Stable Isotope Paleoenvironmental Reconstructions of the Late Pleistocene and early Miocene sites on Rusinga and Mfangano Islands, Lake Victoria, Kenya

A DISSERTATION
SUBMITTED TO THE FACULTY OF
UNIVERSITY OF MINNESOTA
BY

Nicole Diane Garrett

IN PARTIAL FULFILLMENT OF THE REQUIREMENTS
FOR THE DEGREE OF
DOCTOR OF PHILOSOPHY

Kieran P. McNulty, David L. Fox

December 2016

Acknowledgements

I would like to thank my advisors David Fox and Kieran McNulty for this opportunity and their support over these many years. I would also like to thank my committee members Gil Tostevin and Martha Tappen for their help through this process.

Thank you to my many collaborators on these projects: Dan Peppe, Lauren Michel, Holly Dunsworth, Will Harcourt-Smith, Sheila Nightingale, Alex VanPlantinga, Kirsten Jenkins, Christian Tryon, and Tyler Faith. Also, thank you to Kevin Uno and Pratigya Pollisar for their help and expertise in the Biology and Paleo Environment Lab at Lamont Doherty Earth Observatory (Columbia University). I would also like to thank Josef Werne and Sarah Grosshuesch for their introduction into the world of compound-specific isotope analyses.

I am grateful to the many individuals who helped me in the field including Mathew Macharwas, Jared Olelo, Stephen Longoria, Joshua Siembo, Julian Ogondo, Collins Ogongo, and Sina Muteti. Many thanks to Maniko Solheid for her help and advice in the University of Minnesota Stable Isotope Lab. I also am grateful for the many undergraduates who have helped in the lab and the field, specifically Alexi Bessar and Joel Torgenson.

I would like to thank the many graduate students whose help and advice over the past few years has been invaluable: Andrew Elstad-Haveles, Laura Hauff, Claire Kirchoff, Laura Vietti, Jason Massey, Ryan Knigge, Brooke Creager, Katrina Yezzi-Woodley, Dan Maxbauer, and Sam Matson.

Finally, I need to thank my parents David and Stephanie Garrett - without the inspiration of my father, I never would have embarked on the PhD process. Thank you to my

husband Robert Osum who supported me without fail. And lastly, I am grateful to Evelyn for only kicking me a few times during my dissertation defense!

Abstract

Paleoenvironmental reconstructions are a key component when trying to understand a species evolutionary history as environmental pressures play a critical role in the evolution of species. This dissertation, on the Late Pleistocene and early Miocene deposits of Rusinga and Mfangano Islands, Lake Victoria, Kenya, uses carbon and oxygen isotope analyses of paleosol carbonates, bulk sedimentary organic matter, isolated biomarkers from organic matter, and mammalian tooth enamel to reconstruct the various habitats available to the mammalian communities. Present within the Late Pleistocene deposits on Rusinga and Mfangano Island are Middle Stone Age tools, indicating the presence of at least one population of early *Homo sapiens*. The analysis included within (**Chapter 1**) of the Late Pleistocene habitats indicates stream- or spring-side woodlands within a larger C_4 grassland with climates drier than present today. The early Miocene deposits on Rusinga include a well-preserved primate community with remains of the primitive hominoid *Ekembo* as well as specimens from *Dendropithecus* and the lesser-known catarrhines *Limnopithecus* and *Nyanzapithecus*. The paleoenvironmental reconstructions for the early Miocene deposits (**Chapters 2-3**) provide an important evolutionary context for the evolution and diversification of catarrhines, including the earliest members of our own ape-human lineage. The analysis of the Early Miocene habitats indicates a temporally and spatially dynamic mixture of C_3 habitats was available to the faunal community, which included close-canopy habitats experiencing CO_2 recycling as well as environments with plants undergoing light and or water stress (i.e., unshaded areas). The data from the early Miocene also indicates there were distinct

habitats present at Rusinga, with the younger habitats exhibiting either an increase in mean annual temperature, an increase in aridity (evaporation), a decrease in mean annual precipitation or some combination of the three climatic factors. Overall, this analysis indicates the early Miocene primates from Rusinga were able to cope and even thrive in a dynamic and varied landscape by inhabiting both closed and open habitats, including woodlands, bush/shrublands or woody grasslands. For the primitive hominoids, this level of habitat flexibility suggests it may have been an important primitive characteristic for apes.

Table of Contents

Acknowledgements i
Abstract iii
Table of Contents v
List of Tables viii
List of Figures ix

INTRODUCTION 1

CHAPTER 1: STABLE ISOTOPE PALEOECOLOGY OF LATE PLEISTOCENE MIDDLE STONE AGE HUMANS FROM THE LAKE VICTORIA BASIN, KENYA .. 8
Chapter Summary 8
Introduction 10
Pleistocene Records from Rusinga and Mfangano Islands 12
Carbon Isotopes and Paleoecological Reconstruction 14
Aridity Index Based on Mammalian Tooth Enamel Oxygen Isotope Values 21
Materials and Methods 22
Stratigraphic Context 22
Laboratory Analytical Techniques 23
Stable Isotope Results and Interpretations 25
Pedogenic Carbonates and Bulk Soil Organic Matter 25
Mammalian Tooth Enamel: Carbon Isotopes 30
Mammalian Tooth Enamel: Oxygen Isotopes 32
Discussion and Conclusion 33
Acknowledgments 35
Figures and Tables 36

CHAPTER 2: EARLY MIOCENE PALEOENVIRONMENTS OF *EKEMBO* ON RUSINGA ISLAND, KENYA: INTEGRATING BULK SEDIMENTARY ORGANIC AND COMPOUND-SPECIFIC CARBON ISOTOPE ANALYSES OF TERRESTRIAL PALEOSOLS 54
Chapter Summary 54
Introduction 55
Primate Evolution during the Early Miocene 56

Climate and Habitats during the Early Miocene 59
Early Miocene Records from Rusinga Island 61
Materials and Methods 65
Carbon Isotope Composition of Bulk Soil Organic Matter 65
Carbon Isotope Composition of Isolated Biomarkers 68
Paleosol Sampling and Laboratory Analytical Techniques 71
Carbon Isotope Results and Interpretations 75
Carbon Isotope Composition of Bulk Soil Organic Matter 75
Carbon Isotope Composition of Biomarkers 79
Discussion and Conclusions 82
Figures and Tables 86

CHAPTER 3: STABLE ISOTOPE PALEOECOLOGY OF EARLY MIOCENE RUSINGA ISLAND MAMMALIAN COMMUNITIES FROM THE KULU AND HIWEGI FORMATIONS 102
Chapter Summary 102
Introduction 103
Geological Background of Rusinga Island 107
Hiwegi Formation 108
Kulu Formation 110
Stable Isotope Composition of Mammalian Tooth Enamel 110
Materials and Methods 114
Anthracotheriidae 115
Suidae 115
Sanitheridae 116
Tragulidae 116
Chalicotheriidae 116
Rhinocerotidae 117
Proboscidea 118
Hyracoidea 118
Carnivora and Creodonta 119
Laboratory Analytical Techniques 120
Carbon Isotope Results 121
Anthracotheriidae 122
Suidae 123
Sanitheridae 124
Tragulidae 124
Chalicotheriidae 125

Rhinocerotidae 126
Proboscidea 127
Hyracoidea 128
Carnivora and Creodonta 129
Oxygen Isotope Results 129
Discussion 132
Conclusions 136
Figures and Tables 138

CONCLUSION 153

BIBLIOGRAPHY 155

List of Tables

Table 1. Taxonomic list of mammalian fauna from the Wasiriya and Waware Beds as of the 2010 field season. NISP = number of identified specimens. 40

Table 2. Sample ID, corrected paleosol carbonate $\delta^{13}C$ and $\delta^{18}O$ values, SOM $\delta^{13}C$ values, and enrichment value for sediment samples from Rusinga and Mfangano Islands. 42

Table 3. Results of Student's t-tests used to compare the eleven modern ecosystems that exhibit a mean value ± 1 SD overlapping within one standard deviation of the Rusinga mean. 45

Table 4. Field number, locality, tooth, corrected $\delta^{13}C$ value, and $\delta^{18}O$ value for mammalian enamel samples from Rusinga and Mfangano Islands. 48

Table 5. Early Miocene Rusinga Island Paleoenvironmental Reconstructions. 88

Table 6. Carbon isotope composition of Hiwegi Formation paleosol samples collected in 2009 92

Table 7. Carbon isotope composition of Hiwegi Formation paleosol samples collected in 2011 96

Table 8. Carbon isotope composition of *n*-alkanes and *n*-alkanoic acids, as well as corresponding bulk SOM $\delta^{13}C$ values, of selected paleosol samples. 100

Table 9. Early Miocene fossil mammals from Rusinga and Mfangano Islands. 138

Table 10. Carbon and oxygen isotope composition of mammalian enamel samples from Rusinga and Mfangano Islands. 141

Table 11. Results of Student's t-test used to compare the $\delta^{18}O$ values of the rhinocerotids and proboscideans from the Grit/Fossil Bed Member of the Hiwegi Formation, the Kibanga Member of the Hiwegi Formation, and the Kulu Formation. 152

List of Figures

Figure 1. Map of Rusinga and Mfangano Islands, Kenya, showing the Pleistocene sediments and the positions of localities mentioned in the text. 36

Figure 2. Detailed stratigraphic sections from the Late Pleistocene Wasiriya and Waware Beds on Rusinga and Mfangano Islands..... 37

Figure 3. Box-and-whisker plot showing variation of artifact densities (per excavated or surface-collected m^2) from the early Pleistocene Okote Member of the Koobi Fora Formation of Kenya, the Middle Pleistocene of Olorgesailie, Kenya and Maastricht-Bélvèdere, the Netherlands, and Holocene sediments from Sturt National Park, Australia. 39

Figure 4. Correlation between tephra deposits on Rusinga and Mfangano Islands. 41

Figure 5. Paleosol carbonate and organic matter $\delta^{13}C$ values..... 41

Figure 6. Relationships between paleosol carbonate and organic matter $\delta^{13}C$ values from Rusinga and Mfangano Islands and modern soil organic matter samples. 44

Figure 7. Enamel carbon and oxygen isotope values of fossil mammals from Rusinga and Mfangano Islands. 46

Figure 8. Comparison of fossil mammal carbon isotope values from Rusinga and Mfangano Islands to modern Eastern and Southern African mammals. 47

Figure 9. The percentage of bovids belonging to the tribes Alcelaphini and Antilopini against the percentage of C4-consuming bovids across 16 modern wildlife reserves (open and closed habitat) and for the Rusinga and Mfangano fossil samples. 52

Figure 10. Aridity index data from fossil mammals at Rusinga and Mfangano Islands.. 53

Figure 11. Map of fossiliferous Miocene strata on Rusinga and Mfangano Islands, Kenya, in Lake Victoria. 86

Figure 12. Geochronology of the Hiwegi formation..... 87

Figure 13. Summary of Hiwegi Formation geology and SOM analyses. 91

Figure 14. SOM $\delta^{13}C$ values from the Hiwegi Formation at Nyamsingula (R2) and Kaswanga Point (R5). 97

Figure 15. SOM $\delta^{13}C$ values from the Hiwegi Formation at Waregi (R1). 98

Figure 16. SOM $\delta^{13}C$ values from the Hiwegi Formation at Waregi (R1) - lateral sections through the Fossil Bed Member..... 99

Figure 17. Enamel carbon isotope composition by taxa. 147

Figure 18. Mammalian enamel carbon and oxygen isotope composition by taxa. 149

Figure 19. Mammalian enamel carbon and oxygen isotope composition by stratigraphic location. 150

Figure 20. Enamel oxygen isotope composition by taxa. 151

INTRODUCTION

Biologists have long known that environmental pressures play a critical role in the evolution of species. Rusinga (0°24'S, 34°0'E) and Mfangano (0°27'S, 34°0'E) Islands are exceptional in that they record two key stratigraphic intervals in primate evolutionary history that provide an opportunity to document those pressures faced by both early members of our own species (Late Pleistocene sediments) and the earliest members of the ape-human lineage (early Miocene sediments). With regard to the younger deposits, my work on the Late Pleistocene deposits provides the first multi-proxy isotopic reconstruction of the paleoenvironmental context of Middle Stone Age *Homo sapiens* from equatorial East Africa. Additionally, my dissertation research on the older sediments helps to resolve conflicting interpretations of the environmental pressures that shaped the adaptations of early apes and therefore frame later human evolution.

Detailed paleoenvironmental reconstructions are required when attempting to identify a causal relationship between environmental change and evolution, and a variety of methods have been utilized at fossil localities to better understand the adaptive significance of primate morphology. The methods used here include carbon and oxygen isotope analyses of paleosol carbonates, bulk sedimentary organic matter (SOM), isolated biomarkers from SOM, and mammalian tooth enamel.

Carbon isotopic analyses from paleosols, either in the form of sedimentary organic matter, pedogenic carbonates, or isolated biomarkers, are used to infer the relative

proportions of biomass using either the C_3 (Calvin-Benson) or C_4 (Hatch-Slack) photosynthetic pathway present at the time of pedogenesis. C_3 plants include nearly all trees, shrubs, and herbs in addition to cool growing season grasses. C_4 plants are warm growing season grasses, which are generally found in open or unshaded environments, and most sedges. The carbon isotope composition of fossil herbivore tooth enamel is directly related to the relative proportion of C_3 and C_4 plants in the animal's diet during enamel mineralization, which can provide a snapshot of the animal's habitat. The oxygen isotope composition of tooth enamel primarily reflects that of ingested water (either surface drinking water or via as a component of diet via plant matter). Reconstructing the oxygen isotope composition of surface and plant water available for at a site or in a region is often a key component of paleoclimatic reconstructions and provides information on important climatic variables such as aridity, seasonality, and mean annual temperature.

Late Pleistocene Sediments

The Late Pleistocene (126,000 to 10,000 years ago) is a critical time in the evolutionary history of our own species, *Homo sapiens*. After evolving in East Africa between 200,000 and 100,000 years ago, Late Pleistocene modern humans began to disperse both within and out of Africa, rapidly spreading to all six continents now inhabited by *Homo sapiens*. Our understanding of the environmental pressures faced by early modern humans and how those pressures mediated the behavioral and biological diversity of early modern humans and their migration patterns is limited by a dearth of archaeological

evidence associated with detailed paleoenvironmental data. Available paleoenvironmental studies from this period, conducted over large temporal and spatial scales, have suggested that modern human populations in Africa may have retreated to refuges with good access to water during periods of dramatically increased aridity. As such, my research in the Late Pleistocene deposits on Rusinga and Mfangano Islands, which include Middle Stone Age tools, provides a rare look into the behaviors and adaptations of modern *Homo sapiens* during this formative time in human biogeography.

Chapter 1 of this dissertation includes an analysis of the stable carbon and oxygen isotope composition of paleosol carbonate and organic matter and fossil mammalian tooth enamel, including the first isotopic data for several extinct bovids, from the Late Pleistocene deposits on Rusinga and Mfangano Islands. This study represents the first multi-proxy isotopic reconstruction of the paleoenvironmental context on a local/regional scale of early *Homo sapiens* based on data from archaeological sites in equatorial East Africa. This analysis, published in the *Journal of Human Evolution*[1], allows my coauthors and I to place the Rusinga and Mfangano Middle Stone Age humans within a local stream- or spring-side woodland habitat surrounded by a large regional dry grassland ecosystem. Our data suggest that humans were able to remain in East Africa, even during hyper-arid periods with expanded grasslands, by retreating to locally closed and well-watered habitats. Prior to this analysis, researchers interested in this time period where left to hypothesize as to whether or not increased periods of aridity that occurred

[1] Garrett, N.D., Fox, D.L., McNulty, K.P., Faith, J.T., Peppe, D.J., Plantinga, A., Tryon, C.A., 2015. Stable isotope paleoecology of Late Pleistocene Middle Stone Age humans from the Lake Victoria basin, Kenya. Journal of Human Evolution 82, 1-14. http://dx.doi.org/10.1016/j.jhevol.2014.10.005

frequently during the Pleistocene would have driven modern humans out of East Africa. With this analysis, I documented at least one population of humans that was able to survive in East Africa during one of these dry periods without retreating to an isolated refugium.

Early Miocene Sediments

The first members of Hominoidea – the superfamily within Primates that includes all apes including humans – evolved in Africa during the late Oligocene and early Miocene. Understanding the origin and diversification of our hominoid ancestors, including the evolutionary pressures that shaped their adaptive morphology, is a necessary foundation for our understanding of the evolutionary history of all later apes, and is directly relevant to understanding our own hominin ancestors.

The deposits on Rusinga and Mfangano Islands contain one of the richest fossil assemblages from the early Miocene and have been the focus of extensive paleontological research for over eight decades. The fossil mammal community from the islands contains an exceptional number of well-preserved specimens from one of the best-known genera of early Miocene apes, *Ekembo,* which is represented by two species, *E. nyanzae* and *E. heseloni*. Other primates found on Rusinga include *Dendropithecus macinnesi*, and specimens from the less well-known catarrhines *Limnopithecus legetet* and *Nyanzapithecus vancouveringorum*. The fossil primate assemblage therefore provides an excellent setting to examine the adaptation and diversification of the early

Miocene primate community and critical information for our understanding of early ape evolution.

Although decades of research at these sites have produced multiple paleoenvironmental studies, a clear consensus has yet to be reached regarding the ecological context for the island's early apes and other primates. The many paleoenvironmental reconstructions have yielded a wide range of often conflicting results and interpretations, indicating habitats ranging from closed forests, woodlands, or rainforests, mosaic habitats of both open and closed habitats, and even semi-arid environments. Most of these reconstructions have focused on a single formation or locality on the islands, rather than documenting the range of habitats across the entire deposit or any changes to the ecosystems through time. Regardless, the lack of a clear paleoenvironmental context for these sequences has hindered our ability to understand fully the behavior and ecology of these important early Miocene apes.

Chapter 2 of my dissertation includes an analysis of the stable carbon isotope composition of bulk sedimentary organic matter and isolated biomarkers from the early Miocene deposits on Rusinga Island. This study includes a detailed analysis of the spatial and temporal variation within the Hiwegi Formation – the most fossiliferous of the early Miocene formations on Rusinga Island – at multiple localities across the island to provide clearer documentation of the range of habitats present during this crucial period in primate evolution. The data from this portion of the study indicates the early Miocene Hiwegi Formation on Rusinga Island comprised a heterogeneous landscape, which

included a spatially and temporally dynamic mixture of both open and closed habitats such as forests, woodlands, and woody grasslands.

Chapter 3 of my dissertation includes an analysis of the stable carbon and oxygen isotope composition of mammalian tooth enamel from the early Miocene deposits on Rusinga Island. This analysis includes samples from tooth enamel of anthracotheres, suids, sanitherids, tragulids, chalicotheres, titanohyracids, rhinocerotids, gomphotheres, and deinotheres from the early Miocene Hiwegi and Kulu Formations of Rusinga Island. The carbon isotope composition of the mammalian tooth enamel presented in this study suggests a modest degree of habitat variability, which would have included a temporally and/or spatially dynamic mixture of C_3 habitats, although there is very limited evidence for true close-canopy forests. The oxygen isotope data indicates either an increase in mean annual temperature, an increase in aridity (evaporation), a decrease in mean annual precipitation or some combination of the three climatic factors in the Kulu Formation when compared to the Hiwegi Formation demonstrating a marked change in paleoenvironmental stressors facing this early Miocene mammalian community.

With this analysis of the early Miocene bulk sedimentary organic matter, isolated biomarkers, and mammalian tooth enamel (**Chapters 2-3**), I document a range of C_3 habitats present during this period, including a spatially and temporally dynamic mixture of both closed and open habitats. Importantly, these studies do not indicate the early Miocene habitats on Rusinga Island included a large or vast closed-canopy forest. Traditionally, apes are associated with closed habitats such as forests (the majority of

extant apes live in these types of habitats), and this connection is often a major assumption in later ape and human evolutionary theory. This analysis however, indicates the early hominoids from Rusinga were able to cope and even thrive in a dynamic and varied landscape by inhabiting both closed and open habitats, including woodlands, bush/shrublands or woody grasslands. Habitat flexibility in these early apes may have been an important primitive characteristic for hominoids.

CHAPTER 1: STABLE ISOTOPE PALEOECOLOGY OF LATE PLEISTOCENE MIDDLE STONE AGE HUMANS FROM THE LAKE VICTORIA BASIN, KENYA

Note: This chapter was published with co-authors[2] in the Journal of Human Evolution prior to completion of this dissertation.

Formal citation: Garrett, N.D., Fox, D.L., McNulty, K.P., Faith, J.T., Peppe, D.J., Plantinga, A., Tryon, C.A., 2015. Stable isotope paleoecology of Late Pleistocene Middle Stone Age humans from the Lake Victoria basin, Kenya. Journal of Human Evolution 82, 1-14. http://dx.doi.org/10.1016/j.jhevol.2014.10.005

Co-authors: David L. Fox[3], Kieran P. McNulty[4], J. Tyler Faith[5], Daniel J. Peppe[6], Alex Van Plantinga[5,7], Christian A. Tryon[8]

Chapter Summary

Paleoanthropologists have long argued that environmental pressures played a key role in human evolution. However, our understanding of how these pressures mediated the behavioral and biological diversity of early modern humans and their migration patterns

---

[2] **Author contributions:** DLF, KPM, CAT, DLP designed research; NDG performed all isotope analyses and analyzed all isotope data; AVP and DLP performed tephra correlation analyses; CAT performed archaeological artifact density analyses; JTF calculated the bovid tribe distribution across modern and fossil sites; NDG, DLF, and DJP collaborated on field work for geological descriptions; NDG wrote the paper; DLF, CAT, KPM, JTF, DJP, and AVP revised the paper.

[3] Department of Earth Sciences, University of Minnesota, 310 Pillsbury Drive SE, Minneapolis, MN, 55455, USA
[4] Department of Anthropology, University of Minnesota, 395 Hubert H. Humphrey Center, 301 19th Ave S, Minneapolis, MN, 55455, USA
[5] School of Social Science, The University of Queensland, Brisbane, QLD 4072, Australia
[6] Department of Geology, Baylor University, One Bear Place #97354, Waco, TX, 76798, USA
[7] Department of Geology and Geophysics, Texas A&M University, MS3115, College Station, TX 77843, USA
[8] Department of Anthropology, Peabody Museum of Archaeology and Ethnology, Harvard University, 11 Divinity Avenue, Cambridge, MA 02138, USA

within and out of Africa is limited by a lack of archaeological evidence associated with detailed paleoenvironmental data. Here, we present the first stable isotopic data from paleosols and fauna associated with Middle Stone Age (MSA) sites in East Africa. Late Pleistocene (~100-45 ka) sediments on Rusinga and Mfangano Islands in eastern Lake Victoria (Kenya) preserve a taxonomically diverse, non-analog faunal community associated with MSA artifacts. We analyzed the stable carbon and oxygen isotope composition of paleosol carbonate and organic matter and fossil mammalian tooth enamel, including the first analyses for several extinct bovids such as *Rusingoryx atopocranion*, *Damaliscus hypsodon*, and an unnamed impala species. Both paleosol carbonate and organic matter data suggest that local habitats associated with human activities were primarily riverine woodland ecosystems. However, mammalian tooth enamel data indicate that most large-bodied mammals consumed a predominantly C_4 diet, suggesting an extensive C_4 grassland surrounding these riverine woodlands in the region at the time. These data are consistent with other lines of paleoenvironmental evidence that imply a substantially reduced Lake Victoria at this time, and demonstrate that C_4 grasslands were significantly expanded into equatorial Africa compared to their present distribution, which could have facilitated dispersal of human populations and other biotic communities across equatorial Africa. Our results indicate that early populations of *Homo sapiens* from the Lake Victoria region exploited locally wooded and well-watered habitats within a larger grassland ecosystem.

Introduction

Environmental change has been associated with a number of key events in human evolutionary history, including the dispersal of modern humans within and out of Africa (e.g., Scholz et al., 2007; Cowling et al., 2008; Carto et al., 2009; Compton, 2011; deMenocal, 2011; Blome et al., 2012; Potts, 2012; Faith et al., in press). Fossil and genetic data point to an East African origin of *Homo sapiens* between 200,000 and 100,000 years ago (McDougall et al., 2005; Gonder et al., 2007), with Middle Stone Age (MSA) archaeological sites providing the behavioral context for these early populations (McBrearty and Brooks, 2000; Tryon and Faith, 2013). Recent genetic evidence indicates that an East African population, ancestral to many sub-Saharan African lineages and to all non-African lineages, began to disperse within and out of Africa between 70-60 ka (Soares et al., 2012). Several recent studies have focused on the role of late Pleistocene (126 to 12 ka) environmental change in driving these modern human dispersal events (Carto et al., 2009; Blome et al., 2012), including population retreat to well-watered refugia during periods of increased aridity (Basell, 2008; Brandt et al., 2012). However, the impact of these studies is limited because the relevant data archives – particularly proxies for temperature, moisture availability, and vegetation – are poorly resolved spatially and temporally (reviewed in Blome et al., 2012). Available faunal evidence indicates that early modern human populations in East Africa were part of extinct non-analog animal communities that were distinct in terms of taxonomic composition compared to regional modern mammal communities (Marean and Gifford-Gonzales, 1991; Marean, 1992, 1997; Tryon et al., 2010, 2012; Faith et al., 2011,

2012, 2013, 2014), and, as such, the paleoecology of these ancient populations remains poorly understood. Previous paleoenvironmental reconstructions of East African MSA sites using isotopic data have been restricted to the analysis of paleosols from site A5 (dated to ~ 100-80 ka) at Aduma, Ethiopia (Yellen et al., 2005), and no published studies to date have examined the stable isotope composition of fossil mammals from this interval. Thus far, the rarity of detailed paleoenvironmental reconstructions from MSA archaeological and hominin fossil sites has obscured the ecological contexts that shaped the biology and behavior of East African modern humans.

Here we describe the first isotopic reconstruction of the paleoenvironmental context of early *Homo sapiens* from the MSA of East Africa, using data from MSA archaeological sites on Rusinga and Mfangano Islands. These sites are dated to ca. 100-33 ka, overlapping with major dispersals of human populations out of East Africa. We combine the carbon ($\delta^{13}C$)[9] and oxygen ($\delta^{18}O$) isotopic compositions of sediments (pedogenic carbonates, bulk sedimentary organic matter) and fossil mammalian tooth enamel to reconstruct local vegetation composition, assess habitats in the broader landscape sampled by mobile large-bodied ungulates, and estimate regional moisture availability. Taken together, these analyses inform our knowledge of the paleoecological context of early modern humans during this critical time period.

[9] $\delta^{13}C$ and $\delta^{18}O$ values are presented in parts per thousand (permil, ‰), where $\delta X=(R_{sample}/R_{standard}-1) *1000$, X is ^{13}C or ^{18}O, R is $^{13}C/^{12}C$ and $^{18}O/^{16}O$ respectively, and the standard for carbon is Vienna Pee Dee Belemnite (V-PDB) and for oxygen is Vienna Standard Mean Ocean Water (V-SMOW).

Pleistocene Records from Rusinga and Mfangano Islands

Rusinga (0°24'S, 34°0'E) and Mfangano (0°27'S, 34°0'E) are near-shore islands in Lake Victoria (**Fig. 1**) that today receive approximately 1400 mm rainfall per year (Crul, 1995; Fillinger et al., 2004). Prior to substantial human habitation, the islands were likely covered by variably dense woodlands (Andrews, 1973), with the surrounding area on mainland Kenya including woodlands, bushlands, thickets, and forested habitats (White, 1983). Rusinga and Mfangano are remnants of the eruption and deposition of lavas and sediments of the Kisingiri volcano, inactive since the middle Miocene. Both islands share a similar bedrock lithology of Miocene lavas and volcaniclastics, unconformably overlain by poorly consolidated Pleistocene sediments (e.g., Peppe et al., 2009; Tryon et al., 2010). The Pleistocene Wasiriya Beds of Rusinga and the Waware Beds of Mfangano are primarily made up of tuffaceous alluvial and fluvial sediments and weakly developed paleosols suggestive of a relatively unstable landscape dominated by episodic depositional events (**Figs. 1-2**; Tryon et al., 2010, 2012). Rare tufa deposits at the Nyamita locality (Rusinga) are indicative of small, local springs (**Figs. 1-2**; Tryon et al., 2014; Peppe et al., in review). The Wasiriya and Waware Beds comprise identical sedimentary facies and show remarkable similarities in the fauna, the chemical composition of tephra deposits, and age estimates from fossil gastropods, suggesting that the Wasiriya Beds on Rusinga and Waware Beds on Mfangano likely sample the same general interval of time during the late Pleistocene (Tryon et al., 2012, 2014). This is confirmed by tephra correlations made between all fossil-bearing Pleistocene sites on Rusinga, Mfangano, and other nearby sites in the region (Blegen et al., 2014). We

estimate that the artifact and fossil bearing strata on both islands range in age from ca. 100-33 ka. The minimum age for the deposits is constrained by calibrated radiocarbon dates on fossil gastropods (*Limicolaria* cf. *L. martensiana*) that have burrowed into the deposits, and the maximum age is defined by the eruption time of the inferred source volcanoes that produced distal tephra deposits found near the base of the sedimentary sequence (Tryon et al., 2010, 2012).

Both the Wasiriya and Waware Beds contain multiple archaeological sites with MSA artifacts, such as bifacial points and Levallois flakes and cores (Tryon et al., 2010, 2012, 2014). Controlled excavations in 2009-2011 from three locations on Rusinga Island (one at Nyamita and two at Wakondo including the Bovid Hill sub-locality and a second unnamed sub-locality) totaling 28 m^2 produced artifact densities of 1.26-6.50 lithic artifacts/m^2 (Tryon et al., 2010; Jenkins et al., 2012). These *in situ* artifact densities are within the range expected from the "scatter between the patches" (Isaac, 1981) or the "veil of stones" (Roebroeks et al., 1995), typical of open-air Paleolithic artifact scatters across ancient landscapes (**Fig. 3**). Lithic artifacts have been found together in surface collections and in excavations with a diverse fossil fauna, including some specimens with cut-marks (Tryon et al., 2010). The Pleistocene faunas from Rusinga and Mfangano (**Table 1**) contain the largest number of extinct species of any Pleistocene site in East Africa during the last ~ 400 ka (cf. Marean, 1992; Assefa et al., 2008; Domínguez-Rodrigo et al., 2008; Faith et al., 2011, 2012, 2013, 2014), with the extinct species *Rusingoryx atopocranion* (Pickford and Thomas, 1984; Faith et al., 2011) and *Damaliscus hypsodon* (Faith et al., 2012) being the most abundant. Relevant to

paleoenvironmental reconstruction, the faunas include several taxa indicating locally wet conditions, such as *Hippopotamus* and two species of reduncine bovids.

The fluvial, alluvial, and tufa deposits that comprise the Wasiriya and Waware Beds are suggestive of riparian depositional environments (Tryon et al., 2010, 2014; Peppe et al., in review); however, these deposits are likely not representative of the broader, regional landscape. The abundance of bovids belonging to the tribes Alcelaphini (wildebeest and allies) and Antilopini (gazelles and allies) (85% of bovid specimens at Rusinga and 70% at Mfangano), which, together with extinct specialized grazers (*Syncerus antiquus*, *Megalotragus* sp., *Rusingoryx atopocranion*, *Damaliscus hypsodon*) suggest the prevalence of open grassland vegetation (Tryon et al., 2010, 2012, 2014; Faith et al., 2011). Oryx (*Oryx beisa*) and Grevy's zebra (*Equus grevyi*) are both found here well outside their modern ranges where they inhabit arid to semi-arid grasslands and shrublands, suggesting drier conditions compared to the present (Faith et al., 2013).

Carbon Isotopes and Paleoecological Reconstruction

The primary basis for using the stable carbon isotope compositions of pedogenic carbonate, sedimentary organic matter, and mammalian herbivore tooth enamel as paleoecological proxies is the well-established differences in fractionation of carbon isotopes during fixation of atmospheric CO_2 by plants using different photosynthetic pathways. Plants using the C_3 pathway (trees, shrubs, cool growing season grasses) strongly discriminate against ^{13}C during fixation of CO_2 and so have low $\delta^{13}C$ values

relative to atmospheric CO_2 (modern C_3 mean: -27.4 ± 1.6‰; O'Leary, 1981, Passey et al., 2002; Cerling et al., 2003; Kohn, 2010; Diefendorf et al., 2010); C_4 plants (warm growing season grasses, most sedges) discriminate less against ^{13}C and have $\delta^{13}C$ value closer to atmospheric CO_2 (modern C_4: -12.7 ± 1.1‰; O'Leary, 1981, Passey et al., 2002; Cerling et al., 2003; Kohn, 2010; Diefendorf et al., 2010). Plants using the CAM pathway (cacti, other succulents) typically have intermediate $\delta^{13}C$ values but do not comprise a substantial fraction of the diet of modern large bodied herbivores in East Africa and we do not consider them further (Kingdon, 1988a, 1988b). Variation in C_3 plants is primarily driven by environmental factors that must be considered in interpretations of proxy data. Photosynthetic recycling of respired CO_2 in closed forests imparts lower than average $\delta^{13}C$ values to plant tissues (the canopy effect; van der Merwe and Medina, 1991). In contrast, light and water stress in open habitats decrease fractionation during fixation of CO_2, causing higher than average $\delta^{13}C$ values in plants (Ehlringer and Cooper 1988). C_4 plants are uncommon in closed forests today (Edwards and Smith, 2010), and fractionation by C_4 plants does not vary in relation to habitat and rainfall in arid and semi-arid regions of southern Africa (Schulze et al., 1996; Swap et al., 2004; but see Buchmann et al., 1996; Cerling et al., 2003).

The carbon isotope compositions of pedogenic carbonate and organic matter in a paleosol can be used to infer the relative proportions of C_3 and C_4 plants biomass present in the soil at the time of pedogenesis (Cerling and Quade, 1993). Soil organic matter generally preserves the isotopic composition of the overlying plant biomass (Balesdent et al., 1993; Tieszen et al., 1997). Variable contributions of leaves and roots to soil organic matter and

decomposition of organic matter by soil biota can lead to enrichment of organic matter in ^{13}C of several permil relative to standing biomass (Hobbie et al., 2004; Chen et al., 2005; Wynn, 2007). In addition to inputs from the plant component of soil biomass, soil organic matter can include carbon derived from microorganisms, which can shift the $\delta^{13}C$ values from that of the overlying vegetation (Koch, 1998).

Pedogenic carbonates that precipitate at depths greater than ca. 30 cm in soils with moderate to high respiration rates reflect the isotopic composition of plant-derived CO_2 with no direct contribution from atmospheric CO_2 (Cerling, 1991). Soil CO_2 (and therefore soil carbonate) is enriched in ^{13}C by 4.4‰ relative to plant-derived CO_2, due to kinetic fractionation during diffusion of CO_2 from the soil to the atmosphere (Amundson, 1989; Cerling, 1991; Cerling and Quade, 1993). Additionally, equilibrium fractionation during the precipitation of calcite will result in the enrichment of soil carbonates in ^{13}C by ca. +9.8 to +12.4‰ relative to soil CO_2 for the temperature range 25-0°C (Deines et al., 1974; Romanek et al., 1992). Thus, paleosol carbonates formed at depth in productive soils will have $\delta^{13}C$ values that are ca. +14-17‰ higher than unaltered soil organic matter. Deviation from this offset can indicate that one or both phases have been altered and should not be used for paleoenvironmental reconstruction. For example, in habitats with extreme aridity and/or low soil productivity, paleosol carbonates will be even more enriched in ^{13}C due to deeper penetration into the soil of isotopically heavy atmospheric CO_2 (Cerling, 1992; Cerling, 1997; Quade and Levin, 2013).

The $\delta^{13}C$ values of herbivore tissues record the $\delta^{13}C$ values of the plants consumed with tissue-specific enrichments relative to diet (DeNiro and Epstein, 1978). Various methods have been proposed to test for diagenesis in enamel (Morgan et al., 1994; Kohn et al., 1999; Sponheimer and Lee-Thorp, 1999a; Schoeninger et al., 2003), however the consensus is that the isotopic composition of enamel apatite from large-bodied animals is generally resistant to diagenesis during the fossilization process due to its highly crystalline state and extremely low organic content (LeGeros, 1991). Therefore enamel can be used as a proxy for diet during the time over which tooth enamel was mineralizing (DeNiro and Epstein, 1978; Sullivan and Krueger, 1981; Tieszen et al., 1983; Ambrose and DeNiro, 1986; Lee-Thorp et al., 1989; Wang and Cerling, 1994; Cerling and Harris, 1999; Kohn et al., 1999; Lee-Thorp, 2000; Lee-Thorp and Sponheimer, 2013).

For large-bodied ungulates, the generally accepted enrichment factor for tooth enamel relative to diet is +14.1±0.5‰, which is the mean value for numerous ruminant and non-ruminant species of artiodactyls and perissodactyls (Cerling and Harris, 1999; Passey et al., 2002). The carbon isotopic composition of mammalian herbivore tooth enamel reflects the relative dietary proportion of C_3 and C_4 plants during enamel mineralization, which takes place early in an animal's life (DeNiro and Epstein, 1978; Lee-Thorp and van der Merwe, 1987). The total time of enamel mineralization in a single tooth is short (months to years) relative to the time of formation of both paleosol carbonates and organic matter (averaged over hundreds or thousands of years). However, because mammals generally move around the landscape the spatial scale integrated in the tooth enamel isotopic signal can be quite large (Kingston, 2007). In the case of large migratory

herbivores found in the Pleistocene deposits on Rusinga and Mfangano, such as wildebeest (*Connochaetes taurinus*), plains zebra (*Equus quagga*), and probably *Damaliscus hypsodon* (Faith et al., 2012), the paleoenvironmental information extracted from tooth enamel would be on a scale commensurate with that used by mobile populations of human foragers (i.e., tens to hundreds of square kilometers).

To make quantitative interpretations of our carbon isotope data, we must consider long-term and historical changes in the $\delta^{13}C$ of atmospheric CO_2. The $\delta^{13}C$ of atmospheric CO_2 has varied by several permil over geologic time due to natural changes in the global carbon cycle (Leuenberger et al., 1992; Zachos et al., 2001; Gröcke, 2002; Tipple et al., 2010) and has been decreasing over the last 200 years due to the addition of CO_2 from fossil fuel combustion with lower $\delta^{13}C$ values (Friedli et al., 1986; Marino and McElroy, 1991). Many previous paleoenvironmental studies using carbon isotope ratios have not addressed long-term changes in the $\delta^{13}C$ of atmospheric CO_2, so here we layout a detailed methodology. To compare measured $\delta^{13}C$ values of paleosols and fossil mammal tooth enamel to comparable data from modern ecosystems, we first estimated the $\delta^{13}C$ of atmospheric CO_2 during the late Pleistocene using $\delta^{13}C$ and $\delta^{18}O$ values of the benthic foraminifera genus *Cibicidoides* from Deep Sea Drilling Project (DSDP) site 607 (Zachos et al., 2001; Zachos et al., 2008) and the atmospheric CO_2 $\delta^{13}C$ reconstruction method of Tipple et al. (2010) with one modification. Tipple et al. (2010) used a long-term average $\delta^{18}O$ value for seawater of 0.0‰ for 5-0 Ma in their calculations, but to account for the impact of global ice volume during the Pleistocene, we use a $\delta^{18}O$ value for seawater of 1.0‰ in our calculation (Zachos et al., 2001; Miller et al., 2005b).

Using these calculations, our estimated $\delta^{13}C$ value for atmospheric CO_2 from 33-100 ka is -6.6 ± 0.4‰. Our fossil samples are compared to a modern comparative dataset collected from published datasets with publication dates ranging from the 1980s through the 2010s; as most of these publications do not provide collection dates, we chose an approximate average value for modern atmospheric CO_2 value of -8.0‰ based on these sample/publication dates (Keeling et al., 2001). We use the difference between our estimated late Pleistocene $\delta^{13}C$ value and the modern value (1.4‰) to correct our measured values from Rusinga and Mfangano Islands to the equivalent value under the modern atmosphere.

The relative contribution of C_4 biomass to soil organic matter and paleosol carbonates or mammalian diets can be estimated from measured $\delta^{13}C$ values using a simple linear mixing model between end member $\delta^{13}C$ values for C_3 and C_4 plants and enrichments for paleosol carbonates or tooth enamel:

$$\delta^{13}C_{measured} = \delta^{13}C_{C3} * f_{C3} + \delta^{13}C_{C4} * (1 - f_{C3}),$$

where $\delta^{13}C_{C3}$ and $\delta^{13}C_{C4}$ are the assumed end member $\delta^{13}C$ values (and can be modified by adding enrichments appropriate to the measured substrate) and f_{C3} is the fraction of C_3 biomass contributing the measured $\delta^{13}C$ value.

Because fractionation of carbon isotopes during precipitation of pedogenic carbonate is temperature-dependent (Deines et al., 1974; Romanek et al., 1992), enrichments for

paleosol carbonate in the mixing model are partially temperature-dependent and the mixing model also requires information on soil temperature, which we cannot constrain with our data. Thus, we only use the mixing model to interpret our tooth enamel data as large bodied mammals precipitate tooth enamel at an approximately constant body temperature of 37°C (Longinelli, 1984; Luz et al., 1984).

For tooth enamel data, the critical step is the assumption of end member $\delta^{13}C$ values. One approach is to use the mean values for both C_3 and C_4 plants based on large datasets from analyses of modern plants (-27.4 ± 1.6‰ and -12.7 ± 1.1‰, respectively; Cerling and Harris, 1999; Passey et al., 2002; Cerling et al., 2003; Kohn, 2010; Diefendorf et al., 2010). However, modern C_3 and C_4 plants both exhibit considerable variation in $\delta^{13}C$ values, and, as discussed above, the greater variability of C_3 plants is due to environmental effects. Of particular concern here, is that drought-stressed C_3 plants can have mean $\delta^{13}C$ values as high as -24.6 ± 1.1‰ (Cerling and Harris, 1999; Passey et al., 2002), and, given that paleoecological evidence from the Rusinga and Mfangano fauna suggests a predominantly open and semi-arid grassland, mean C_3 and C_4 end member values are likely to overestimate the proportion of C_3 plants and underestimate the proportion of C_4 plants in the diets of herbivores. Given the importance of aridity as a climatic factor in the late Pleistocene East African paleoenvironmental record, we want to be cautious about our assumptions to avoid circularity in our interpretations. Rather than use a single set of assumptions about end member values, we present five different versions of the mixing model that are increasingly conservative in their assumptions about aridity and the abundance of C_4 biomass and cover the plausible range of

quantitative reconstructions of diet. This approach allows us to interpret the paleoenvironmental implication of the diet reconstructions from tooth enamel $\delta^{13}C$ values under all end-member assumptions. In these versions, the end member values used are: (A) mean C_3 and C_4 modern plant $\delta^{13}C$ values, (B) mean C_3 end member shifted positively by one standard deviation (1.6‰) and unaltered mean C_4 end member, (C) arid climate C_3 end member and unaltered mean C_4 end member, (D) arid climate C_3 end member and mean C_4 end member shifted positively by one standard deviation (1.1‰), (E) arid climate C_3 end member shifted positively by one standard deviation (1.1‰) and mean C_4 end member shifted positively by one standard deviation (1.1‰).

Aridity Index Based on Mammalian Tooth Enamel Oxygen Isotope Values

The oxygen isotope composition of tooth enamel reflects the $\delta^{18}O$ value of body water/fluids and body temperature. Bioapatite and body fluids are assumed to form in oxygen isotope equilibrium as oxygen exchange between body water, blood phosphate, and blood carbonate occurs rapidly (Koch, 1998, 2007; Nagy, 1989; Ambrose and Norr, 1993; Tieszen and Fagre, 1993). Because leaf water is enriched in ^{18}O relative to meteoric water due to evaporation, animals that obtain a large proportion of their water from leaves (i.e., evaporation sensitive or ES taxa) will have enriched enamel bioapatite $\delta^{18}O$ values relative to contemporaneous and sympatric animals that must drink from a surface water source (i.e., evaporation insensitive or EI taxa). Local relative humidity and surface temperatures will influence the total amount of enrichment for leaf water; these variables ultimately affect the total amount of evaporation (Flanagan et al., 1991;

Fricke et al., 1998; Luz et al., 1990; Sponheimer and Lee-Thorp, 1999b; Levin et al., 2006).

We use the index of Levin et al. (2006) to estimate aridity from measured $\delta^{18}O$ values of mammalian tooth enamel. This aridity index relies on the relationship between water deficit and the ^{18}O enrichment (ε^*) between ES and EI taxa based on measured $\delta^{18}O$ enamel values. Water deficit (WD) is the difference between potential evapotranspiration (PET) and mean annual precipitation (MAP). The $\delta^{18}O$ value of the body water of ES taxa (hence tooth enamel) will track ^{18}O enrichment in leaf water due to evaporation, and, conversely, the $\delta^{18}O$ value of body water (and tooth enamel) of EI will track the $\delta^{18}O$ value of meteoric water. As many of the same species Levin et al. (2006) used in their calibration study have been recovered from Rusinga and Mfangano Islands, we can apply the aridity index to these species and do not need to rely on assumptions of taxonomic uniformitarianism. For comparison, we calculated modern WD values for Rusinga Island and nearby Kisumu (75 km east-northeast) (WD = 774 and 562 mm, respectively) using PET and MAP values from the WORLDCLIM model (Hijmans et al. 2005).

Materials and Methods

Stratigraphic Context

Isotopic analyses focused on paleosol carbonate and bulk organic samples collected from stratigraphic sections measured through the Nyamita and Wakondo localities on Rusinga

Island and the Kakrigu locality on Mfangano Island. Weakly developed paleosols found within the Wasiriya and Waware beds include pedogenic features such as small carbonate nodules (<1 cm), granular texture, pressure faces, Mn-staining, and calcified root traces. The majority of our samples derive from Nyamita, where an approximately 14-m-thick succession of Wasiriya Beds sediments is exposed for ~1 km along a single north-south trending valley (Van Plantinga, 2011). Correlative tephra deposits (as determined by electron probe microanalyses of the volcanic glass phase; termed: Nyamita Tuff and Wakondo Tuff, respectively) link the Nyamita and Wakondo localities (**Fig. 4**) and have facilitated the study of lateral variation among sedimentary facies, which is described in detail by Tryon et al. (2010), Van Plantinga (2011) and Peppe et al. (in review). Sampled fossil teeth derive largely from surface contexts where original stratigraphic position within the late Pleistocene deposits could be determined.

Laboratory Analytical Techniques

Paleosol samples were collected from ten stratigraphic sections at the Wakondo and Nyamita localities in the Wasiriya beds of Rusinga Island, and one section at the Kakrigu locality in the Waware Beds on Mfangano Island during the 2009-2011 field seasons (**Fig. 2**).

Paleosol samples for carbonate analysis were roasted *in vacuo* for one hour at 400°C to eliminate water and organic matter and then reacted with 100% phosphoric acid in a Kiel automatic carbonate extraction device. The carbon and oxygen isotopic composition of

the resulting carbon dioxide gas was measured using a Finnigan MAT 252 isotope ratio mass spectrometer and normalized by repeated analysis of both a commonly used (but uncertified) laboratory standard (Carrara marble) and a certified international carbonate standard (NBS-19). Paleosol samples for bulk soil organic matter analysis were reacted with 0.5 M hydrochloric acid for 24 hours to eliminate any carbonates and then rinsed with deionized water five times. Samples were then dried in a 60°C oven for 48+ hours to remove any remaining water. Following combustion in a Costech ECS 4010 elemental analyzer, the carbon isotopic composition of the resulting CO_2 was measured using Thermo Delta V+ isotope ratio mass spectrometer and normalized by in sequence analyses of a laboratory standard (UCSC Pugel) and NIST 2711a (Montana soil). Analytical precision for all measured values is better than 0.1‰ based on repeated analyses of the standards.

Fifty-nine teeth identifiable to tribe, genus, or species were sampled from eight Rusinga Island localities and two Mfangano Island localities. Approximately 7 mg of tooth enamel were drilled from each specimen using a diamond bur. Care was taken to avoid any cracks in the enamel or specimens with evidence of alteration (such as discoloration). Following one of several established and commonly used protocols (Koch et al., 1997; e.g., Bibi, 2007; Clementz et al., 2009; Feranec et al., 2009; Gehler et al., 2012; McLean and Emslie, 2012; Domingo et al., 2013; Feranec and Pagnac, 2013; Clementz et al., 2014), sample powders were reacted with 30% hydrogen peroxide at 8°C for 48 hours to remove any organic contaminants. The enamel samples were then rinsed five times with water and reacted with 1 M acetic acid with a 1 M calcium acetate buffer (pH: 5) at 8°C

for 24 hours to remove any exogenous carbonate. Samples were again rinsed five times and then freeze dried for 24 hours. The cleaned enamel samples and approximately 2 cm of silver thread (to react with any SO_2 generated during acidification) were reacted with 100% phosphoric acid in a Kiel automatic carbonate extraction device. A Finnigan MAT 252 isotope ratio mass spectrometer was used to measure the carbon and oxygen isotopic composition of the resulting CO_2. Values were normalized by repeated analysis of carbonate standards (Carrara marble, NBS-19) and analytical precision for all values is better than 0.1‰. All isotope analyses of paleosols and teeth were completed at the University of Minnesota Stable Isotope Lab.

Stable Isotope Results and Interpretations

Pedogenic Carbonates and Bulk Soil Organic Matter

Twenty of the 75 sediment samples exhibit the expected +14-17‰ offset in $\delta^{13}C$ values of pedogenic carbonate and organic matter ($\Delta_{CO3\text{-}OM}$), indicating that these are appropriate for use in paleoenvironmental reconstructions. (**Fig. 5, Table A.1**). This subset of paleosols comes from several stratigraphic sections along a ~1 km transect at the Nyamita locality on Rusinga (**Fig. 1, Table 2**). The stratigraphic sections at Nyamita and Wakondo were correlated using the chemical composition of volcanic glass in the Nyamita and Wakondo Tuffs, allowing us to demonstrate that the paleosol carbonates discussed here are from roughly contemporaneous strata that sample different parts of the landscape (Tryon et al., 2010; Van Plantinga, 2011; Peppe et al., in review). Although

we do not have unambiguously reliable isotopic data from paleosols in other Wasiriya or Waware Bed localities (**Fig. 1**), tephra correlations indicate that all of the Wasiriya and Waware Bed deposits are contemporaneous (Blegen et al. 2014). Furthermore, the similarities in large mammal taxonomic composition and in the sedimentary facies at all localities on both islands (e.g., Tryon et al., 2012, 2014) indicate that the deposits at Nyamita are representative of local environments on Rusinga and Mfangano Islands during the late Pleistocene.

For those samples with $\Delta_{CO3\text{-}OM}$ = +14-17‰, percent carbon and $\delta^{13}C$ value of organic matter are not correlated ($r = 0.07$, $p = 0.78$), but for the samples that have $\Delta_{CO3\text{-}OM}$ values outside of the range of 14-17‰, percent carbon and $\delta^{13}C$ value of organic matter have a weak but statistically significant positive correlation ($r = 0.54$, $p < 0.001$). Additionally, for most of those samples, $\Delta_{CO3\text{-}OM}$ is less than 14‰. One interpretation is that the carbonate $\delta^{13}C$ values are reliable and that degradation of organic matter by soil microbiota shifted organic matter systematically to lower $\delta^{13}C$ values. This requires preferential consumption of isotopically heavy compounds by soil microbiota during degradation, leaving a residue of organic matter with low $\delta^{13}C$ values. Degradation would have to have been completed after the bulk of carbonate precipitated. Under this interpretation, samples with higher carbon content and higher $\delta^{13}C$ values (i.e., greater C_4 biomass) would be closer to pristine than those with lower carbon content and lower $\delta^{13}C$ values. However, early organic matter diagenesis in modern soils enriches residual organic matter in ^{13}C (Wynn et al., 2005; Wynn, 2005), which would lead to a negative correlation between percent carbon and organic matter $\delta^{13}C$ value. Thus, it is possible

that all organic matter $\delta^{13}C$ values are within a couple permil of original soil organic matter values and most carbonate $\delta^{13}C$ do not reflect only soil derived CO_2.

All but three carbonate samples were a mix of very small, distributed nodules and disseminated carbonate within the matrix that could reflect later, non-pedogenic precipitation of cements that could be influenced by the sub-surface hydrology related to the nearby tufa deposits. Additionally, equilibrium fractionation of carbon isotopes during precipitation of carbonate is temperature-dependent, and the enrichment of pedogenic carbonate in ^{13}C relative to source CO_2 is inversely proportional to soil temperature (Deines et al., 1974; Romanek et al., 1992). Thus, for the range of soil temperatures (40-25°C) measured in modern Kenyan soils (Passey et al., 2010), we would expect less enrichment of soil carbonates in ^{13}C than for the temperature range of 25-0° C that is commonly assumed (ca. +7.2 to +9.8‰ vs. +9.8 to +12.4‰, respectively). We do not have independent estimates of soil temperatures for our samples, but many of the samples with $\Delta_{CO3\text{-}OM}$ less than 14‰ may reflect higher than expected soil temperature and actually be reliable for paleoenvironmental interpretation. It is notable in this regard that the samples with high soil organic matter $\delta^{13}C$ values and relatively low carbonate $\delta^{13}C$ values indicate higher proportions of C_4 biomass and therefore less woody cover and shade, which would result in higher soil temperatures.

As there is no simple means to determine whether the pedogenic carbonate or organic matter preserves original isotopic composition, and given that we do not have constraints on soil temperature at the time of carbonate precipitation, the conservative approach

taken here is to consider only those samples from Nyamita (n = 20) for which carbonate and organic matter $\delta^{13}C$ values reflect the expected offset range (14-17‰) for modern soils (**Fig. 5**). To interpret the paleosol carbonate and organic matter carbon isotopic values within the context of modern biomes, we use published $\delta^{13}C$ values from modern tropical soils and the UNESCO classification of African vegetation based on woody cover as well as more commonly used ecosystem classifications (**Figs. 6A and 6B**; White, 1983; White et al., 2010; Cerling et al., 2010, 2011). Of 11 modern tropical ecosystems with soil organic matter $\delta^{13}C$ values within one standard deviation of the mean $\delta^{13}C$ for our samples (after correction to the equivalent modern value), five have are statistically indistinguishable based on Student's t-tests (**Table 3**): dry deciduous forest, woodland, Ethiopian riparian woodland, (riparian) woodland, and shrubland/bushland. From this list, and based on the fluvial character of the Wasiriya and Waware Beds and presence of spring deposits, the most consistent interpretation is that the Rusinga and Mfangano habitats sampled were riparian woodlands. This implies 40-80% woody cover with an open stand of trees and a field layer of grasses (White, 1983).

For the 20 samples which have $\Delta_{CO3\text{-}OM}$ = 14-17‰, the distribution of both organic matter and carbonate $\delta^{13}C$ values indicate dominantly C_3 biomass at Nyamita with a few samples that suggest the presence of a minor C_4 grass component (**Fig. 6C**). These samples include the three carbonate nodules that were larger (although still less than ca. 1 cm in diameter) and distinct enough to be analyzed separately from matrix. However, if we assume that all of the organic matter samples are unaltered, the distribution of the 75 organic matter $\delta^{13}C$ values also indicates a broad, dominantly C_3 mode and a second,

narrower C_4 mode consistent with a temporally or spatially variable woodland and tropical grassland ecosystem. Despite our uncertainty as to the reliability of the carbonate data, the distribution for all 75 paleosol carbonate $\delta^{13}C$ values notably has a similar shape although with a secondary mode that suggests a lower percentage of C_4 grasses at these sites than the secondary mode for the organic matter $\delta^{13}C$ values (**Fig. 6D**).

As the Rusinga and Mfangano faunal community does not have a clear modern analog, it is possible that the ecosystem does not have a single modern analog either. Cerling et al. (2010, 2011) demonstrated that $\delta^{13}C$ values of soil organic matter could be used to estimate percent woody cover for tropical soils (using average end member $\delta^{13}C$ values for C_3 and C_4 biomass of ca. -26.2 and -12.5‰ respectively; see Fig. 1 in Cerling et al., 2010). This method allows for a paleoenvironmental reconstruction that is not dependent on a modern ecosystem analog and indicates an average of 64% woody cover (± 18%) for the 20 samples which have $\Delta_{CO3\text{-}OM}$ = 14-17‰ – a woodland habitat that is consistent with our reconstruction from carbonate and organic matter $\delta^{13}C$ values. Interestingly, we see local variability in paleosol ^{13}C values across the ~1 km Nyamita transect (see **Table 2**), with samples collected above the Nyamita Tuff pointing to an increase in C_3 plant cover towards the spring deposit, suggestive of a moisture gradient influencing local biomass composition.

Mammalian Tooth Enamel: Carbon Isotopes

Tooth enamel $\delta^{13}C$ values are presented in **Figs. 7 and 8**, and are given by specimen with summary statistics for each taxon in **Table 4**. Regardless of which end members are assumed in the linear mixing model, most (≥76%) of the individual mammal specimens sampled consumed > 70% C_4 plants. The different mixing models result in only ~10% variation in the reconstructed amount of C_4 biomass in the diet of each specimen because most individuals consumed such a high proportion of C_4 biomass. For example, *Rusingoryx atopocranion* (mean $\delta^{13}C$ = -0.6‰) is estimated to have consumed 74-86% C_4 plant biomass, depending on the mixing model assumed. The isotopic data confirm that the late Pleistocene fauna is dominated by grazing species, with the only pure C_3 feeder represented by a single *Hippopotamus* specimen from Mfangano Island which exhibited an uncommonly low $\delta^{13}C$ value. Taxa with a predominantly C_4 diet ($\delta^{13}C$ > -1‰; cf. Kingston, 2007; Kingston and Harrison, 2007) account for 87% and 74% of the ungulate specimens sampled from Rusinga and Mfangano, respectively. The abundance of C_4 feeders relative to C_3 browsers or C_3-C_4 mixed feeders implies the existence of an expansive C_4 grassland in the region. Indeed, the relative abundance of C_4 feeders at Rusinga exceeds the proportions observed in modern open habitat areas in Africa, including Ngorongoro, Serengeti, and Lake Turkana (Sponheimer and Lee-Thorp, 2003; **Fig. 9**).

The extinct bovids analyzed from Rusinga and Mfangano show a strong preference for C_4 grasses. For the previously unsampled extinct alcelaphine bovids, *Rusingoryx*

atopocranion and *Damaliscus hypsodon*, the average enamel $\delta^{13}C$ values (-0.6 ± 1.9‰ and -0.2 ± 2.7‰, respectively) demonstrate they were consuming a diet of almost exclusively C_4 grasses, consistent with inferences derived from their morphology (Faith et al., 2011, 2012). A single measurement for the extinct unnamed impala, distinguished from modern *Aepyceros melampus* by its large size and exceptional hypsodonty (Faith et al., 2014, in press), yields a $\delta^{13}C$ value toward the C_4 end member value for tooth enamel (-2.7‰). This is likewise consistent with its dental morphology, although the $\delta^{13}C$ value also falls within the range of observed values of modern impala – a species characterized by exceptional dietary flexibility ranging from C_4 to C_3 dominated diets (e.g., Sponheimer et al. 2003a; Codron et al., 2006) (**Fig. 8**). Our data also include the first isotopic analyses for the extinct giant buffalo (*Syncerus antiquus*; average $\delta^{13}C = 0.5‰$) and giant wildebeest (*Megalotragus* sp.; average $\delta^{13}C = 0.2‰$) from the late Pleistocene of East Africa, with results showing that both consumed at least 80% C_4 plant biomass, consistent with isotopic evidence for these taxa in South Africa (Lee-Thorp and Beaumont, 1995; Codron et al., 2008).

Although the $\delta^{13}C$ values from most of the late Pleistocene taxa sampled in this study fall within the range of their modern conspecifics (**Fig. 8**), the suids in particular suggest a substantial departure from their modern representatives. The bushpig (*Potamochoerus* sp.) sampled from the Wasiriya Beds was consuming an unusually high proportion of C_4-derived foods ($\delta^{13}C = 0.9‰$; 77 to 87% C_4), overlapping with extant warthog (*Phacochoerus*). In contrast, extant *Potamochoerus porcus* from equatorial Africa has a mixed C_3-C_4 diet, although consisting primarily of C_3 plants (mean $\delta^{13}C = -9.4 \pm 5.3‰$),

whereas extant *Phacochoerus aethiopicus* ($\delta^{13}C$ = -0.5 ± 1.2‰) and *Phacochoerus africanus* ($\delta^{13}C$ = -1.4 ± 1.0‰) are grazers and consume diets of pure C_4 biomass (Kingston and Harrison, 2007, Harris and Cerling, 2002). Bushpigs are omnivorous, with preferred plant foods including roots, tubers, bulbs, rhizomes, grasses, berries and fruits (Bishop, 2010). The strong C_4 signal found in these fossil bushpigs further attests to the dominance of C_4 plant species in the environment, and may reflect a greater reliance on C_4 grasses or consumption of C_4 underground storage organs (e.g., Yeakel et al., 2007).

Mammalian Tooth Enamel: Oxygen Isotopes

Using the ES-warthog aridity index regression (from Levin et al., 2006), $\delta^{18}O$ values for the Rusinga and Mfangano Island fauna predict a water deficit (WD) of 974 mm (**Fig. 10**), which is considerably more arid than present day Rusinga Island and nearby Kisumu, (WD = 774 and 562 mm, respectively). Based on our current sample size of isotopic data for fossil mammals, we do not yet have sufficient statistical power to compare this estimate quantitatively to modern values for the region or to values for other late Pleistocene fossil sites. However, the aridity implied by our estimated WD is consistent with previous paleoecological inferences based on the fauna, which also suggest that the surrounding region consisted of habitats that were more arid than present day environments (Tryon et al., 2010, 2012, 2014; Faith et al., in press). Assuming comparable evapotranspiration in the past, the WD of 974 mm implies a 200 mm (>20%) reduction in annual rainfall (to ~820 mm/yr). A drop in annual rainfall of this magnitude would initiate a series of feedback mechanisms leading to a reduction in lake level

(Broecker et al., 1998; Milly, 1999). The estimated reduction in precipitation and lake levels would be even greater if evapotranspiration were lower between 100-33 ka, as is likely under cooler temperatures. A significantly reduced Lake Victoria is also consistent with bathymetric and ecological models suggesting a minimum ~25 m drop in lake level, connecting Rusinga and Mfangano to the mainland at the time of hominin occupation (Tryon et al., 2012, 2014).

Discussion and Conclusion

Regional approaches to reconstructing paleoenvironments typically provide resolution at temporal or spatial scales that exceed those relevant to hominin populations (e.g., Blome et al., 2012). However, the combined evidence here from sediments, fauna, and isotopic analyses of paleosol carbonates and soil organic matter documents both the microhabitats where MSA artifacts and fauna accumulated as well as the broader landscape that would have been exploited by human foragers. Our analyses suggest that the late Pleistocene deposits on Rusinga and Mfangano Islands sample stream- or spring-side woodland settings (64 ± 18% woody cover) within a larger C_4 grassland environment that was drier than today. The dominance of ungulates with a diet of primarily C_4 vegetation provides strong evidence for a substantially greater expansion of C_4 grasslands into equatorial eastern Africa than was previously known. In comparison with ~2 Ma sediments from the nearby site of Kanjera (Plummer et al., 2009), it may be that C_4 grasslands repeatedly expanded and contracted across the Lake Victoria region in relation to Pleistocene climate fluctuations. However, the association of stone tools with the paleosols and

fossils sampled here suggest that, in some cases, humans persisted during intervals of drier conditions with expanded grassland cover rather than migrating into wetter habitats. They did this by exploiting locally closed and well-watered habitats within the larger grassland communities.

The aridity index, although based on limited data, suggests an increased water deficit and as much as a 20% reduction in annual precipitation compared to the region today. As the expanse of Lake Victoria is largely rainfall dependent (Broecker et al., 1998; Milly, 1999; Kendall, 1969), this and other lines of evidence imply a substantial reduction in water level, likely transforming Rusinga and Mfangano into topographic highpoints on a grassland landscape, which would have supported more wooded habitats in an otherwise rich open grassland ecosystem (Tryon et al., 2014).

The association of lake level decline together with the expansion of grasslands across the Lake Victoria basin has also been documented during the Last Glacial Maximum (Kendall, 1969; Talbot and Livingstone, 1989; Talbot et al., 2006), suggesting a general pattern that may have occurred repeatedly during drier phases of the Pleistocene. These environmental changes would have facilitated hominin dispersal between equatorial East Africa and Central Africa by the removal of probable biogeographic barriers, including the lake itself and the equatorial forest belt (reviewed in Faith et al., in press). Genetic evidence for possibly environmentally mediated dispersals during the late Pleistocene is provided by Soares et al. (2012), who document the dispersal of hominin populations from East Africa to Central Africa between 60-35 ka and their dispersal out of Africa

between 70-60 ka. Thus, climatically driven changes in past environments may have played a central role in facilitating hominin dispersals during the late Pleistocene.

Acknowledgments

Research presented here was conducted under research permit NCST/5/002/R/576 issued to Tryon by the government of the Republic of Kenya and an Exploration and Excavation License issued by the National Museums of Kenya. Funding was provided by the National Science Foundation (BCS-0841530, BCS-1013199, BCS-1013108, and BCS-1013134), the National Geographic Society's Committee for Research and Exploration (8762-10), the Leakey Foundation, McKnight Foundation, the Geological Society of America, New York University, Baylor University, the University of Minnesota, and the University of Queensland. We thank Drs. Idle Farah and Emma Mbua for facilitating our research at the National Museums of Kenya, and the British Institute in Eastern Africa and Rusinga Island Lodge for logistical and material support. We are grateful to the many individuals who helped us in the field and laboratory, including Mathew Macharwas, Jared Olelo, Stephen Longoria, Joshua Siembo, Julian Ogondo, Sheila Nightingale, Kirsten Jenkins, Andrew Haveles and Maniko Solheid.

Figures and Tables

Figure 1. Map of Rusinga and Mfangano Islands, Kenya, showing the Pleistocene sediments and the positions of localities mentioned in the text.

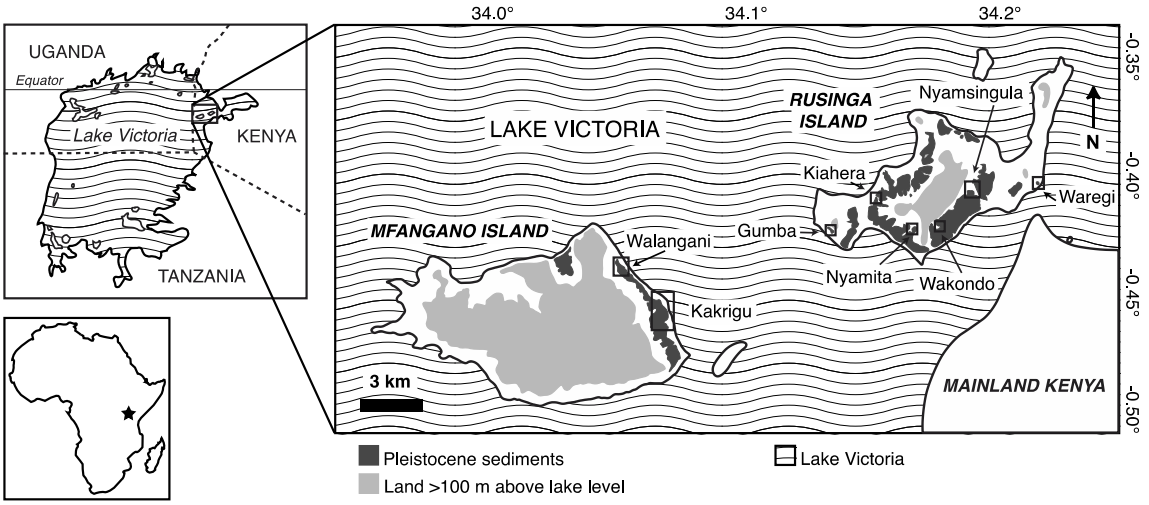

Figure 2. Detailed stratigraphic sections from the Late Pleistocene Wasiriya and Waware Beds on Rusinga and Mfangano Islands. Sections measured at the Wakondo (12.07.09.01) and Nyamita (AV1001, AV1002, AV1003, AV1004, AV1005, AV1006, AV1008, 11.07.09.01, 11.07.09.02) localities from the Wasiriya Beds on Rusinga Island in 2009 and 2010, and stratigraphic section measured at the Kakrigu locality (DP1011) from the Waware Beds on Mfangano Island in 2010. Correlation between stratigraphic sections (indicated by solid line) is based on field observations and geochemical correlations of tephra deposits (Van Plantinga, 2011; Peppe et al., in review). Solid stars are those paleosol samples that fall within the expected enrichment range (+14-17‰ offset in δ13C values of carbonate and organic matter), and open stars are those that fall outside of the expected enrichment range.

FIGURE ON NEXT PAGE

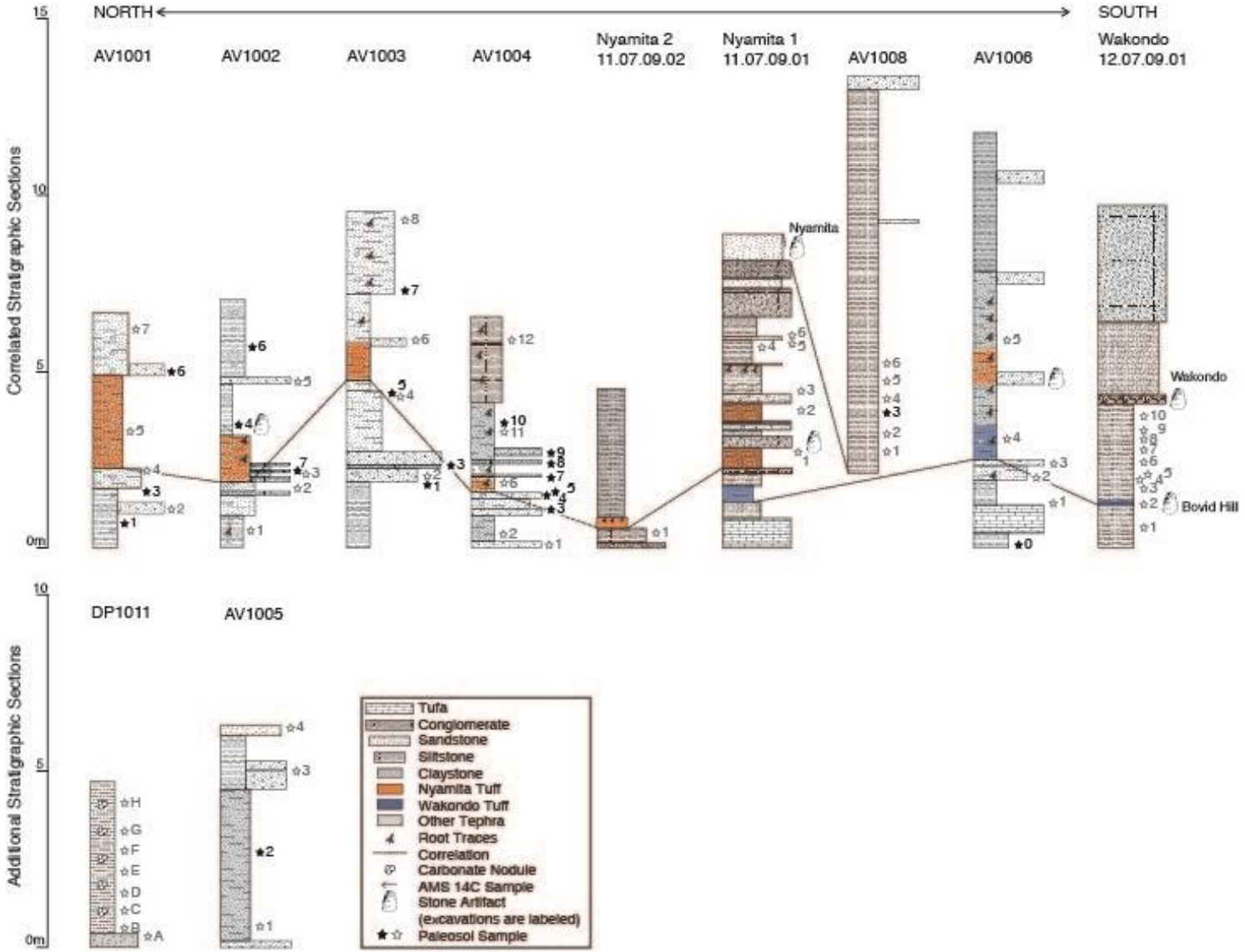
NORTH
SOUTH
AV1001
AV1002
AV1003
AV1004
Nyamita 2
11.07.09.02
Nyamita 1
11.07.09.01
AV1008
AV1006
Wakondo
12.07.09.01
Correlated Stratigraphic Sections
15
10
5
0m
Nyamita
Wakondo
Bovid Hill
DP1011
AV1005
Additional Stratigraphic Sections
Tufa
Conglomerate
Sandstone
Siltstone
Claystone
Nyamita Tuff
Wakondo Tuff
Other Tephra
Root Traces
Correlation
Carbonate Nodule
AMS 14C Sample
Stone Artifact
(excavations are labeled)
Paleosol Sample

Figure 3. Box-and-whisker plot showing variation of artifact densities (per excavated or surface-collected m2) from the early Pleistocene Okote Member of the Koobi Fora Formation of Kenya (Rogers and Harris, 1992; Stern, 1993), the Middle Pleistocene of Olorgesailie, Kenya (Potts et al., 1999) and Maastricht-Bélvèdere, the Netherlands (Roebroeks et al., 1995), and Holocene sediments from Sturt National Park, Australia (Holdaway et al., 1998). Artifact densities from excavations on Rusinga Island (Jenkins et al., 2012; Tryon et al., 2012) are shown for comparison. To reduce spread, all data are log-transformed, with zero values removed. The number of excavations from each locality is shown in parentheses.

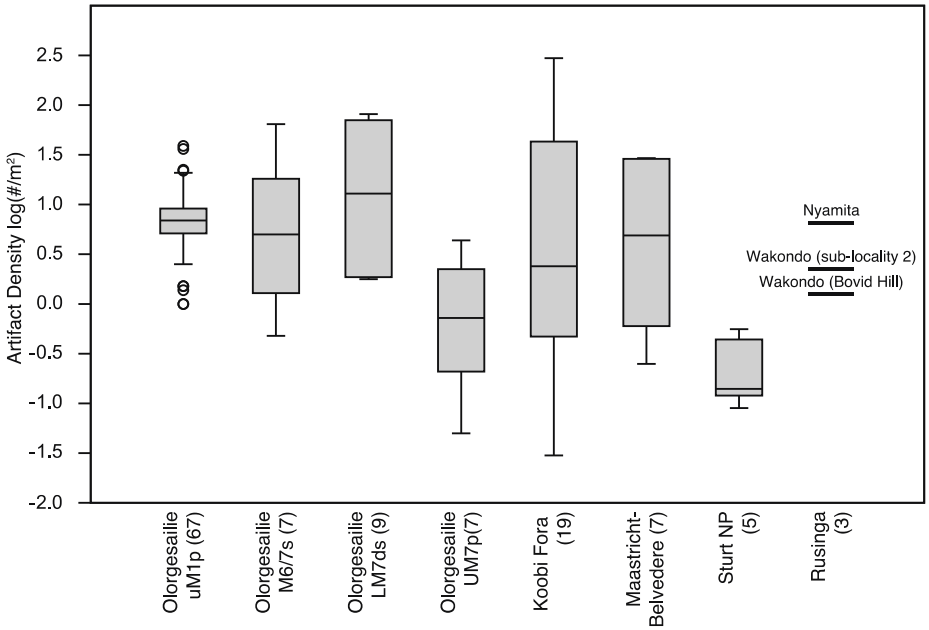

Table 1. Taxonomic list of mammalian fauna from the Wasiriya and Waware Beds as of the 2010 field season. NISP = number of identified specimens.

Taxon	Rusinga Wasiriya	Mfangano Waware
	NISP	NISP
Crocuta crocuta	3	0
Procavia sp.	0	1
Orycteropus crassidens†	1	0
Lepus capensis	0	1
Elephantidae cf. *Loxodonta africana*	1	0
Rhinocerotidae	0	1
Equus quagga	4	1
Equus grevyi	5	0
Equus sp. indet.	11	3
Hippopotamus cf. *amphibius*	4	1
Phacochoerus sp.	9	1
Potamochoerus larvatus	0	1
Taurotragus oryx	2	0
Tragelaphus strepsiceros	1	0
Oryx beisa	3	0
Redunca sp.	11	2
Kobus kob/*Redunca arundinum*	5	1
Connochaetes taurinus	35	3
Megalotragus sp. indet.†	3	0
Alcelaphini cf. *Alcelaphus buselaphus*	11	3
Damaliscus hypsodon†	26	2
Rusingoryx atopocranion†	140	13
Alcelaphini indet.	34	10
Aepyceros sp.†	7	0
Gazella thomsoni	7	2
Antilopini indet.	2	0
Ourebia ourebi	8	3
Oreotragus sp./*Raphicerus* sp.	0	1
Madoqua sp.	0	1
Syncerus caffer	6	2
Syncerus antiquus†	2	3
Bovini indet.	2	1
ΣNISP	343	57

† = *Extinct*

Figure 4. Correlation between tephra deposits on Rusinga and Mfangano Islands. UPGMA dendrogram calculated using the modified Euclidean method, showing the nodes defining each of the two correlated tephra deposits. Correlation figure based on analyses from Van Planting (2011) and Peppe et al. (in review).

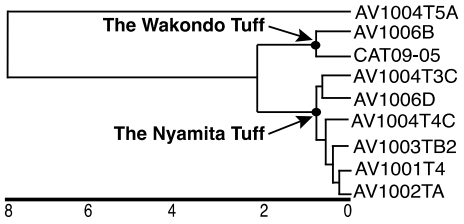

Figure 5. Paleosol carbonate and organic matter $\delta^{13}C$ values. Diamonds are those samples from the Nyamita locality, squares represent samples from the Wakondo locality, and circles represent samples from the Kakrigu locality. Solid symbols are those samples that fall within the expected enrichment range (+14-17‰ offset in δ13C values of carbonate and organic matter), and open symbols are those that fall outside of the expected enrichment range. The shaded area indicates the expected enrichment range. Samples that fall outside this shaded area most likely represent sediments with a significant soil microbiota contribution, carbonates formed under low soil respiration rates, or non-pedogenic carbonates.

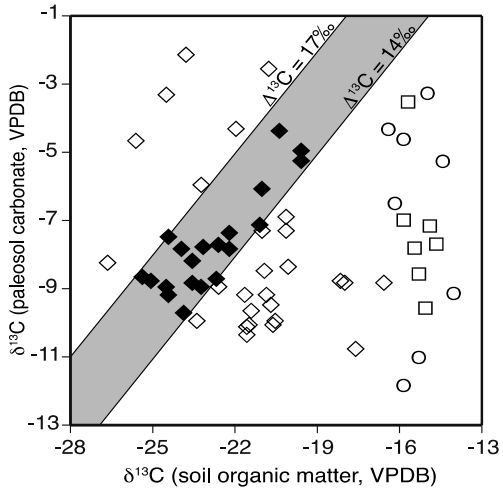

Table 2. Sample ID, corrected paleosol carbonate $\delta^{13}C$ and $\delta^{18}O$ values, SOM $\delta^{13}C$ values, and enrichment value for sediment samples from Rusinga and Mfangano Islands. Paleosol and SOM $\delta^{13}C$ values have been corrected for changes in carbon isotope composition of atmospheric CO_2 (see Methods). Samples for which carbonate and SOM $\delta^{13}C$ values exhibit the expected offset (14-17‰) are in boldface.

	Paleosol Carbonates		SOM	$\Delta^{13}C$
Sample ID	$\delta^{13}C$ (VPDB)	$\delta^{18}O$ (VSMOW)	$\delta^{13}C$ (VPDB)	(SOM-$CaCO_3$)
Wasiriya Beds				
Nyamita Locality				
11.07.09.01.01	-8.89	27.60	-18.06	-9.2
11.07.09.01.02			-20.27	
11.07.09.01.03	-10.21	27.16	-21.65	-11.4
11.07.09.01.04	-9.28	27.68	-20.97	-11.7
11.07.09.01.05	-8.42	27.79		
11.07.09.01.06	-9.40	28.61		
11.07.09.02.01	-8.29	26.46		
AV1001 Sed 1	**-7.85**	**27.13**	**-23.21**	**-15.4**
AV1001 Sed 2	-8.59	26.12	-21.04	-12.5
AV1001 Sed 3	**-9.77**	**26.21**	**-23.98**	**-14.2**
AV1001 Sed 4	-10.02	25.73	-23.49	-13.5
AV1001 Sed 5	-10.15	26.10	-20.67	-10.5
AV1001 Sed 6	**-5.36**	**27.61**	**-19.69**	**-14.3**
AV1001 Sed 7	-8.92	27.01	-16.65	-7.7
AV1002 Sed 1	-9.06	26.79	-22.71	-13.7
AV1002 Sed 2	-8.87	27.63	-18.22	-9.4
AV1002 Sed 3	-7.41	27.32	-21.11	-13.7
AV1002 Sed 7	**-7.78**	**26.53**	**-22.69**	**-14.9**
AV1002 Sed 4	**-8.82**	**27.46**	**-22.79**	**-14.0**
AV1002 Sed 5			-20.57	
AV1002 Sed 6	**-6.13**	**26.81**	**-21.10**	**-15.0**
AV1003 Sed 1	**-5.05**	**26.64**	**-19.67**	**-14.6**
AV1003 Sed 2	-9.54	26.27	-20.75	-11.2
AV1003 Sed 3	**-4.46**	**27.26**	**-20.48**	**-16.0**
AV1003 Sed 4	-6.96	27.96	-20.21	-13.3
AV1003 Sed 5	**-9.01**	**27.01**	**-23.31**	**-14.3**
AV1003 Sed 6	-9.26	27.07	-21.75	-12.5
AV1003 Sed 7	**-7.23**	**28.18**	**-21.21**	**-14.0**
AV1003 Sed 8	-10.83	26.18	-17.66	-6.8
AV1004 Sed 1			-21.75	
AV1004 Sed 2	-8.31	26.82	-26.75	-18.5
AV1004 Sed 3	**-8.29**	**26.81**	**-23.62**	**-15.3**
AV1004 Sed 4	**-8.93**	**26.45**	**-23.67**	**-14.8**
AV1004 Sed 5	**-8.83**	**26.50**	**-25.18**	**-16.4**
AV1004 Sed 6	-3.42	26.50	-24.63	-21.2
AV1004 Sed 7	**-7.59**	**26.61**	**-24.48**	**-16.9**
AV1004 Sed 8	**-7.90**	**26.46**	**-22.29**	**-14.4**
AV1004 Sed 9	**-7.45**	**26.68**	**-22.26**	**-14.8**
AV1004 Sed 11	-10.44	26.16	-21.63	-11.2
AV1004 Sed 10	**-9.02**	**25.87**	**-24.60**	**-15.6**
AV1004 Sed 12	-10.12	27.57	-21.60	-11.5
AV1005 Sed 1	-2.20	26.94	-23.91	-21.7
AV1005 Sed 2	**-8.72**	**27.47**	**-25.47**	**-16.8**
AV1005 Sed 3	-10.03	25.98	-20.64	-10.6

Sample ID	Paleosol Carbonates $\delta^{13}C$ (VPDB)	$\delta^{18}O$ (VSMOW)	SOM $\delta^{13}C$ (VPDB)	$\Delta^{13}C$ (SOM-$CaCO_3$)
AV1005 Sed 4	-9.75	26.73	-21.49	-11.8
AV1006 Sed 0	**-9.29**	**26.77**	**-24.49**	**-15.2**
AV1006 Sed 1	-4.77	27.30	-25.68	-20.9
AV1006 Sed 2	-2.65	27.23	-20.87	-18.2
AV1006 Sed 3	-7.39	27.81	-20.22	-12.8
AV1006 Sed 4	-4.40	26.51	-22.09	-17.7
AV1006 Sed 5	-6.04	26.62	-23.31	-17.3
AV1008 Sed 1			-23.70	
AV1008 Sed 2			-19.65	
AV1008 Sed 3	**-7.93**	**27.89**	**-24.06**	**-16.1**
AV1008 Sed 4	-8.45	27.90	-20.13	-11.7
AV1008 Sed 5			-17.67	
AV1008 Sed 6			-18.08	
Wakondo Locality				
12.07.09.01.01	-8.61	27.84	-15.38	-6.8
12.07.09.01.02			-15.83	
12.07.09.01.03			-13.99	
12.07.09.01.04	-9.61	27.84	-15.16	-5.6
12.07.09.01.05			-15.77	
12.07.09.01.06	-7.74	28.48	-14.73	-7.0
12.07.09.01.07	-7.83	29.20	-15.52	-7.7
12.07.09.01.08	-7.02	27.58	-15.98	-9.0
12.07.09.01.09	-7.24	27.51	-14.98	-7.8
12.07.09.01.10	-3.59	27.82	-15.82	-12.2
Waware Beds				
Kakrigu Locality				
DP1011A	-11.17	25.08	-15.43	-4.3
DP1011B	-11.99	24.92	-15.95	-4.0
DP1011C	-6.63	26.82	-16.26	-9.6
DP1011D	-3.42	26.88	-15.08	-11.7
DP1011E	-4.72	26.86	-15.98	-11.3
DP1011F	-4.46	26.96	-16.48	-12.0
DP1011G	-5.42	25.69	-14.50	-9.1
DP1011H	-9.26	25.84	-14.12	-4.9

Figure 6. Relationships between paleosol carbonate and organic matter $\delta^{13}C$ values from Rusinga and Mfangano Islands and modern soil organic matter samples. The light grey stripe throughout indicates ± 1 SD around the mean paleosol organic matter value for Rusinga and Mfangano based on samples that fell within the expected enrichment range. Notably, a similar construction based on paleosol carbonate samples would yield a nearly identical stripe. (A) Carbon isotope values for modern soil organic matter samples based on UNESCO definitions from Cerling et al. (2011). Bars indicate mean values for modern localities ± 1 SD. (B) Carbon isotope values for modern soil organic matter samples based on commonly used ecosystem definitions from Cerling et al. (2010). Bars indicate mean values ± 1 SD. In both panels, grey bars indicate modern samples that are significantly different from the Rusinga and Mfangano whereas black ones indicate localities that are not significantly different. (C) Histogram of Rusinga and Mfangano paleosol organic matter $\delta^{13}C$ values in 1‰ bins. (D) Histogram of Rusinga and Mfangano paleosol carbonate $\delta^{13}C$ values in 1‰ bins. The paleosol carbonate values are offset by 15‰ (the average expected enrichment value between paleosol carbonate and organic matter $\delta^{13}C$ values) from the soil organic matter values. In panels C and D, the black bars indicate those samples that fall within the expected enrichment range and the dark grey bars indicate the entire sample set.

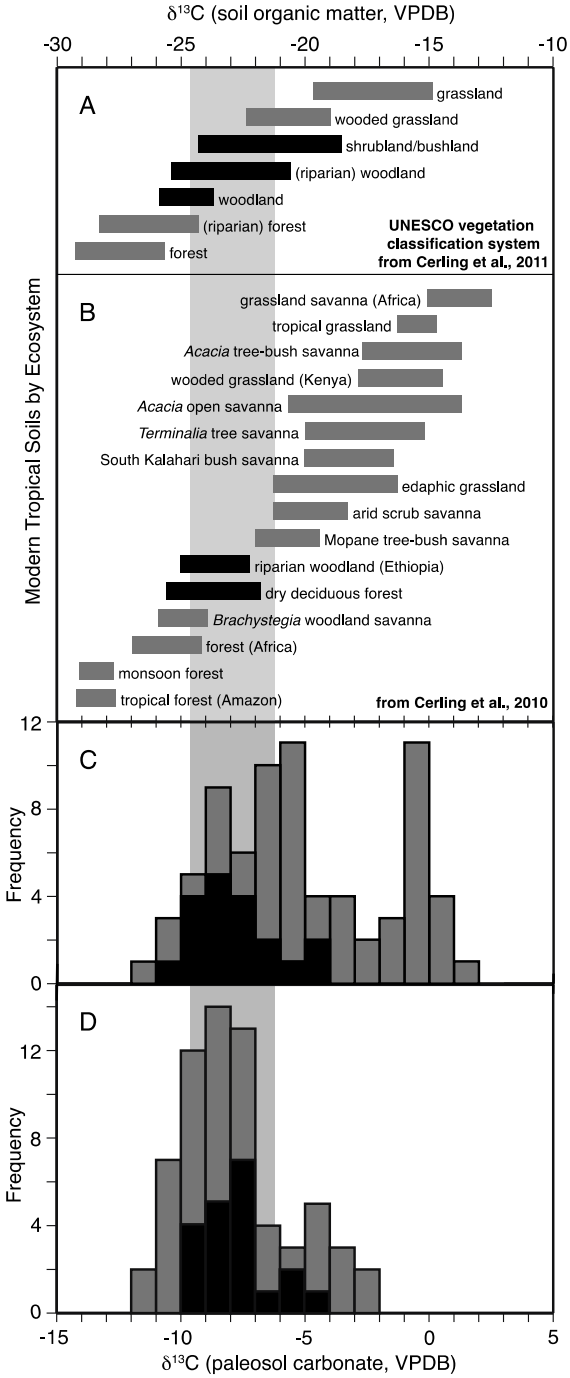

Table 3. Results of Student's t-tests used to compare the eleven modern ecosystems that exhibit a mean value ± 1 SD overlapping within one standard deviation of the Rusinga mean. Bonferroni-adjusted *p*-values are reported, and those that are most similar to the Wasiriya samples (i.e., *not* significantly different) are in boldface.

Ecosystem	$\delta^{13}C$ mean	SD	n	df	t-value	*p*-value
UNESCO Vegetation Classification System from Cerling et al. (2011)						
(Riparian) Forest	-26.2	2.0	4	22	3.45	0.022
Woodland	**-24.7**	**1.1**	**9**	**27**	**2.90**	**0.077**
(Riparian) Woodland	**-22.9**	**2.4**	**3**	**21**	**0.00**	**0.999**
Shrubland/Bushland	**-21.5**	**2.9**	**13**	**31**	**1.75**	**0.999**
Wooded Grassland	-20.6	1.7	11	29	3.60	0.011
Ecosystem classifications from Cerling et al. (2010)						
Brachystegia woodland savanna	-24.9	1	271	289	8.14	<0.001
dry deciduous forest	**-23.7**	**1.9**	**4**	**22**	**0.84**	**0.999**
riparian woodland (Ethiopia)	**-23.6**	**1.4**	**11**	**29**	**1.16**	**0.999**
Mopane tree-bush savanna	-20.7	1.3	44	62	5.69	<0.001
arid scrub savanna	-19.8	1.5	4	22	3.38	0.033
edaphic grassland	-18.8	2.5	8	26	5.03	<0.001

Figure 7. Enamel carbon and oxygen isotope values of fossil mammals from Rusinga and Mfangano Islands. Enamel $\delta^{13}C$ values expressed as modern equivalents based on mean estimated $\delta^{13}C$ value of late Pleistocene atmospheric CO_2 of -6.6±1.0‰ (see text) and modern $\delta^{13}C$ value of -8.0‰. Heavy dashed lines represent expected $\delta^{13}C$ values of enamel for herbivores eating end member diets with mean C_3 and C_4 plant $\delta^{13}C$ values of -27.4 and -12.7‰, respectively; grey boxes indicate one standard deviation around mean values for C_3 and C_4 plants (±1.6 and 1.1‰, respectively). Long dashed line represents the expected enamel $\delta^{13}C$ value for end member C_3 diet under arid conditions (-24.6‰, all plant values from Passey et al., 2002). Percent C_4 is calculated using a linear mixing model: $\delta^{13}C_{(measured)} = xC_4 + (1\text{-}x)C_3$, where x is the percent C_4 and end member $\delta^{13}C$ values are given by C_4 and C_3. We calculated mixing models for five pairs of end members using an apparent enamel enrichment relative to diet of +14.1‰ (Cerling and Harris, 1999): (A) mean C_3 and C_4 plant $\delta^{13}C$ values (i.e., heavy dashed lines), (B) mean C_3 end member shifted positively by one standard deviation (1.6‰) and mean C_4 end member, (C) arid climate C_3 end member (i.e., long dashed line) and mean C_4 end member, (D) arid climate C_3 end member and mean C_4 end member shifted positively by one standard deviation (1.1‰), which is the most conservative model with regards to estimated C_4 percent in diet, (E) arid climate C_3 end member shifted positively by one standard deviation (1.1‰) and mean C_4 end member shifted positively by one standard deviation (1.1‰).

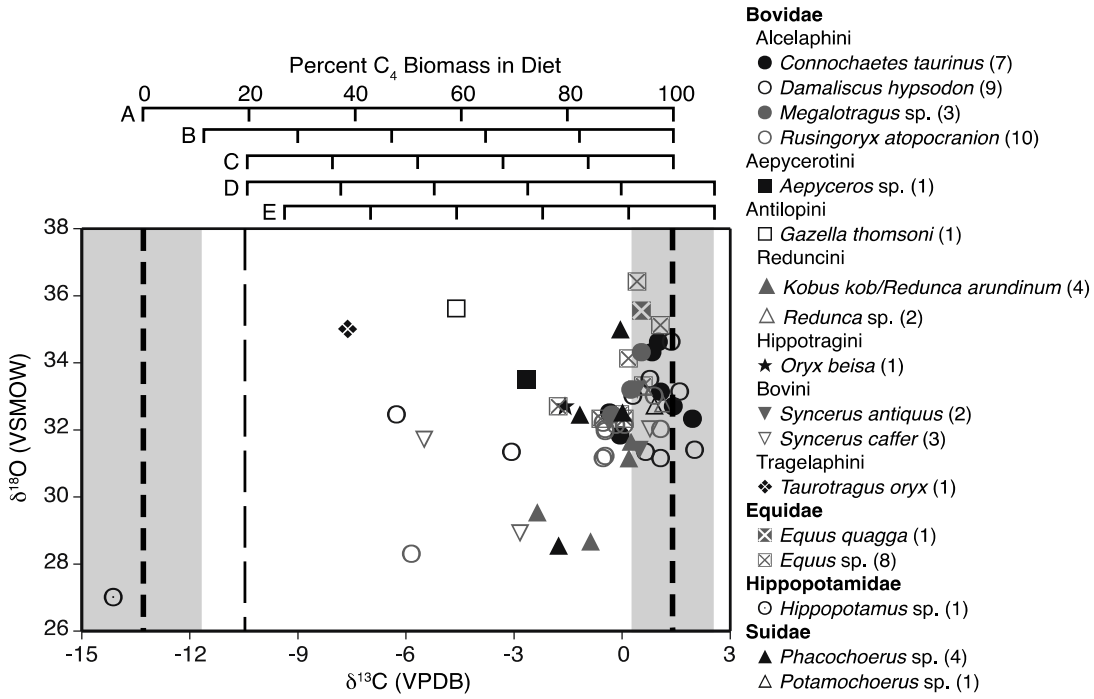

Figure 8. Comparison of fossil mammal carbon isotope values from Rusinga and Mfangano Islands to modern Eastern and Southern African mammals. Solid diamonds are fossil mammals. Open, grey diamonds are modern mammals. Percent C_4 axes are the same as those in **Fig. 7**. Modern data compiled from Kingston and Harrison, 2007, Sponheimer and Lee-Thorp, 2003, Bocherens et al., 1996; Koch et al., 2001; Cerling et al., 2003; Sponheimer et al., 2003b; Cerling et al., 2008; Harris and Cerling, 2002.

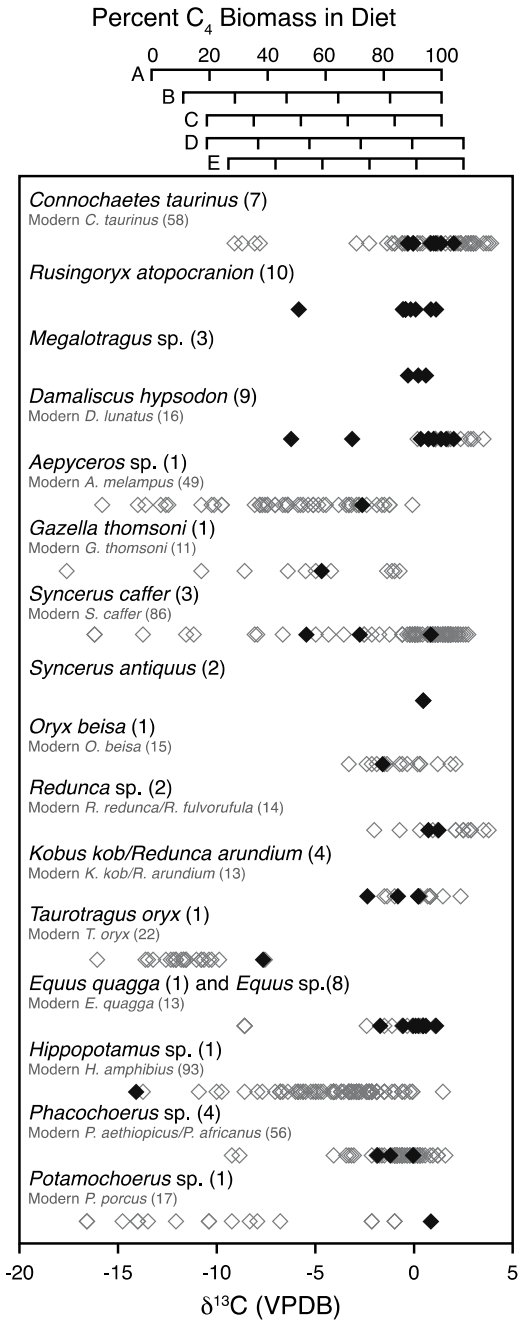

Table 4. Field number, locality, tooth, corrected $\delta^{13}C$ value, and $\delta^{18}O$ value for mammalian enamel samples from Rusinga and Mfangano Islands. Enamel $\delta^{13}C$ values have been corrected for changes in carbon isotope composition of atmospheric CO_2 (see methods). Average and standard deviation are provided for each species. Percent C_4 in diet is calculated for each specimen using the five mixing models discussed in the text (see methods and figure 7). † indicates species that are currently extinct.

	Locality	Tooth	$\delta^{13}C$ (VPDB)	$\delta^{18}O$ (VSMOW)	% C_4 in diet (A)	% C_4 in diet (B)	% C_4 in diet (C)	% C_4 in diet (D)	% C_4 in diet (E)
Bovidae									
Connochaetes taurinus									
1	Waregi	LM2	1.40	32.7	100	100	100	92	91
MFP10-06	Mfangano, no locality	m	-0.10	32.1	90	89	87	80	78
RU2007-421	Nyamsingula	Lm3	1.10	33.1	98	98	97	89	88
RU2008-248	Nyamita	Rm3	1.96	32.3	100	100	100	96	95
RUP10-121	Nyamsingula	Lm3	1.04	34.6	98	97	97	89	88
RUP10-122	Nyamsingula	Lm3	-0.30	32.3	88	87	86	79	77
RUP10-211	Nyamsingula	RM	0.82	34.3	96	96	98	87	86
			0.86±0.8	33.1±1.0	96	96	95	87	86
Damaliscus hypsodon†									
MFP10-04	Mfangano, no locality	Rm3	1.36	34.6	100	100	100	91	90
RU2006-433	Nyamsingula	Rm3	1.61	33.1	100	100	100	93	93
RUP10-139	Nyamsingula	Rm	1.05	31.1	98	97	97	89	88
RUP10-329	Nyamita	RM3	2.04	31.4	100	100	100	96	96
RUP10-335	Nyamita	LM1/2	0.77	33.5	96	95	95	87	85
RUP10-34	Nyamita	Rm3	0.68	31.3	95	95	94	86	85
RUP10-395	Nyamita	LM2	-3.09	31.3	69	66	62	57	53
RUP10-48	Nyamita	Rm3	-6.28	32.4	48	41	35	32	26
RUP10-50	Nyamita	M	0.29	33.0	92	92	91	83	81
			-0.17±2.73	32.4±1.1	89	88	87	79	78

	Locality	Tooth	$\delta^{13}C$ (VPDB)	$\delta^{18}O$ (VSMOW)	% C_4 in diet (A)	% C_4 in diet (B)	% C_4 in diet (C)	% C_4 in diet (D)	% C_4 in diet (E)
Aepyceros sp.†									
RU2009-11			-2.68	33.5	72	69	66	60	56
Rusingoryx atopocranion†									
MFP10-75	Kakrigu	Rm3	-0.55	31.1	89	85	84	77	74
RUP10-240	Nyamsingula	Rm3	-0.47	31.9	87	86	84	77	75
RUP10-303	Wakondo	Lm1	-0.47	31.2	87	86	84	77	75
RUP10-343	Nyamita	RM1	-0.52	32.2	87	85	84	77	75
RUP10-406	Wakondo	Lm1	0.89	33.0	97	96	96	88	86
RUP10-412	Wakondo	m	0.09	32.1	91	90	89	81	80
RUP10-435	Nyamsingula	RM2	-5.83	28.3	51	45	39	36	30
RUP10-47		RM2	1.10	32.0	98	98	97	89	88
RUP2007-364	Nyamsingula	M	-0.19	32.1	89	88	87	79	77
RUW-1A	Wakondo	M	-0.44	32.0	87	86	85	77	75
			-0.64±1.92	31.6±1.3	86	84	83	76	74
Megalotragus sp.†									
RU2009-3			0.54	34.3	94	93	93	85	84
RU2007-361	Nyamsingula	m	-0.31	32.4	88	87	86	78	76
RUP10-332	Nyamita	Lm1/2	0.26	33.2	92	91	90	83	81
			0.16±0.43	33.3±1.0	92	91	90	82	80
Gazella thomsoni									
T1015	Nyamsingula	Lm1/2	-4.63	33.6	59	54	49	45	40

	Locality	Tooth	$\delta^{13}C$ (VPDB)	$\delta^{18}O$ (VSMOW)	% C_4 in diet (A)	% C_4 in diet (B)	% C_4 in diet (C)	% C_4 in diet (D)	% C_4 in diet (E)
Syncerus antiquus†									
MFP10-23	Kakrigu	Lm3	0.48	31.4	94	93	92	84	83
RU2007-410	Wakondo	RM2	0.42	33.2	93	93	92	84	83
			0.45±0.04	33.3±1.3	94	93	92	84	83
Syncerus caffer									
MFP10-41	Walangani	Lm2	-5.48	31.7	53	47	42	39	33
RU2006-142	Gumba	Rm3	0.80	32.0	96	95	95	87	86
RUP10-138	Nyamsingula	Lm3	-2.81	28.9	72	68	65	59	55
			-2.50±3.15	30.9±1.7	73	70	67	62	58
Oryx beisa									
T2000	Nyamsingula	m	-1.53	32.7	80	78	75	69	66
Redunca sp.									
RUP10-351	Nyamita	LM1/2	1.19	32.8	99	98	98	90	89
RUP10-86	Nyamita	Lm3	0.67	33.3	95	94	94	86	85
			0.93±0.37	33.0±0.4	97	96	96	88	87
Kobus kob/*Redunca arundinum*									
MFP10-55	Kakrigu	Lm3	-2.30	29.6	75	72	69	63	60
None	Nyamsingula	Lm1/2	0.28	31.7	92	91	91	83	81
RUP10-116	Nyamsingula	Rm	-0.81	28.7	85	83	81	75	72
RU2007-457	Nyamsingula	Rm	0.23	31.2	92	91	90	83	81
			-0.65±1.21	30.3±1.4	86	84	83	76	74
Taurotragus oryx									
RU2009-6	Nyamita	M	-7.64	35.0	39	31	24	22	15

	Locality	Tooth	$\delta^{13}C$ (VPDB)	$\delta^{18}O$ (VSMOW)	% C_4 in diet (A)	% C_4 in diet (B)	% C_4 in diet (C)	% C_4 in diet (D)	% C_4 in diet (E)
Equidae									
Equus quagga									
RUP10-76	Kiahera	Lm1/2	0.52	35.5	94	93	93	85	83
Equus sp.									
MFP10-40	Kaswanga		0.45	36.4	94	93	92	84	83
MFP10-71	Kakrigu		0.04	32.3	91	90	89	81	79
RU2007-503	Nyamsingula	M	-0.59	32.3	86	85	83	76	74
RU2008-237	Nyamita		0.02	32.5	91	89	88	81	79
RU2009-1174	Nyamsingula		0.58	33.3	94	94	93	85	84
RUP10-137	Nyamsingula	Rm	-1.76	32.7	79	76	73	67	64
RUP10-501	Gumba		0.18	34.1	92	91	90	82	81
RUP10-503	Gumba		1.07	35.1	98	97	97	89	88
			0.00±0.86	33.6±1.5	90	89	88	81	79
Hippopotamidae									
Hippopotamus sp.									
MFP1-0-45	Kakrigu		-12.74	27.0	0	0	0	0	0
Suidae									
Phacochoerus sp.									
RU2007-469	Nyamsingula	m3	-0.01	32.5	90	89	88	81	79
RUP10-154	Nyamsingula		-1.79	28.5	78	76	73	67	64
RUP10-262	Nyamsingula		-0.05	35.0	90	89	88	80	79
RUP11-7	Nyamita		-1.16	32.4	83	80	78	72	69
			-0.75±0.87	32.1±2.7	85	84	82	75	73
Potamochoerus sp.									
T99/124	Nyamsingula	m	0.89	32.7	97	96	96	88	86

Figure 9. The percentage of bovids belonging to the tribes Alcelaphini and Antilopini against the percentage of C4-consuming bovids across 16 modern wildlife reserves (open and closed habitat) and for the Rusinga and Mfangano fossil samples. Open, grey squares are open habitats. Solid, grey squares are closed habitats. Solid, black triangles are fossil sites. Modern data from Sponheimer and Lee-Thorp (2003: **Table 1**).

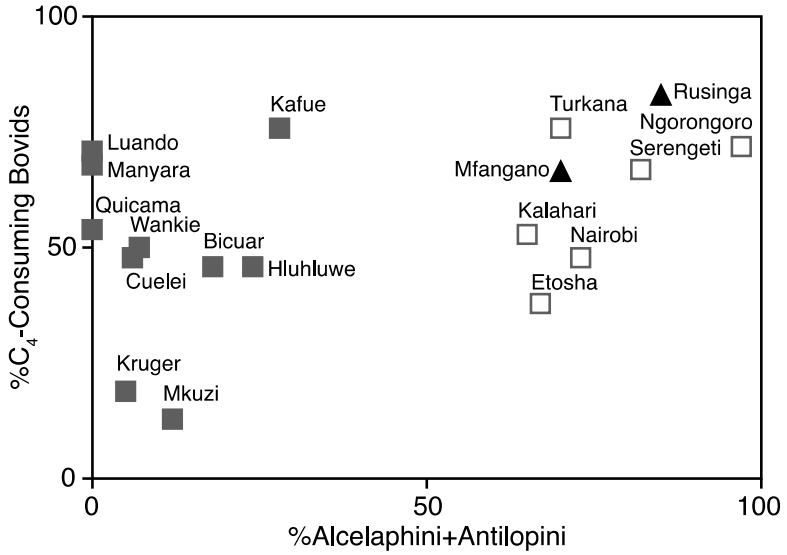

Figure 10. Aridity index data from fossil mammals at Rusinga and Mfangano Islands. The measured ^{18}O enrichment (ε*) between evaporation sensitive taxa (ES; warthogs) and evaporation insensitive taxa (EI; buffalo, Grant's gazelle, and oryx) $\delta^{18}O$ enamel values from Rusinga and Mfangano (open circle) plotted on the regression between water deficit (WD) and ε*ES-EI for extant warthogs (ES animals) and extant EI animals from Levin et al. (2006). The light grey bars indicate the water deficit at some of the east African localities where samples were collected for the regression analysis from Levin et al. (2006). Dark grey bars indicate the water deficit at Rusinga Island and Kisumu calculated following Levin et al. (2006) using climate data obtained from (Hijmans et al., 2005; Zomer et al., 2007).

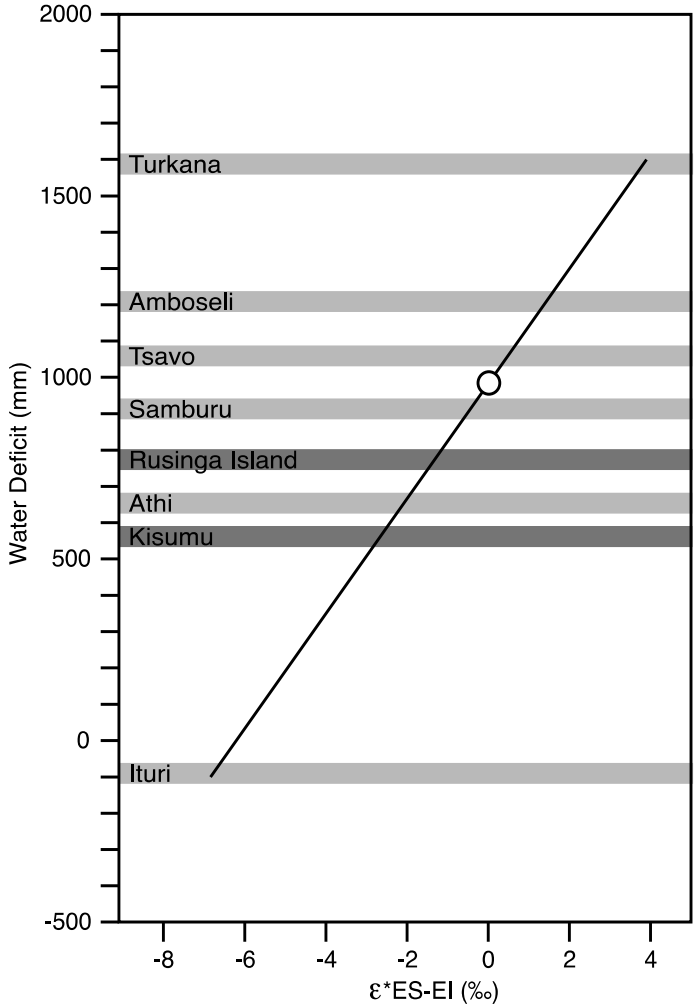

CHAPTER 2: EARLY MIOCENE PALEOENVIRONMENTS OF *EKEMBO* ON RUSINGA ISLAND, KENYA: INTEGRATING BULK SEDIMENTARY ORGANIC AND COMPOUND-SPECIFIC CARBON ISOTOPE ANALYSES OF TERRESTRIAL PALEOSOLS

Chapter Summary

The Miocene was a critical epoch in the evolutionary history of Hominoidea (apes). During this time period, both stem and crown hominoids appear in Africa and the adaptive radiation that shaped these primates is the foundation for our own hominin evolutionary history. The early Miocene deposits on Rusinga Island have produced numerous fossil remains from two species of the early hominoid *Ekembo, E. nyanzae* and *E. heseloni*, as well as many other catarrhine species. Accurately reconstructing the habitats for these early apes, and thus identifying the evolutionary pressures that shaped the adaptive morphologies for these and perhaps all later hominoids, has long been a goal of paleoanthropologists. Here, we present a detailed paleoenvironmental reconstruction from the Hiwegi Formation – the most fossiliferous of the early Miocene formations on Rusinga Island – incorporating data from multiple localities across the island as well as from a densely sampled set of stratigraphic sections, to document the full temporal and spatial range of potential primate habitats present during this ca. 2 million years of deposition. We analyzed the stable carbon isotope composition of bulk sedimentary organic matter and isolated *n*-alkanes and *n*-alkanoic acids and the results document a spatially and temporally dynamic mixture of C_3 habitats ranging from close canopy forests undergoing CO_2 recycling to open or unshaded habitats with plants experiencing light and/or water stress. This analysis demonstrates that the early Miocene primate

community from Rusinga Island was not living in a stable habitat of any type, but rather was able to thrive in a range of habitats for an extended period of hominoid evolutionary history. Additionally, this habitat flexibility exhibited by *Ekembo* may have been an important primitive characteristic for all of Hominoidea.

Introduction

Rusinga Island (0°24'S, 34°0'E; **Fig. 11**), located on the eastern edge of Lake Victoria, is one of the most important early Miocene sites in East Africa because of the exceptional abundance, diversity, and quality of preservation of vertebrate fossils at many fossil localities. The Rusinga Island faunas include a rich fossil primate community, which contains catarrhines, primitive hominoids, and strepsirhines. Identifying the ecological context for the evolution and diversification of these primates, particularly the early members of Hominoidea (our own family), is critical for understanding the relationship between past environmental change and primate evolution as well as the adaptive significance of various primate morphologies. Here we describe the carbon isotope ($\delta^{13}C$[10]) composition of bulk sedimentary organic matter (SOM) and the abundance, distribution, and $\delta^{13}C$ values of biomarkers from the early Miocene Hiwegi Formation on Rusinga Island. Our results indicate the early Miocene on Rusinga Island included a dynamic range of both closed and open habitats (such as forests, woodlands, bushlands/shrublands). These findings suggest the early Miocene primates were

[10] $\delta^{13}C$ values are presented in parts per thousand (permil, ‰), where $\delta^{13}C=(R_{sample}/R_{standard}-1) *1000$, R is $^{13}C/^{12}C$, and the standard is Vienna Pee Dee Belemnite (V-PDB).

generally adapted to a range of habitat types, rather than being specialized, and indicate habitat flexibility may have been a primitive feature for many primates including the early hominoids.

Primate Evolution during the Early Miocene

The Miocene was an interval of major changes in the mammalian faunas and biomes of Africa. In addition to a number of global climatic and tectonic changes that occurred during the Miocene, such as a reduction in atmospheric pCO_2 (Zachos et al., 2001) and the formation of the East African Rift System (Jacobs et al., 2010), there is also a marked faunal turnover in Africa resulting from the contact between Eurasia and the previously isolated African continent (Partridge, 2010). Prior to this event, the endemic African fauna was dominated by Afrotheria, a clade of lineages that evolved on the continent and share an ancient common ancestor, including proboscideans, sirenians, hyradoids (Stanhope et al., 1998; Asher and Sieffert, 2010), as well as by many non-afrothere lineages, including rodents, primates, and anthracotheres (Winkler et al., 2010; Seiffert et al., 2010; Holroyd et al., 2010). The Miocene faunas were noticeably different from the endemic Oligocene mammalian communities, due to the replacement of many endemic taxa by immigrant species or by evolutionary diversification in response to increased competition (e.g., Winkler, 2002; Cote, 2008). Some of the endemic taxa, such as the proboscideans, were able to diversify and expand both within and emigrate out of Africa during this period (Sanders et al., 2010). Although there is some debate as to the role of Asia in primate evolutionary history, specifically an Asian or Afro-Arabian origin for

stem anthropoids (e.g., Godinot, 1994; Beard, 2002; Marivaux et al., 2005; Miller et al., 2005a; Beard, 2005; Rossie and Seiffert, 2006), the African primate record provides the most continuous record with the greatest diversity of anthropoid fossils (Seiffert et al., 2010), and therefore an ideal location to understand the primate adaptive changes at the end of the Paleogene and throughout the Neogene, which laid the framework for the evolution of our own species.

The first members of Catarrhini evolved in Afro-Arabia during the late Eocene and early Oligocene (Andrews, 1985; Fleagle, 1986; Harrison, 1987; Harrison, 2002), and by the early Miocene, stem catarrhines and stem and possibly crown members of both Cercopithecoidea (Old World monkeys) and Hominoidea (apes) were present in Africa (Benefit and McCrossin, 2002; Harrison, 2002; Jablonski, 2002; Andrews and Harrison, 2005; Stevens et al., 2013). *Ekembo hesleoni* and *E. nyanzae*, (formerly classified as *Proconsul*; McNulty et al., 2015), are found exclusively on Rusinga and Mfangano Islands and are perhaps the best known of the early hominoids, as multiple individuals of both sexes have been recovered from the islands and nearly every skeletal element is documented in the fossil record. *Ekembo* exhibits features that directly link it to extant hominoids, including its lack of tail (Ward et al., 1991; Ward, 1997; Ward et al., 1999), and numerous hominoid synapomorphies, including features in the hand (Walker et al., 1993), wrist (Davers and Nakatsukasa, 2015), elbow (Rose, 1988), and ankle (Dunsworth, 2006). New research indicates *Ekembo* shares a high degree of mobility as well as strengthening and stability at the wrist – as indicated by the enlarged and kidney-shaped distal ulnar surface, well-developed indentation on the palmar surface of the

radial styloid process, and deep ulnar fovea – with extant apes (Sarmiento, 1988; Daver and Nakatsukasa, 2015). Although *Ekembo* engaged in quadrupedalism and did not exhibit the shoulder adaptations for suspensory behaviors (suspension, brachiation, orthograde climbing) found in extant hominoids, several postcranial features are indicative of extensive climbing and clambering behaviors. These include the ability for a high degree of hallux flexion and powerful forelimb and hindlimb grasping (Sarmiento, 1983; Langdon, 1986; Rose, 1992; Rose, 1993; Walker et al., 1993; Begun et al., 1994; Rose, 1994; Dunsworth, 2006) and enhanced joint mobility throughout the forelimb (Jenkins, 1973; Rose, 1998) and hindlimb (Rose, 1993; Ward, 1993; Rose, 1994; Ward et al., 1995; Ward, 1997; Bacon, 2001). These features suggest phylogenetic placement near the base of the hominoid clade, making *Ekembo* an excellent model for understanding the origins of orthograde climbing and the other locomotor specializations exhibited by later apes. Placing the species of *Ekembo*, as well as the other primate species with which they are sympatric, within their paleoenvironmental context and identifying the evolution and ecological pressures that shaped their functional anatomy, therefore, is critical for understanding the evolution of later hominoids.

The early Miocene Rusinga Island localities have produced a large collection of the primitive hominoid *Ekembo*, including a dozen partial skeletons and the type specimens of *Ekembo nyanzae* and *Ekembo heseloni* (Leakey, 1943; MacInnes, 1943; Napier and Davis, 1959; Walker and Teaford, 1988; Walker, 2007). Rusinga also preserves remains of the catarrhine primates *Dendropithecus macinnesi* (Andrews and Simons, 1977), *Limnopithecus legetet*, and *Nyanzapithecus vancouveringorum* (Harrison, 2002), as well

as three strepsirhine genera *Komba*, *Progalago*, and *Mioeuoticus* (Drake et al., 1988; Harrison et al., 2010). Although the phylogenetic status of the catarrhine primates is still under considerable debate, particularly that of the *Ekembo* (e.g., Walker, 1997; Harrison, 2010; McNulty et al., 2015), these fossils still provide critical information about the early Miocene catarrhine community. The rich fossil primate community from Rusinga Island is particularly interesting as it has the potential to address issues of niche partitioning among sympatric species, including, in the case of *Ekembo*, congeneric sympatric species.

However, the lack of a clear paleoenvironmental context for these species has hindered our ability to understand fully the behavior and ecology of these important early Miocene catarrhines and also the diverse assemblages of mammals and other vertebrates with which they are associated. Identification of specific adaptive morphologies present in the primates from Rusinga Island is dependent on a reliable understanding of the environmental conditions these animals faced in their habitats.

Climate and Habitats during the Early Miocene

Coinciding with the evolution and early diversification of the hominoids, the early Miocene is characterized by major tectonic and climatic shifts including the expansion of the Antarctic Ice Sheet and the formation permanent glaciers (Flower and Kennett, 1994; Holbourn et al., 2005; Pagani et al., 2011), a reduction in atmospheric pCO_2 (Zachos et al., 2001; DeConto and Pollard, 2003; Pagani et al., 2005; Tipple et al., 2010; Zhang et

al., 2013), the enhancement of the Asian and East African monsoons driven by the accelerations of the Tibetan uplift (Ruddiman, 2007; Zhisheng et al., 2001; Zhang et al., 2015), and global cooling prior to the Mid-Miocene climatic optimum (17-15Ma; Zachos et al, 2001), which was period of global warming coupled with relatively high atmospheric pCO_2 and a decrease in the Antarctic Ice Sheet (Zachos et al., 2001; Foster et al., 2012). The Mid-Miocene climatic optimum was following by a reestablishment of global cooling, reduction in pCO_2, and expansion of the Antarctic Ice Sheet (Zachos et al., 2001).

Perhaps the most dramatic tectonic event, specifically with regard to East Africa, of the Cenozoic was the development of the East African Rift System (EARS); the period of volcanism and extensive rifting throughout East Africa not only resulted in drastic changes in the African landscape, but also played a causal role in local, regional, and global climate change during the Cenozoic (Jacobs et al., 2010). The 6000-km long EARS, which stretches from the Red Sea in the north to the southern tip of Lake Malawi, is directly linked to the expansion of grassland habitats and changes in rainfall patterns resulting in increased aridity throughout East Africa (Sepulchre et al., 2006). By the late Miocene, as a result of these global and regional-scale climatic changes, C_4 grasslands spread across Africa resulting in more modern-like environments. Understanding the impact these global events had on species evolution requires a clear picture of the local habitats as well as evidence for the spatial and temporal variability of those ecosystems. These detailed records will provide a paleoenvironmental context not only for early

hominoid evolution but also a framework for interpreting the behavior and ecology of early Miocene faunal communities.

Early Miocene Records from Rusinga Island

Rusinga Island is a remnant of the early Miocene Kisingiri volcano and its deposits of lavas and volcaniclastic sediments (**Figs. 11A-C**). The Rusinga Group, which are the early Miocene deposits on the island, comprise ca. 300 m of strata, which contains dozens of fossil bearing layers. The first Miocene fossils associated with the Kisingiri volcano were reported in 1909 by R. Chesnaye, and members of the third East African Archaeological Expedition led by L.S.B. Leakey and D.G. MacInnes first explored Rusinga Island in the 1930s. The initial expeditions revealed the fossil deposits on Rusinga contain some of the richest samples of early Miocene floral and faunal communities found throughout East Africa; the exceptional preservations of these fossil layers is mainly due to the volcanic origin, and resulting hyper-alkaline chemistry, of the sediments (Harris and Van Couvering, 1995; Drake et al., 1988). Vertebrate fossils from more than 90 species of mammals, in addition to the multiple primate species, are known from the early Miocene Rusinga Group, which comprises in stratigraphic order, the Wayando Formation, Kiahera Formation, Rusinga Agglomerate, Hiwegi Formation, and Kulu Formation (**Fig. 11**). The Wayando, Kiahera and Hiwegi Formations include numerous poorly to moderately developed paleosols (Van Couvering, 1972; Thackray, 1989; Bestland, 1990; Bestland and Retallack, 1993; Retallack et al., 1995; Bestland and Krull, 1999; Michel et al., 2014).

K-Ar dates from Rusinga Island suggested all fossil mammal sediments were deposited at ca. 17.8 Ma in less than 0.5 million years (Drake et al., 1988). However, renewed research on the Miocene fossil localities on Rusinga Island has provided new insights into the temporal context for these deposits. Following a re-interpretation of the Rusinga Group formation stratigraphy, Peppe et al. (2009) estimated the age of the Kulu Formation to be ~17-15 Ma. New $^{40}Ar/^{39}Ar$ incremental heating analyses of biotite plus magnetostratigraphic analyses indicate most of the fossiliferous deposits within the Wayando and Hiwegi Formations are 20-18 Ma (Peppe et al., 2011a; Peppe et al., 2011b; McCollum et al., 2013).

Prior paleoenvironmental reconstructions for the early Miocene sediments on Rusinga Island have indicated habitats ranging from closed forests, woodland, or rainforest, mosaic habitats of both open and closed habitats, and even semi-arid environments (see **Table 5**). These various habitats would imply drastically different contexts for the mammalian fauna and notably for the selective pressures on the locomotor adaptations of the two sympatric species of Ekembo. However, many of these paleoenvironmental reconstructions lump more than one fossil locality, and in some instances more than one formation, which makes interpreting them exceptionally difficult. The prior inaccuracies in fossil site groupings and locality identification within formations may be the cause of the often conflicting Rusinga habitat reconstructions (see Peppe et al., 2009).

A majority of the fossils recovered from Rusinga Island have come from several localities within the Hiwegi Formation. **Fig. 12** illustrates the geochronology of the Hiwegi Formation, which comprises in stratigraphic order, the Kaswanga Point Member, Grit Member, Fossil Bed Member and Kibanga Member. Historically, all of the paleontological and paleoenvironmental studies of this formation have considered these fossil sites to be contemporaneous and treated the deposits as synchronous (e.g., Van Couvering, 1972; Bestland et al., 1995). New magnetostratigraphic analyses document a series of reversals throughout the formation indicating the fossil localities do not represent a single, short, synchronous interval (McCollum et al., 2013). As such, these fossil collections and subsequent paleoenvironmental reconstructions, which were provenienced by locality, are now clearly time-average multiple separate fossil-bearing units.

Recent paleoenvironmental reconstructions from the Hiwegi Formation have been undertaken to consider the proper temporal and geological context and have identified multiple different habitats within this formation. For example, at the oldest Hiwegi Formation fossil localities at near Kaswanga Point (R5), which are dated to ~18.5 Ma, the presence of a large accumulation of crocodiles (*Brochuchus pigotti*) and fluvial sedimentary features is suggestive of riverine habitats (Conrad et al., 2013). The presence of fossil Hippopotamidae and Rhinocerotidae in this same fossil layer may suggest open habitats, although that invokes assumptions of taxonomic uniformitarianism. Maxbauer et al. (2013) described 12 dicot morphotypes, two monocot morphotypes, and two distinct dicot fragments, from a site stratigraphically near but

below the R5 vertebrate locality, which suggest this riparian environment had a strongly seasonal, warm climate and included a mixture of woodland and forested biomes. Similarly, at the youngest of the Hiwegi Formation vertebrate localities discussed within, R3, Michel et al. (2014) documented the presences of an *in situ* fossil forest. The density of tree stumps on the exposed stratum plus percent whole margin and leaf area analyses of the fossil leaves found in association suggest this was an extremely dense close-canopied tropical seasonal forest. *Ekembo* has been recovered from both of these Hiwegi Formation localities, and the stem catarrhine *Dendropithecus* has also been recovered from the R3 locality. This discovery of these catarrhine primates within the R3 tree stump layer definitively places them within a forested environment. However, their association with more open habitats, as has been interpreted for R5 (Andrews et al., 1979), may indicate at least some of the early hominoids were able to persist in a variety of habitats. Open habitat use is found among modern apes (see Pruetz and Bertolani, 2009), and may indicate habitat flexibility is a primitive ape characteristic rather than a modern development (see Andrews, 2015).

Prior paleoenvironmental reconstructions using SOM carbon isotope composition from the Hiwegi Formation resulted in $\delta^{13}C$ values that indicated C_3 plants from a sub-humid or semi-arid climate (i.e., water stressed conditions; Bestland and Krull, 1999; Forbes et al., 2004). However, these studies did not correct measured $\delta^{13}C$ values either for short-term anthropogenic or long-term natural changes in the $\delta^{13}C$ value of atmospheric CO_2, which would lead to an overestimate of water or light stressed C_3 vegetation and bias their reconstruction toward a more arid or semi-arid C_3 habitat.

To help further resolve the Rusinga Group paleoenvironments, we present here a paleoenvironmental reconstruction integrating both bulk sedimentary organic and compound-specific carbon isotope analyses of terrestrial paleosols from throughout the Hiwegi Formation including the Kaswanga Point (R5), Nyamsingula (R2), and Waregi (R1 and R3) localities to further clarify our understanding of the range of habitats present within this ~2 million year formation and associated with fossil primates and other early Miocene mammals.

Materials and Methods

Carbon Isotope Composition of Bulk Soil Organic Matter

The primary basis for using stable carbon isotope composition of sedimentary organic matter as a paleoenvironmental proxy is the well-established differences in fractionation of carbon isotopes during fixation of atmospheric CO_2 by plants using different photosynthetic pathways. Plants using the C_3 photosynthetic pathway (Calvin-Benson; trees, shrubs, and cool growing season grasses) strongly discriminate against ^{13}C during fixation of CO_2 and so have low $\delta^{13}C$ values relative to atmospheric CO_2 (modern C_3 mean: -27.4 ± 1.6‰; O'Leary, 1981, Passey et al., 2002; Cerling et al., 2003; Kohn, 2010; Diefendorf et al., 2010). Among C_3 plants, gymnosperms (woody trees) are more ^{13}C enriched than angiosperms (flowering plants, includes flowering trees and C_3 grasses; Chikaraishi and Naraoka, 2003). C_4 plants (Hatch-Slack or Kranz; warm growing season

grasses and sedges) discriminate less strongly against ^{13}C and have $\delta^{13}C$ values closer to atmospheric CO_2 (modern C_4: -12.7 ± 1.1‰; O'Leary, 1981, Passey et al., 2002; Cerling et al., 2003; Kohn, 2010; Diefendorf et al., 2010).

Although there is evidence that C_4 plants evolved during the Oligocene and therefore may have been present in East Africa by this time (see Sage, 2004; Christin et al., 2008; Vicentini et al., 2008; Edwards et al., 2010; Sage et al., 2011; Christin and Osborne, 2014), most evidence indicates these plants would have been extremely rare, if at all present, and therefore did not contribute to the overall biomass or $\delta^{13}C$ value of paleosols until later in the Miocene (Kingston et al., 1994). It is often assumed that C_3 ecosystems are limited to woody or forested environments, however ~85% of all plant species (97% of extant terrestrial species) utilize the C_3 photosynthetic pathway including open-habitat plants such as shrubs and a number of temperate grass species (e.g., wheat, rye, and Kentucky bluegrass; Jacobs et al., 1999). C_3 grasses evolved near the K-T boundary and pollen evidence suggests open habitats with C_3 grasses spread throughout the world before the evolution of C_4 photosynthesis (Bonnefille, 1995; Jacobs et al., 1999; Kellogg, 2001; Christin et al., 2013). The expectation for the early Miocene on Rusinga Island is a pure C_3 ecosystem, regardless of how open or closed those habitats were or the relative percentages of C_3 grasses and woody plants. Identifying a modern analog for the pure C_3 ecosystems present during the early Miocene is difficult. Although North American grasslands north of 45°N latitude are dominated by C_3 species, these may still contain some C_4 grass species (Teeri and Stowe, 1976; Stowe and Teeri, 1978; Ehleringer et al.,

1991; Tieszen et al., 1997; Sage et al., 1999). Similarly, in extant C_3 dominated forest ecosystems, C_4 sedges are common understory plants.

Variation in the carbon isotopic composition of C_3 plants is primarily driven by environmental factors and can be utilized as a paleoenvironmental proxy; this variation is particularly important in a C_3-only ecosystem. Photosynthetic recycling of isotopically light respired CO_2 in closed forests results in ^{13}C depleted plant tissues and lower than average $\delta^{13}C$ values to plant tissues (the canopy effect; van der Merwe and Medina, 1991). In contrast, light and water stress in open habitats results in physiological and biochemical responses from the plants to prevent excess water loss, decreasing carbon isotope fractionation during fixation of CO_2, resulting in more ^{13}C enriched tissues and higher than average $\delta^{13}C$ values (Ehlringer and Cooper, 1988; Cerling and Harris, 1999). For example, modern drought-stressed C_3 plants, all dicots, collected from Mpala reserve had a mean bulk $\delta^{13}C$ value of -24.6 ± 1.1‰ (*n*=15; Cerling and Harris, 1999; Passey et al., 2002).

Bulk SOM generally preserves the isotopic composition of the overlying plant biomass (Balesdent et al., 1993; Tieszen et al., 1997). However, variable contributions of leaves and roots to SOM and decomposition of organic matter by soil biota can lead to enrichment in ^{13}C of older and more recalcitrant organic matter at depth in soils by several permil relative to standing biomass (Hobbie and Werner, 2004; Wynn, 2007). In addition to inputs from the plant component of soil biomass, the total organic component

can include carbon derived from microorganisms, which can shift the $\delta^{13}C$ values from that of the overlying vegetation (Koch, 1998).

Carbon Isotope Composition of Isolated Biomarkers

Long, straight-chain (i.e., normal or *n*-) alkanes and alkanoic acids are major components of the protective epicuticular waxes that coat the leaf surface of almost all land plants. These biologically specific compounds or biomarkers are can be persistent in sediments over geologic time and retain the carbon isotopic composition incorporated during biosynthesis (Eglinton and Hamilton, 1967; Freeman and Colarusso, 2001; Schefuss et al., 2003). Because these compounds are generally resistant to biodegradation, they serve as an exceptional proxy for ancient vegetation in terrestrial or terrigenous sediments. While biomarker approaches have been commonly utilized on both marine and lacustrine sediments (e.g., Huang et al., 1999; Feakins et al., 2005), the utility of compound-specific isotope analysis from terrestrial sediments is now being recognized (Zech et al., 2012; Agrawal et al., 2014).

Alkanes are organic compounds composed exclusively of carbon and hydrogen molecules and single bonds; alkanes are often referred to as saturated hydrocarbons because they have only C–C and C–H bonds. Alkanes are considered straight-chained or normal (*n*-) if the carbon molecules are connected in a row rather than branching. Alkanoic acids are a specific type of carboxylic acid, which are organic compounds that contain a carboxyl group (C(=O)OH). In the case of alkanoic acids, the carboxyl group is

single bonded to an alkane and straight-chained (i.e., normal or *n*-) alkanoic acids have only single bonds and do not contain any branches. The general formula for these and other hydrocarbons is C_x, where *x* refers to the number of carbon atoms in the molecule (i.e., C_{21} *n*-alkane has a chain of 21 single-bonded carbon atoms with hydrogen atoms single-bonded along the entire length).

The presence (or absence) of specific alkanes and alkanoic acids in a substrate can provide valuable information about the source of the organic compounds. C_{27}-C_{33} *n*-alkanes with a predominance of homologues with odd over even chain lengths and C_{26}-C_{32} *n*-alkanoic acids with a predominance of even over odd chain lengths are diagnostic of a terrestrial higher plant leaf wax source (Eglinton and Hamilton, 1967; Kolattukudy, 1969). In contrast, predominance of short-chain *n*-alkanes (C_{15}, C_{17}, C_{19}) and *n*-alkanoic acids (C_{16} and C_{18}) is indicative of algal or cyanobacterial source (Han et al., 1968; Gelpi et al., 1970) and aquatic plants have C_{23} and C_{25} *n*-alkanes in abundance (Baas et al., 2000; Ficken et al., 2000). The soil carbon preference index (CPI; following Marzi et al., 1993) is a common method of quantifying chain length predominance and is widely used for interpreting the source of biomarkers from lacustrine and marine sites (e.g., Feakins et al, 2007). However, processes contributing to CPI values measured in paleosol samples are as yet poorly understood and require further study, most likely owing to the fact that current studies have focused on plant CPI values rather than the soils/paleosols. The relative abundance of long-chained *n*-alkanes can also be informative of the type of plants from which the leaf waxes originated; for example, C_3 and C_4 grasses have a higher abundance of the longer chained *n*-alkanes (C_{33} and $C_{31} > C_{29}$) relative to the

abundances found in C_3 tree (angiosperms) species; C_3 woody trees have the highest abundances for the long chained *n*-alkanes (C_{35} and C_{31}; Rommerskirchen et al., 2006). For these reasons, as well as the fact that their concentrations in C_3 and C_4 plants are the most similar, the C_{31} *n*-alkane and C_{30} *n*-alkanoic acid are often the focus of isotopic analysis (for example, Uno et al., 2016) although all of the compounds can provide paleoenvironmental information.

Measuring the carbon isotope ratios of specific biomarkers allows for the analysis of carbon that was unambiguously derived from terrestrial plants, eliminating the confounding influence of other carbon sources on the composition of bulk sedimentary organic matter (Collister et al., 1994). *n*-Alkanes from C_3 plants are ^{13}C depleted by approximately 4‰ (observed range is 1-10‰) relative to the bulk plant tissue and therefore the bulk soil organic matter (Collister et al., 1994; Chikaraiski and Naraoka, 2001; Conte et al., 2003). Similarly, relative to bulk plant tissue values, *n*-alkanoic acids from C_3 plants were ~5‰ depleted, resulting in a ~1‰ difference between *n*-alkane and *n*-alkanoic acid homologues (Conte et al., 2003). This relationship between corresponding organic compounds is consistent regardless of photosynthetic pathway (C_3, C_4, and CAM) and C_3 plant types (angiosperms and gymnosperms; Chikaraishi and Naraoka, 2007). Based on this depletion between biomarkers and bulk plant tissues, the *n*-alkanes and *n*-alkanoic acids from C_3 plants range from approximately -25 to -45‰ and an approximate range of -19 to -25‰ for C_4 plant *n*-alkanes and *n*-alkanoic acids (see Feakins et al., 2007; Garcin et al., 2014). Importantly, similar to the pattern seen in bulk SOM samples, *n*-alkanes from C_3 angiosperms (mean $\delta^{13}C$: -36.1±2.7‰; Chikaraishi and

Naraoka, 2003) are depleted in ^{13}C relative to those from C_3 gymnosperms (mean $\delta^{13}C$: -31.6±1.7‰; Chikaraishi and Naraoka, 2003).

Magill et al. (2013) used the $\delta^{13}C$ values for the C_{31} *n*-alkane to estimate fraction of woody cover using the UNESCO classification of African vegetation. Using published data from plants and soils at a variety of xeric and tropical localities, Magill et al. (2013) found that C_{31} is ^{13}C depleted by ~9‰ relative to SOM in both C_3 and C_4 plants (although for different reasons). This allowed Magill et al. (2013) to extend the estimation of woody cover fraction using SOM $\delta^{13}C$ values (Cerling et al., 2011) to C_{31} *n*-alkane $\delta^{13}C$ values.

Paleosol Sampling and Laboratory Analytical Techniques

Paleosol samples for bulk soil organic matter (SOM) analyses were collected from eleven stratigraphic sections of the Hiwegi Formation at the Waregi (R1), Nyamsingula (R2), and Kaswanga Point (R5) localities of Rusinga Island during the 2009 field season. The Hiwegi Formation includes the Grit/Kaswanga Point Member, the Fossil Bed Member, and the Kibanga Member (see **Figs. 11-12**). The samples from Nyamsingula (R2) and Kaswanga Point (R5) are from the Grit/Kaswanga Point Member of the Hiwegi Formation. The Hiwegi Formation at Waregi (R1) includes all three members; those samples below the "marker bed" have been traditionally considered the Grit Member, and above the Fossil Bed Member. Pedogenic features, such as carbonate nodules and slickensides, are present in the numerous poorly to moderately developed Hiwegi

Formation paleosols. Paleosol samples were crushed and homogenized in a ceramic mortar and pestle. Approximately 5-50 mg of sample (depending on organic content) was loaded into 5x9 mm Ag capsules and reacted *in situ* with 1M hydrochloric acid in a PTFE tray with 6x6 mm wells on a 60°C hotplate until the reaction ceased to eliminate any carbonates. The samples were then allowed to dry fully on the hotplate or in a 60°C drying oven. The Ag capsules were wrapped in Sn capsules to facilitate complete combustion. Following combustion in a Costech ECS 4010 elemental analyzer, the carbon isotopic composition of the resulting CO_2 was measured using Thermo Delta V+ isotope ratio mass spectrometer and normalized by in sequence analyses of a laboratory standard (UCSC Pugel or UM Kansas soil). Analytical precision for all measured values is better than 0.1‰ based on repeated analyses of the laboratory standards and acetanilide supplied by Costech. All bulk isotope analyses of R1, R2, and R5 paleosols were completed at the University of Minnesota Stable Isotope Lab.

Paleosol samples for SOM analyses were collected from the Kibanga Member of Hiwegi Formation at Waregi (R3) during the 2011 field season. Two additional samples from stratigraphically equivalent deposits at Waregi (R1) and Nyamsingula (R2) were also collected during 2011. Samples for analyses of soil organic matter were crushed in a porcelain mortar and pestle. Approximately 70 to 90 mg of samples were loaded in silver capsules and treated in situ with 10% HCl on a hot plate at 50ºC. This method was repeated until visible reaction ceased. Samples were then loaded in a Costech elemental analyzer connected to a Thermo Delta V isotope ratio mass spectrometer via a Thermo Scientific Conflo IV interface. Replicate analyses of an in-house standard were run with a

standard error of <0.04‰. All bulk isotope analyses of R3 paleosols were completed at Baylor University.

A subset (*n*=20) of the largest paleosol samples collected for SOM analyses from R1, R2, and R5 in 2009 were selected for compound-specific (*n*-alkane and fatty acid) carbon isotope analyses and were crushed and homogenized in a ceramic mortar and pestle. Due to the sandy and friable nature of the paleosols, solvent rinsing was not possible prior to crushing. Total lipids were extracted (TLE) from~50-200 g of crushed and homogenized paleosol sample with a Dionex ASE-350 using 9:1 dichloromethane/methanol (v/v). Excess water was removed from the TLE with a sodium sulfate column by elution with 4 mL of dichloromethane when necessary. The TLE was separated with a silica gel column (Sigma-Aldrich, 70-230 mesh, 60 Å pore size) by elution with 4 mL each of hexane (aliphatic), dichloromethane (ketone/ester), and methanol (acid/polar). The acid/polar fraction was further separated with an aminopropyl column by elution with 4 mL each of 2:1 dichloromethane/isopropanol (neutral compounds), 4% acetic acid in diethyl ether (v/v, acidic compounds), and methanol (polar, non-acidic compounds). The acid fraction was transesterified using 95:5 methanol/acetyl chloride (v/v) at 60°C for at least 2 hours, producing fatty acid methyl esters, which were further separated with a second silica gel column by elution with 4mL each of hexane, dichloromethane (free *n*-alkanoic acid esters), and methanol (hydroxyl alkanoic acid esters). The purified *n*-alkanes (aliphatic fraction) and *n*-alkanoic acids were quantified and identified using a gas chromatograph equipped with mass selective detector (GC-MSD) and a flame ionization detector (GC-FID) and the isotope

analyses were performed using a continuous-flow isotope ratio mass spectrometer. All extractions and compound-specific isotope analyses were completed at the Organic Geochemistry Laboratory at Lamont-Doherty Earth Observatory of Columbia University.

The fundamental source of carbon in plant tissues is atmospheric CO_2; therefore, to make quantitative interpretations of any carbon isotope data, long-term and historical changes in the isotopic composition of atmospheric CO_2 must be considered. The 2014 mean monthly carbon isotope composition of atmospheric CO_2 was -8.4‰ as measured at Mauna Loa, although it has been steadily decreasing since then. The $\delta^{13}C$ of atmospheric CO_2 has varied by several permil over geologic time due to natural changes in the global carbon cycle (Leuenberger et al., 1992; Zachos et al., 2001; Gröcke, 2002; Tipple et al., 2010) and has been decreasing over the last 200 years due to the addition of ^{13}C-depleted CO_2 from fossil fuel combustion (the Suess effect; Friedli et al., 1986; Marino and McElroy, 1991). The $\delta^{13}C$ value for atmospheric CO_2 from 18-20 Ma was estimated as -6.0±0.2‰ using $\delta^{13}C$ and $\delta^{18}O$ values of the benthic foraminifera genus *Cibicidoides* from Deep Sea Drilling Project (DSDP) site 607 (Zachos et al., 2001; Zachos et al., 2008) and the atmospheric CO_2 $\delta^{13}C$ reconstruction method of Tipple et al. (2010). To allow for comparison to modern published datasets, we chose an approximate average value for modern atmospheric CO_2 value of -8.0‰ based on sample/publication dates ranging from the 1980s through the 2010s (Keeling et al., 2001). We have corrected our measured $\delta^{13}C$ values from Rusinga Island to the equivalent value under the modern atmosphere using the difference between our estimated early Miocene $\delta^{13}C$ value and the modern value (2.0‰).

Carbon Isotope Results and Interpretations

Carbon Isotope Composition of Bulk Soil Organic Matter

Tables 6-7 and Figs. 13-16 show the $\delta^{13}C$ vales for the paleosol SOM samples; the $\delta^{13}C$ values of all of these paleosols samples fall within the range expected for a pure C_3 ecosystem. The oldest paleosol samples come from contemporaneous Hiwegi Formation deposits at Kaswanga Point (R5), Nyamsingula (R2), and the Grit Member at Waregi (R1; i.e., stratigraphically below the "marker bed") and date to approximately 18.5 Ma. The $\delta^{13}C$ values for these 21 roughly contemporaneous SOM samples range from -23.5 to -31.5‰ (mean: -28.0 ± 2.4‰); seven fall within one standard deviation of the modern mean for C_3 vegetation, six have $\delta^{13}C$ values indicate water or light stressed C_3 vegetation, and eight have $\delta^{13}C$ values that indicate CO_2 recycling in a closed canopied environment. This suggests a high degree of variability within the ecosystems and habitats that included a temporally and/or spatially dynamic mixture of forest, woodland and more open habitats (such as shrublands, bushlands, or woody grasslands). Plant macrofossils from these same deposits indicate a strongly seasonal, warm climate, which included a mixture of woodland and tropical forested biomes (Maxbauer et al., 2013); the sedimentology indicates deposition by fluvial processes, which is corroborated by the presence of a large accumulation of crocodiles (Conrad et al., 2013).

The next set of paleosol samples are from the Fossil Bed Member at Waregi (R1), and are stratigraphically younger then the samples from Kaswanga Point (R5), Nyamsingula (R2) and Grit Member (i.e., below the marker bed at R1) deposits. The Fossil Bed Member is an extremely fossil rich unit of the Hiwegi Formation and has produced numerous specimens of proboscideans (*Deinotherium* and cf. *Archaeobeledon*), rhinocerotids, and primates (including *Ekembo*). Seven lateral sections of the Fossil Bed Member that are stratigraphically below the "Rhino Quarry" fossil site were measured and sampled (see **Figure 16**) in addition to one main long section through the entire Hiwegi Formation at Waregi (R1), which included samples from the Grit and Kabanga Members not included within the Fossil Bed Member set discussed here.

The $\delta^{13}C$ values for the 89 SOM samples of the Fossil Bed Member at Waregi (R1) range from -20.0 to -33.5‰ (mean: -27.9 ± 1.8‰); fifty-nine (~66%) of these samples fall within one standard deviation of the modern mean for C_3 vegetation with only nine samples indicating water or light stressed C_3 vegetation, and 21 indicating CO_2 recycling in a closed canopied environment. The isotopic data from the Fossil Bed Member indicate a heterogeneous landscape of forested, woodland, and more open habitats similar to those from the older samples at Kaswanga Point, Nyamsingula, and the Grit Member at Waregi (R1), and there does not appear to be any spatial trend in overall ecosystem composition. This type of heterogeneous (open and closed) mixture of purely C_3 biomes does not exist in modern equatorial Africa today, as the open tropical areas are dominated by C4 species, although this type of heterogeneous mixture of C_3 forest, woodland, and prairie/grassland habitats can be found in the northern Great Plains (Sage et al., 1999;

Nordt et al., 2008; von Fischer et al., 2008). Although the northern Great Plains may be a suitable analog for the heterogeneous habitat structure present on Rusinga during the early Miocene, C_4 plants are still present in these high latitude ecosystems. There are no extant pure C_3 ecosystems to use as an analog for both the ecosystem composition and habitat structure.

There does appear to be a slight trend towards increased open habitats in the youngest samples from the Fossil Bed Member (top ~1m of sections). Five of the nine SOM samples that indicate water or light stressed C_3 vegetation come from the stratigraphically highest SOM samples in the Fossil Bed Member, and there are no SOM samples with $\delta^{13}C$ values indicating closed canopied forests from this portion of the Fossil Bed Member. This suggests that the most closed forested habitats were gradually lost and replaced by woodlands and more open habitats during deposition of the Fossil Bed Member at Waregi, although the overall habitat remains a heterogeneous mixture of ecosystems.

The remaining six SOM samples from the Hiwegi Formation at Waregi (R1) are from the Kibanga Member; these samples are stratigraphically below the fossilized forest recently documented from the Hiwegi Formation at Waregi (R3; see Michel et al., 2014). The $\delta^{13}C$ values for these six samples range from -19.1 to -30.2‰ (mean: -24.1 ± 4.2‰) and contain three relatively ^{13}C enriched paleosol samples. There is a chance that these three samples (12.07.09.02.14, 12.07.09.02.15a, 12.07.09.02.15b; **Table 6**) were contaminated by modern roots or vegetation as these samples were collected at the top of a hill from

close to the modern surface. As these samples indicate the same trend towards more open environments suggested by the top ~1m of the Fossil Bed Member samples, it is plausible that they represent a real shift in habitat openness before a shift back towards ecosystems including more closed forested habitats at the top of this section.

The final set of paleosol samples was collected in 2011 and all but two come from the Kibanga Member of the Hiwegi Formation at Waregi (R3), which is stratigraphically above the major fossil bearing layers at Waregi (R1). The other two samples come from stratigraphically equivalent paleosols at R1 and Nyamsingula (R2). In this same paleosol layer at R3, calcified tree stump and roots casts were recovered. Fossil leaves were collected from the overlying sandstone layer; these macrobotanical remains indicate the paleosol layer contained a close-canopied tropical seasonal forest (see Michel et al., 2014).

The $\delta^{13}C$ values for 23 paleosol samples from this fossilized forest paleosol layer range from -23.7 to -27.8‰ (mean: -25.7 ± 1.1‰); thirteen of these samples fall within one standard deviation of mean modern C_3 vegetation, and the remaining ten samples are more ^{13}C enriched indicating water or light stressed C_3 pants. Surprisingly, none of these samples have $\delta^{13}C$ values that indicate CO_2 recycling in a closed canopy forest. Modern water stressed plants have a mean $\delta^{13}C$ of -24.6 ± 1.1‰ (Cerling and Harris, 1999; Passey et al., 2002), and 9 of the fossil forest layer paleosol $\delta^{13}C$ values exhibit this level of ^{13}C enrichment. However, this level of water stress is unlikely in the close-canopy forest indicated by the density of tree stump cases found in this same paleosol layer

(Michel et al., 2014). An alternative explanation for the somewhat enriched values could be an abundance of gymnosperms in this forest, as woody trees are more ^{13}C enriched than C_3 angiosperms (Chikaraishi and Naraoka, 2003), however the macrobotanical remains from the sandy layer directly overlying this paleosol does not support this (Michel et al., 2014). Another possible explanation for the depleted $\delta^{13}C$ values in this layer is the presence of C_4 sedges (Cyperceae). Sedges can be found among forest understory plants and based on molecular clock estimates, first evolved the C_4 photosynthetic pathway as early as 19.6 Ma (Besnard et al., 2009). However, alone, neither of these explanations is wholly adequate. Future compound-specific isotope analyses from sediments in and around the fossil forest layer may help clarify the discrepancy between isotope and botanical data.

Carbon Isotope Composition of Biomarkers

One major factor with compound specific stable isotope analysis of plant biomarkers in terrestrial sediments is contamination by modern plants. Modern roots may penetrate deeply into sediments, and organic compounds may leach into sediments and can be transported large distances by water. A subset (n=20) of the paleosol samples collected for SOM analyses from R1, R2, and R5 in 2009 were selected for compound-specific (*n*-alkane and fatty acid) carbon isotope analyses based purely on size (i.e., only the largest samples were chosen with no other considerations). Five of these paleosol samples may have sources of modern contamination; two samples (12.07.09.02.13 and 12.07.09.02.15a) had modern roots infiltrating the layer nearby, two samples

(12.07.09.02.17 and 16.07.09.01.04) had modern vegetation within 1m of sample, and one sample (17.07.09.01.12) had potentially modern carbonates based on field observations. One method of testing for contamination is compound specific radiocarbon dating, which will show whether or not contamination has occurred within the last ~45 kyr. Although this type of test would not establish whether or not abundance data or $\delta^{13}C$ values for the biomarkers were contaminated at any other time, it is most likely that contamination would be due to recent erosion bringing the paleosols into close proximity with modern soils and vegetation. However, compound specific radiocarbon dating was cost prohibitive for this small pilot study; therefore the five paleosol samples with the potential for contamination should be interpreted with caution and, although the $\delta^{13}C$ values are presented in **Table 8**, the values are not used here in our paleoenvironmental reconstruction. One additional paleosol sample (16.07.09.01.01) was too small for isotopic analysis leaving 14 total paleosol samples available for *n*-alkanoic acid composition and isotopic analyses.

Low CPI values (1.4-4.3 over C_{28}-C_{34}) for the *n*-alkanoic acids (see **Table 8**) may indicate a non-terrestrial plant origin such as an additional bacterial source for the long-chain *n*-alkanoic acids, however, the low CPI values may also be the result of early diagenesis. The low organic content of paleosols and relatively old early Miocene age supports diagenesis as the cause for these values. As stated above, CPI values in soils generally, and paleosols specifically, are poorly understood and require further study. The good agreement (~1‰) between $\delta^{13}C$ values of *n*-alkane and corresponding *n*-alkanoic acid supports terrestrial plant origin for the biomarkers, and offers additional support to

the hypothesis that the low CPI values are the result of diagenesis and not due to non-plant source contamination.

The $\delta^{13}C$ values for the *n*-alkanoic acids from the 14 paleosol samples range from -22.9 to -34.8‰ (see **Table 8**). The $\delta^{13}C$ values of *n*-alkanoic acids falls within the range of those for measured modern C_3 ecosystems, including the Lethbridge grassland, a C_3 dominated prairie from Alberta, Canada (Conte et al., 2003). The relatively equivalent C_{28}-C_{34} *n*-alkanoic acid abundance found in the Rusinga paleosol data is similar to that observed in the C_3 prairie species by Conte et al. (2003), and may suggest a similarly open habitat during the early Miocene, although more samples are needed to support this argument.

Only four of the paleosol samples had *n*-alkane abundances high enough for carbon isotope analysis of the *n*-alkanes. These *n*-alkane samples exhibited the odd/even chain length preference through C_{27}-C_{33} indicative of terrestrial vegetation; all four samples also showed a large unresolved complex mixture (UCM) hump indicative of diagenesis, and may simply be due to the sample age; additional analyses of relatively geological old paleosol samples will help to resolve the origin of the UCM hump. The $\delta^{13}C$ values for the *n*-alkanes (C_{27} to C_{35}) from these four samples range from -29.6 to -34.5‰ (**Table 8**). Magill et al. (2013) used the $\delta^{13}C$ values for the C_{31} *n*-alkane to estimate fraction of woody cover using the UNESCO classification of African vegetation; applied to the four *n*-alkane samples measured here ($\delta^{13}C$ values of -32.3 to -33.3‰), the early Miocene ecosystem was a woodland with at least 40% woody plant cover and an understory of

grasses, herbs, or sedges (see also White, 1983). The $\delta^{13}C$ values for the four early Miocene C_{27}-C_{35} *n*-alkanes is more ^{13}C depleted than extant C_3 angiosperm trees and grasses ($\delta^{13}C_{27\text{-}35}$ mean: -35.6 ± 2.1‰ and -35.6 ± 3.1‰ respectively) and falls within the range of that measured for extant C_3 gymnosperms ($\delta^{13}C_{27\text{-}35}$ mean: -30.9 ± 1.3‰; Rommenskirchen et al., 2006). The abundance and $\delta^{13}C$ values from the *n*-alkanes and *n*-alkanoic acids support the paleoenvironmental reconstructions based on the bulk SOM $\delta^{13}C$ values indicating a heterogeneous landscape with both closed forest and open woodland or bush/shrubland habitats and indicates the need to further consider C_3 gymnosperms as important components of the overall early Miocene biomass.

Discussion and Conclusions

The early ape *Ekembo* provides an exceptional model for understanding the paleoenvironmental pressures that shaped early hominoid evolution. As the early Miocene is a period of major transition – due to major global climatic and tectonic events that result in major ecological and faunal turnover – it is important to identify the local habitats and ecosystems that shape the framework for this evolution.

The deposits on Rusinga Island provide an ideal site to reconstruct early Miocene paleoenvironments; there is an extensive collection of early Miocene mammalian fauna present in the fossil deposits consisting of more than 100 vertebrate species including a large collection of multiple catarrhine species (*Ekembo*, *Dendropithecus*, *Limnopithecus*, and *Nyanzapithecus*). The diversity of mammalian orders represented in the collection as

well as the overall quantity and quality of preservation makes the Rusinga fossil fauna the best comparative collection for East African Miocene paleobiology.

It is often assumed that the pure C_3 ecosystems present throughout Africa prior to the evolution and expansion of C_4 grasses were closed forested ecosystems. This assumption is fundamental to the savanna hypothesis, which states that hominins diverged from other hominoids as they moved out of the forests and into the open grasslands, facing evolutionary pressures that led to bipedality, stone tool production, and a number of other adaptations (e.g., Darwin, 1871; Dart, 1925; Bartholomew and Birdsell, 1953; Robinson, 1954; Jolly, 1970; Laporte and Zihlman, 1983; Hill and Ward, 1988; Andrews, 1992).

The carbon isotope ($\delta^{13}C$) composition of bulk sedimentary organic matter (SOM) and the abundance, distribution, and $\delta^{13}C$ values of biomarkers presented here indicate the early Miocene Hiwegi Formation on Rusinga Island comprised a heterogeneous landscape, which included a spatially and temporally dynamic mixture of both open and closed habitats such as forests, woodlands, and woody grasslands. Within this mosaic C_3 ecosystem, the $\delta^{13}C$ values also hint at the presence of gymnosperms, although further evidence is needed to support this interpretation. Our results indicate that early Miocene primate habitats, at least at the Rusinga Island localities, were not exclusively the closed-canopy forests that the majority of extant hominoids inhabit today.

When other fossil ape localities from the greater region are considered, a heterogeneous landscape is not extraordinary. The paleoenvironmental reconstructions from the early

Miocene Tinderet primate sites support more closed-canopy forest habitats (e.g., Nesbit Evans et al., 1981; Andrews et al., 1997), but those from the other sites indicate more open C_3 habitats, such as at Karungu on eastern shore of Lake Victoria in Kenya (Andrews et al., 1979; Nesbit Evans et al., 1981) and Moroto in eastern Uganda (Andrews et al., 1997). This indicates the dynamic and heterogeneous landscape represented at Rusinga Island may be typical of some of the early Miocene East African hominoid habitats and therefore played an integral role in primate evolution. Andrews (2015) argues that the ability to thrive in highly seasonal tropical woodland habitats is what may have allowed hominoids to spread into Asia and Europe during the Miocene.

Repeated eruptions by the Kisingiri volcano may have directly contributed to the heterogeneous nature of the local habitats and may as well explain the conflicting nature of previous paleoenvironmental reconstructions. Disturbances caused by volcanic eruptions and the resulting fire, tephra deposits, and/or increased soil alkalinity may not have impacted the landscape in a uniform way, resulting in a mosaic of ecological effects and succession patterns (Heinselman, 1973; Denslow, 1980; Turner and Bratton, 1987; del Moral and Wood, 1993; Miller and Urban, 1999). Repeated eruption of the Kisingiri volcano may have acted to maintain the heterogeneous and dynamic nature of the landscape, constantly compounding the temporal and spatial succession of the local and regional habitats. Additionally, the carbonatitic and hyperalkaline nature of the Kisingiri volcano can produce sedimentary strata that have signals of mock aridity (i.e., the effects of volcanism can mimic aridity and xeric environmental conditions), leading to the possible misinterpretation paleoenvironmental proxies (Harris and Van Couvering, 1995).

Finally, past paleoenvironmental reconstructions, especially those that combined or averaged multiple localities, should be reconsidered in light of the dynamic nature of volcanically driven successional ecosystems indicated at Rusinga Island. The isotopic results from the Kibanga Member at Waregi (R1 and R3) highlights the dynamic nature of the early Miocene habitats with the presence of a fossilized forest which, based on the light/water stressed isotope signal from the paleosols, may have been short lived. With spatial or temporal averaging, the presence of a true close-canopy forest separate from more open habitats may have been confused with either a heterogeneous landscape or a woodland-type habitat.

The placement of Rusinga Island hominoids within spatially and temporally varied habitats indicates they were able to cope and even thrive in this dynamic landscape by inhabiting both closed and open habitats. The adaptations for extensive climbing and clambering capabilities seen in *Ekembo* may have been a biological adaptation to environmental and ecosystem fluctuations, suggesting habitat flexibility may be a primitive characteristic for all hominoids.

Figures and Tables

Figure 11. Map of fossiliferous Miocene strata on Rusinga and Mfangano Islands, Kenya, in Lake Victoria. Generalized geologic map of fossiliferous formations on Rusinga Island (A). Major fossil localities and collection sites are indicated (adapted from Van Couvering, 1972; B). Stratigraphy of Miocene strata on Rusinga Island (C). Figure modified from Peppe et al., 2009.

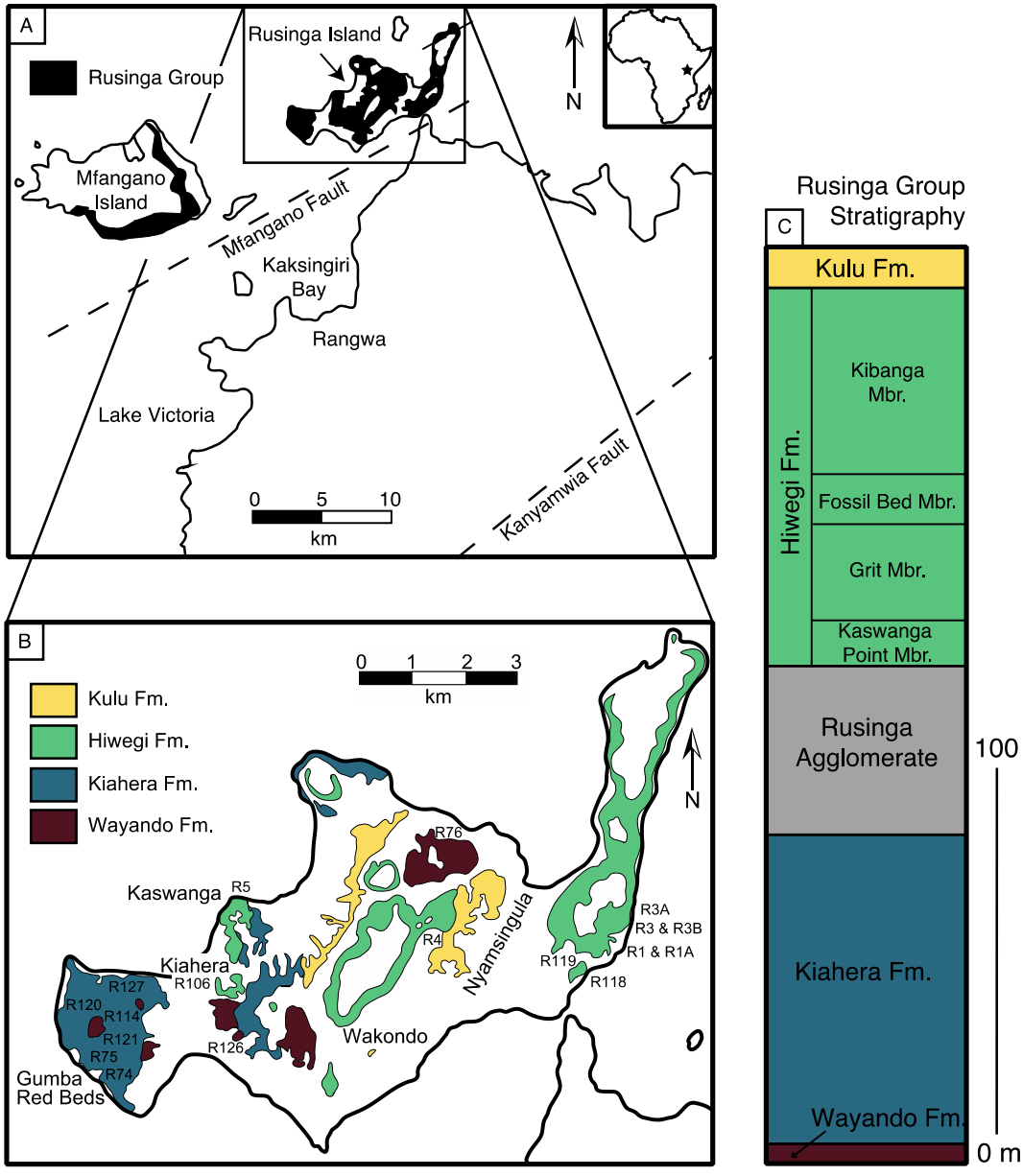

Figure 12. Geochronology of the Hiwegi formation. Summarized geochronological sequence of the Hiwegi formation on Rusinga Island depicting the paleomagnetism results (see McCollum et al., 2013) as well as the location of fossiliferous sediments, fossilized leaves, and approximate locations of paleosol samples. Figure from original provided by Daniel J. Peppe.

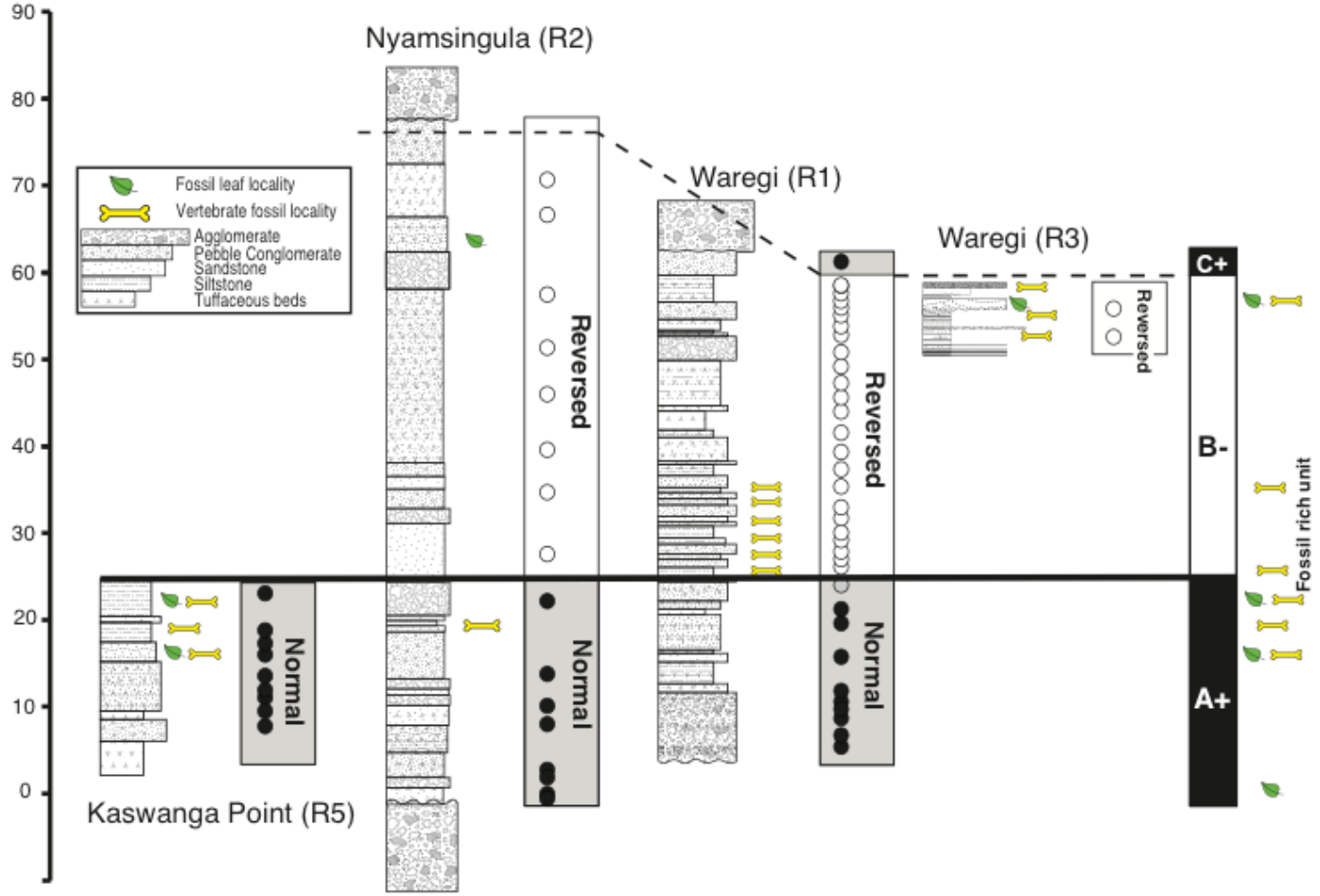

Table 5. Early Miocene Rusinga Island Paleoenvironmental Reconstructions.

Site	Publication	Methodology	Original Environmental Reconstruction	Vegetation Type
	Chesters, 1957	Analysis of fruits and nuts obtained during Leakey expeditions	Tropical forest with abundant lianas suggesting a riverine forest	Forest
	Andrews and Van Couvering, 1975	Faunal indicator species and reanalysis of Chesters (1957) plant materials	Lowland evergreen forest; waterside conditions, perhaps with associated forest	Forest
Hiwegi; R5	Andrews et al., 1979	Analysis of ecological diversity of fossil mammalian assemblages	Forest community with some similarity to floodplain communities (mixed-source)	Forest
Hiwegi; R5	Nesbit Evans et al., 1981	Faunal indicator species, habitat spectra, taxonomic habitat indices, ecological spectra, socio-ecology	Forest	Forest
Hiwegi, Kiahera	Pickford, 1983	Terrestrial gastropod assemblages	Dry forest	Forest
Hiwegi; R117	Collinson, 1985	Fossil plant remains including fruits, nuts, twigs, wood and bark fragments	Disrupted forest or woodland edges with a high proportion of shrubs and woody climbers	Forest or woodland/bushland/ thicket/shrubland
	Pickford, 1985	Terrestrial gastropod assemblages	Dry forest to woodland communities with 80-100% tree cover	Forest
Hiwegi; Kibanga Member	Thackray, 1989	Analysis of paleosols including XRD analysis and associated invertebrate fossils	Humid climate with seasonally dry conditions; mid-successional forest with an open canopy (possibly grasses on forest floor) with areas of more dense forest (and more moist climates)	Forest or woodland/bushland/ thicket/shrubland
Kiahera	Bestland, 1990; Bestland and Retallack, 1993	Paleosol analysis including XRF and atomic absorption studies	Dry woodland or grassy, shrubby woodland; drier climate and more open vegetation	Woodland/bushland/ thicket/shrubland or wooded grassland
Hiwegi; Kibanga Member	Thackray, 1994	Presence of fossil bee nests	Sub-humid to humid climate; angiosperm dominated vegetation with dense or shade-providing habitats	Forest or woodland/bushland/ thicket/shrubland

Site	Publication	Methodology	Original Environmental Reconstruction	Vegetation Type
Hiwegi; R106	Retallack et al., 1995	Paleosol analysis including analysis of major and trace elements and molecular weathering ratios	Mosaic of well-drained colonizing forest, riparian woodland, and dry forest, with local less well-drained areas under wooded grassland or grassy woodland, riparian woodland, and floodplain grassy woodland	Forest or woodland/bushland/ thicket/shrubland or wooded grassland
Hiwegi; Waregi, R1, R122, R107	Retallack et al., 1995	Leaf margin size and shape	Modern dry tropical forest or woodland, but not rain forest or dry wooded grassland	Forest or woodland/bushland/ thicket/shrubland
	Andrews et al., 1997	Analysis of fauna specifically primate locomotor adaptations	Woodland habitats	Woodland/bushland/ thicket/shrubland
	Bestland and Krull, 1999	Carbon isotopic composition of soil organic matter	Semi-arid (water stressed) paleoclimatic conditions; pure C_3 vegetation	Unknown
	Retallack, 2002	Analysis of paleosols and associated primate fauna	Gallery woodland with well-drained floodplain forest; possible lowland, seasonally wet, wooded grassland	Forest or woodland/bushland/ thicket/shrubland or wooded grassland
Wayondo, Hiwegi, and Kiahera	Forbes et al., 2004	Carbon isotopic composition of soil organic matter	Comparable with modern humid (Wayondo) to sub-humid/semi-arid (Hiwegi and Kiahera) temperate, or sub-tropical environments; pure C_3 vegetation	Unknown
Hiwegi; R117	Collinson et al., 2009	Fossil plant remains	Flora is dominated by woodland tree species and climbers with little evidence of forest species; trees, shrubs, lianas and climbers present	Woodland/bushland/ thicket/shrubland
	Ungar et al., 2012	Tragulid dental microwear	Tragulid microwear consistent with lowland forests with mixed open/closed or wet/dry habitats; tragulids were mixed feeders indicating both browse and graze available	Forest or woodland/bushland/ thicket/shrubland

Site	Publication	Methodology	Original Environmental Reconstruction	Vegetation Type
Hiwegi; R5	Maxbauer et al., 2013	Fossil plant remains	Riparian environments that supported woodland and forest environments	Forest or woodland/bushland/ thicket/shrubland
Hiwegi; R3	Michel et al., 2014	*in situ* fossil forest and associated plant remains	Forest	Forest

The specific formation and/or location for each of the Rusinga Island sites has been noted whenever provided in the publication. The vegetation type is based on the UNESCO definitions from White, 1983. "Unknown" is used when the paleoclimatic reconstruction does not include or allow for an ecological reconstruction.

Figure 13. Summary of Hiwegi Formation geology and SOM analyses. R3 Kibanga Member, R1 Fossil Bed Member, and R1, R2, and R5 Grit Member SOM $\delta^{13}C$ values presented as box-and-whisker plots, with whiskers extending to maximum and minimum values. SOM $\delta^{13}C$ values are grouped by generalized stratigraphic position, with all R1 Fossil Bed Member samples presented together and all R1, R2, and R5 Grit Member samples presented together. The circles indicate the R1 Kibanga Member SOM samples, with open circles indicating the three values that may have modern plant contamination, and the closed circles indicating the remaining samples. Geology and stratigraphy image from original by Daniel J. Peppe.

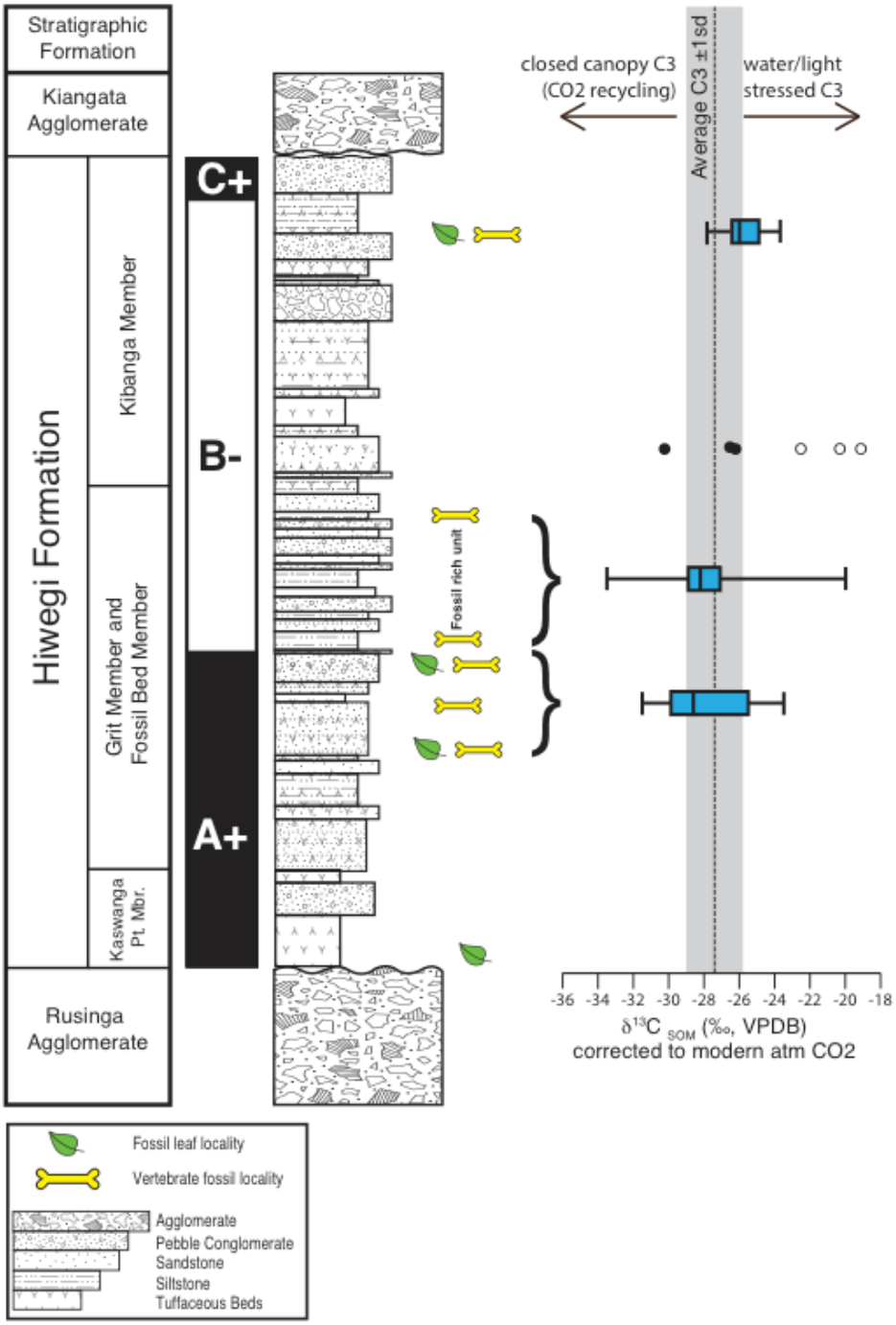

Table 6. Carbon isotope composition of Hiwegi Formation paleosol samples collected in 2009 and analyzed at the University of Minnesota Stable Isotope Lab. All $\delta^{13}C$ values corrected to modern atmospheric CO_2.

Sample	Locality	Member	$\delta^{13}C$ value (‰)	Possible Contaminant
12.07.09.02.01	Waregi (R1)	Kaswanga Point/Grit	-27.1	
12.07.09.02.02	Waregi (R1)	Kaswanga Point/Grit	-29.7	
12.07.09.02.03	Waregi (R1)	Fossil Bed	-28.5	
12.07.09.02.04	Waregi (R1)	Fossil Bed	-29.6	
12.07.09.02.05	Waregi (R1)	Fossil Bed	-28.3	
12.07.09.02.06	Waregi (R1)	Fossil Bed	-27.6	
12.07.09.02.07	Waregi (R1)	Fossil Bed	-28.4	
12.07.09.02.08	Waregi (R1)	Fossil Bed	-29.2	
12.07.09.02.09	Waregi (R1)	Fossil Bed	-28.6	
12.07.09.02.10	Waregi (R1)	Fossil Bed	-28.9	
12.07.09.02.11	Waregi (R1)	Fossil Bed	-28.5	
12.07.09.02.12a	Waregi (R1)	Fossil Bed	-29.5	
12.07.09.02.12b	Waregi (R1)	Fossil Bed	-28.3	
12.07.09.02.13	Waregi (R1)	Kibanga	-26.2	
12.07.09.02.14	Waregi (R1)	Kibanga	-22.5	modern roots?
12.07.09.02.15a	Waregi (R1)	Kibanga	-20.3	modern roots?
12.07.09.02.15b	Waregi (R1)	Kibanga	-19.1	modern roots?
12.07.09.02.16	Waregi (R1)	Kibanga	-26.5	
12.07.09.02.17	Waregi (R1)	Kibanga	-30.2	
14.07.09.01.01	Nyamsingula (R2)	Kaswanga Point/Grit	-30.6	
14.07.09.01.02	Nyamsingula (R2)	Kaswanga Point/Grit	-31.1	
14.07.09.01.03	Nyamsingula (R2)	Kaswanga Point/Grit	-25.1	
14.07.09.01.04	Nyamsingula (R2)	Kaswanga Point/Grit	-23.9	
14.07.09.01.05	Nyamsingula (R2)	Kaswanga Point/Grit	-25.1	
14.07.09.01.06	Nyamsingula (R2)	Kaswanga Point/Grit	-28.1	
14.07.09.01.07	Nyamsingula (R2)	Kaswanga Point/Grit	-28.9	
14.07.09.01.08	Nyamsingula (R2)	Kaswanga Point/Grit	-30.0	
14.07.09.02.01	Kaswanga Point (R5)	Kaswanga Point/Grit	-30.5	
14.07.09.02.02	Kaswanga Point (R5)	Kaswanga Point/Grit	-28.6	
14.07.09.02.03	Kaswanga Point (R5)	Kaswanga Point/Grit	-28.7	
14.07.09.02.04	Kaswanga Point (R5)	Kaswanga Point/Grit	-25.5	
14.07.09.02.05	Kaswanga Point (R5)	Kaswanga Point/Grit	-29.9	
14.07.09.02.06	Kaswanga Point (R5)	Kaswanga Point/Grit	-27.3	

Sample	Locality	Member	$\delta^{13}C$ value (‰)	Possible Contaminant
16.07.09.01.01	Waregi (R1)	Kaswanga Point/Grit	-29.3	
16.07.09.01.02	Waregi (R1)	Fossil Bed	-30.0	
16.07.09.01.03	Waregi (R1)	Fossil Bed	-25.0	
16.07.09.01.04	Waregi (R1)	Fossil Bed	-24.4	
16.07.09.01.05	Waregi (R1)	Fossil Bed	-28.0	
16.07.09.01.06	Waregi (R1)	Fossil Bed	-28.8	
16.07.09.01.07	Waregi (R1)	Fossil Bed	-28.9	
16.07.09.02.01	Waregi (R1)	Kaswanga Point/Grit	-23.5	
16.07.09.02.02	Waregi (R1)	Kaswanga Point/Grit	-24.8	
16.07.09.02.03	Waregi (R1)	Fossil Bed	-26.8	
16.07.09.02.04	Waregi (R1)	Fossil Bed	-29.3	
16.07.09.02.05	Waregi (R1)	Fossil Bed	-27.1	
16.07.09.02.06	Waregi (R1)	Fossil Bed	-28.0	
16.07.09.02.07	Waregi (R1)	Fossil Bed	-28.0	
16.07.09.02.08	Waregi (R1)	Fossil Bed	-24.0	
16.07.09.02.09	Waregi (R1)	Fossil Bed	-26.8	
16.07.09.02.10	Waregi (R1)	Fossil Bed	-29.7	
16.07.09.03.01	Waregi (R1)	Kaswanga Point/Grit	-31.5	
16.07.09.03.02	Waregi (R1)	Fossil Bed	-29.6	
16.07.09.03.03	Waregi (R1)	Fossil Bed	-26.0	
16.07.09.03.04	Waregi (R1)	Fossil Bed	-28.5	
16.07.09.03.05	Waregi (R1)	Fossil Bed	-28.3	
16.07.09.03.06	Waregi (R1)	Fossil Bed	-29.0	
16.07.09.03.07	Waregi (R1)	Fossil Bed	-30.0	
16.07.09.03.08	Waregi (R1)	Fossil Bed	-33.5	
16.07.09.03.09	Waregi (R1)	Fossil Bed	-25.6	
17.07.09.01.01	Waregi (R1)	Fossil Bed	-28.2	
17.07.09.01.02	Waregi (R1)	Fossil Bed	-28.0	
17.07.09.01.03	Waregi (R1)	Fossil Bed	-28.6	
17.07.09.01.04	Waregi (R1)	Fossil Bed	-29.1	
17.07.09.01.05	Waregi (R1)	Fossil Bed	-27.8	
17.07.09.01.06	Waregi (R1)	Fossil Bed	-27.6	
17.07.09.01.07	Waregi (R1)	Fossil Bed	-26.7	
17.07.09.01.08	Waregi (R1)	Fossil Bed	-26.5	
17.07.09.01.09	Waregi (R1)	Fossil Bed	-27.7	

Sample	Locality	Member	$\delta^{13}C$ value (‰)	Possible Contaminant
17.07.09.01.10	Waregi (R1)	Fossil Bed	-30.0	
17.07.09.01.11	Waregi (R1)	Fossil Bed	-27.2	
17.07.09.01.12	Waregi (R1)	Fossil Bed	-23.7	
17.07.09.01.13	Waregi (R1)	Fossil Bed	-27. 3	
17.07.09.01.14	Waregi (R1)	Fossil Bed	-25.0	
17.07.09.02.01	Waregi (R1)	Fossil Bed	-28.8	
17.07.09.02.02	Waregi (R1)	Fossil Bed	-28.1	
17.07.09.02.03	Waregi (R1)	Fossil Bed	-30.2	
17.07.09.02.04	Waregi (R1)	Fossil Bed	-28.8	
17.07.09.02.05	Waregi (R1)	Fossil Bed	-29.3	
17.07.09.02.06	Waregi (R1)	Fossil Bed	-31.4	
17.07.09.02.07	Waregi (R1)	Fossil Bed	-30.0	
17.07.09.02.08	Waregi (R1)	Fossil Bed	-29.5	
17.07.09.02.09	Waregi (R1)	Fossil Bed	-28.7	
17.07.09.02.10	Waregi (R1)	Fossil Bed	-28.1	
17.07.09.02.11	Waregi (R1)	Fossil Bed	-24.4	
17.07.09.02.12	Waregi (R1)	Fossil Bed	-27.1	
17.07.09.02.13	Waregi (R1)	Fossil Bed	-27.6	
18.07.09.01.01	Waregi (R1)	Kaswanga Point/Grit	-28.1	
18.07.09.01.02	Waregi (R1)	Fossil Bed	-29.9	
18.07.09.01.03	Waregi (R1)	Fossil Bed	-27.0	
18.07.09.01.04	Waregi (R1)	Fossil Bed	-27.7	
18.07.09.01.05	Waregi (R1)	Fossil Bed	-27.7	
18.07.09.01.06	Waregi (R1)	Fossil Bed	-28.1	
18.07.09.01.07	Waregi (R1)	Fossil Bed	-29.4	
18.07.09.01.08	Waregi (R1)	Fossil Bed	-26.5	
18.07.09.01.09	Waregi (R1)	Fossil Bed	-28.3	
18.07.09.01.10	Waregi (R1)	Fossil Bed	-28.6	
18.07.09.01.11	Waregi (R1)	Fossil Bed	-26.2	
18.07.09.01.12	Waregi (R1)	Fossil Bed	-26.7	
18.07.09.01.13	Waregi (R1)	Fossil Bed	-20.0	
18.07.09.01.14	Waregi (R1)	Fossil Bed	-23.7	
20.07.09.01.01	Waregi (R1)	Fossil Bed	-28.4	
20.07.09.01.02	Waregi (R1)	Fossil Bed	-28.5	
20.07.09.01.03	Waregi (R1)	Fossil Bed	-29.2	

Sample	Locality	Member	$\delta^{13}C$ value (‰)	Possible Contaminant
20.07.09.01.04	Waregi (R1)	Fossil Bed	-26.1	
20.07.09.01.05	Waregi (R1)	Fossil Bed	-26.0	
20.07.09.01.07	Waregi (R1)	Fossil Bed	-27.8	
20.07.09.01.08	Waregi (R1)	Fossil Bed	-28.4	
20.07.09.01.09	Waregi (R1)	Fossil Bed	-29.0	
20.07.09.01.10	Waregi (R1)	Fossil Bed	-27.3	
20.07.09.01.11	Waregi (R1)	Fossil Bed	-27.2	
20.07.09.01.12	Waregi (R1)	Fossil Bed	-28.6	
20.07.09.01.13	Waregi (R1)	Fossil Bed	-26.9	
20.07.09.01.14	Waregi (R1)	Fossil Bed	-29.2	
20.07.09.01.15	Waregi (R1)	Fossil Bed	-28.2	
20.07.09.01.16	Waregi (R1)	Fossil Bed	-27.5	
20.07.09.01.17	Waregi (R1)	Fossil Bed	-27.9	

Table 7. Carbon isotope composition of Hiwegi Formation paleosol samples collected in 2011 and analyzed at the Baylor University. All $\delta^{13}C$ values corrected to modern atmospheric CO_2. This unpublished dataset includes samples prepared and run on a mass spectrometer by Lauren Michel (Baylor University).

Sample	Locality	Member	$\delta^{13}C$ value (‰)	Possible Contaminant
p1 0-9	Waregi (R3)	Kibanga	-23.7	
p1-9-22	Waregi (R3)	Kibanga	-24.3	
p1 22-32	Waregi (R3)	Kibanga	-25.0	
p1 32-48	Waregi (R3)	Kibanga	-26.4	
p1 48-71	Waregi (R3)	Kibanga	-25.1	
p1 71-80	Waregi (R3)	Kibanga	-24.2	
p1 80-100	Waregi (R3)	Kibanga	-24.7	
p1 100-112	Waregi (R3)	Kibanga	-24.0	
p1 112-141	Waregi (R3)	Kibanga	-24.7	
r3-p2 0-26	Waregi (R3)	Kibanga	-26.7	
r3-p2 0-26	Waregi (R3)	Kibanga	-26.4	
r3-p2 26-66	Waregi (R3)	Kibanga	-26.7	
r3-p2 66-101	Waregi (R3)	Kibanga	-27.8	
r3-p5 38-51	Waregi (R3)	Kibanga	-26.6	
r3-p5 51-62	Waregi (R3)	Kibanga	-26.8	
r3-p5 62-102	Waregi (R3)	Kibanga	-25.8	
r3-p6 5-15	Waregi (R3)	Kibanga	-26.2	
r3-p6 5-15	Waregi (R3)	Kibanga	-26.0	
r3-p6 5-15	Waregi (R3)	Kibanga	-26.1	
r3-p6 30-50	Waregi (R3)	Kibanga	-26.4	
r3-p6 60-80	Waregi (R3)	Kibanga	-25.3	
ny-p3 25.2-36.2	Nyamsingula (R2)??	Kibanga	-26.3	
r1-p9b 7-32	Waregi (R1)??	Kibanga	-26.0	

Figure 14. SOM $\delta^{13}C$ values from the Hiwegi Formation at Nyamsingula (R2) and Kaswanga Point (R5).

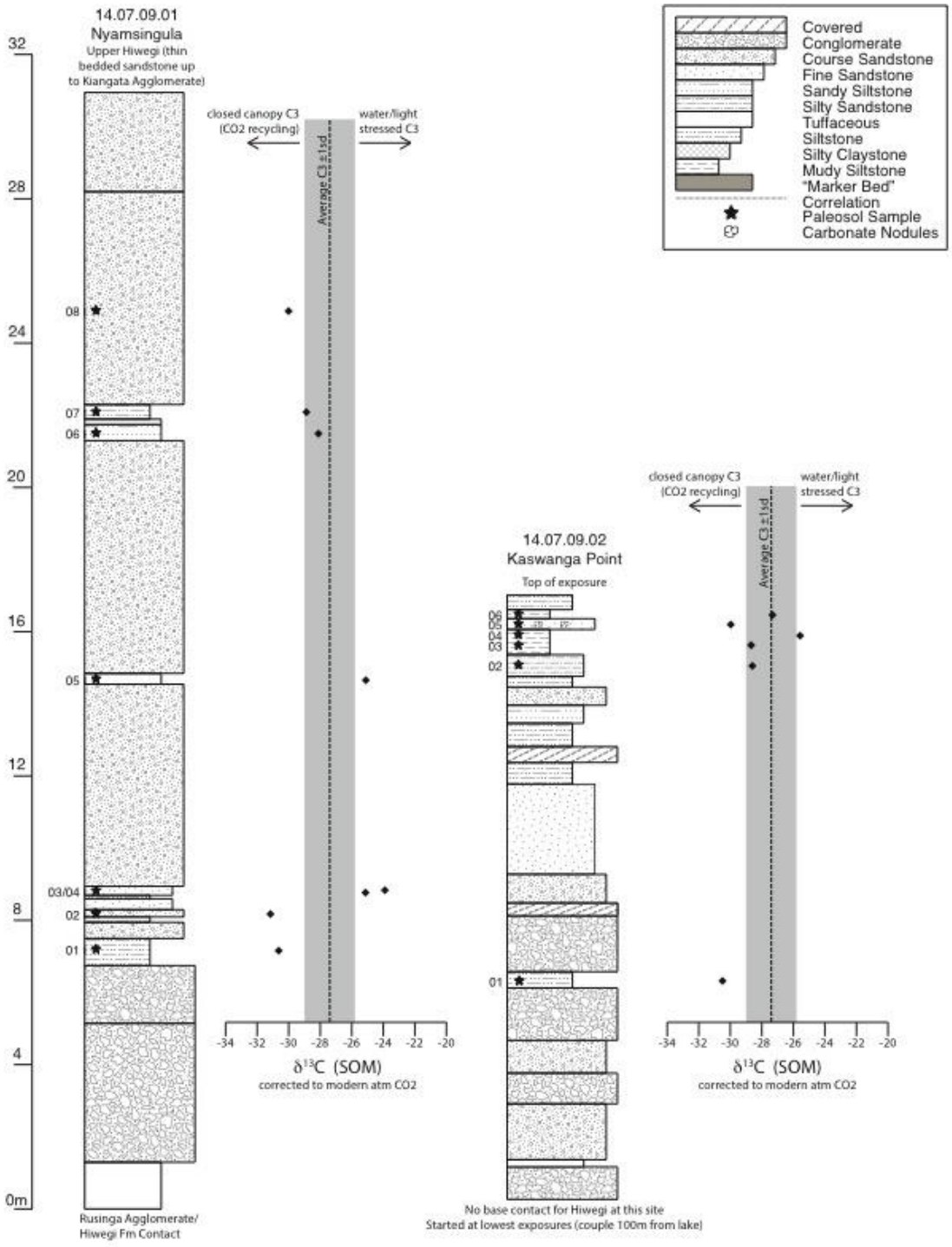

Figure 15. SOM $\delta^{13}C$ values from the Hiwegi Formation at Waregi (R1). Geology and stratigraphy image from original by Daniel J. Peppe.

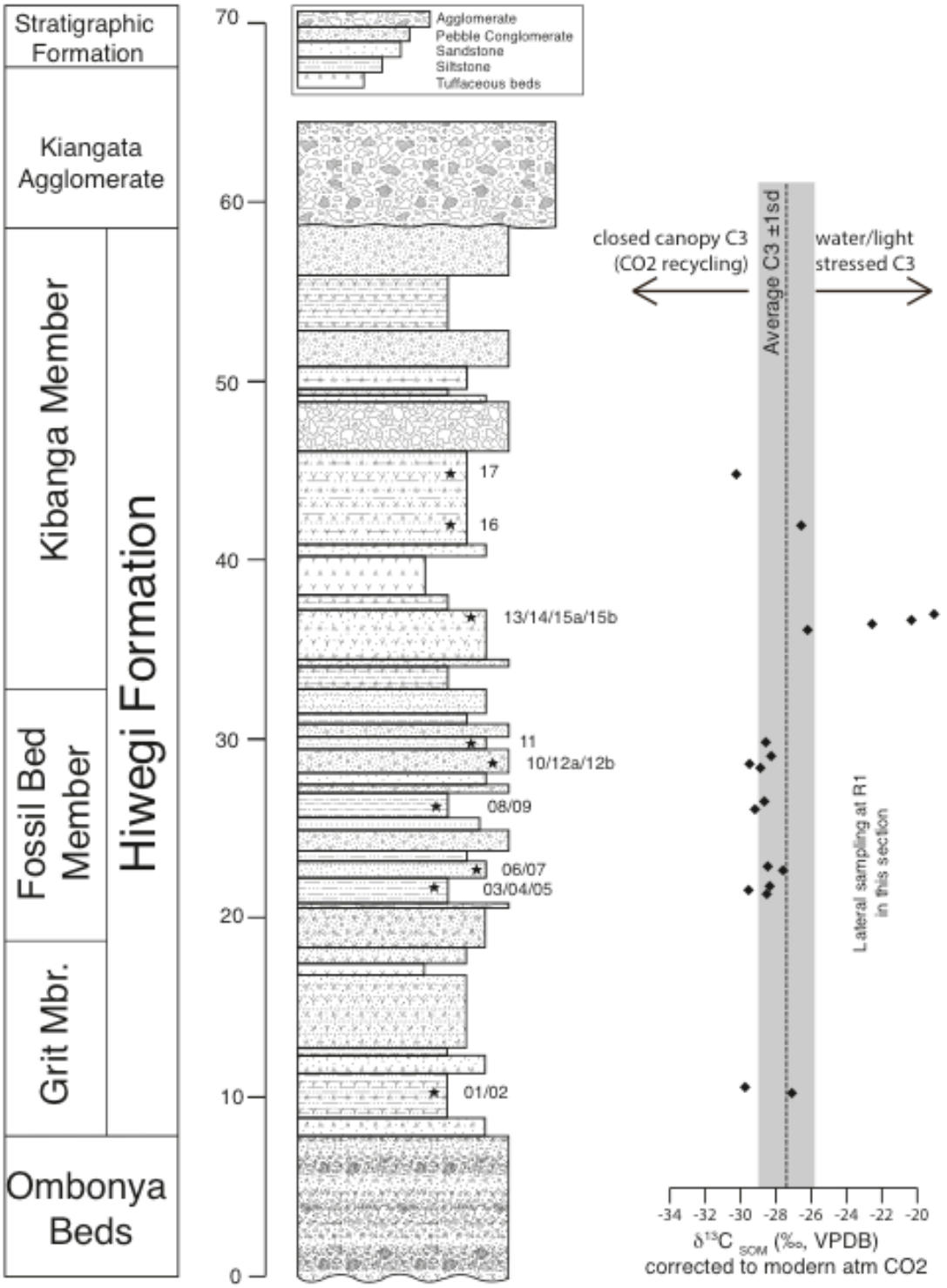

Figure 16. SOM $\delta^{13}C$ values from the Hiwegi Formation at Waregi (R1) - lateral sections through the Fossil Bed Member.

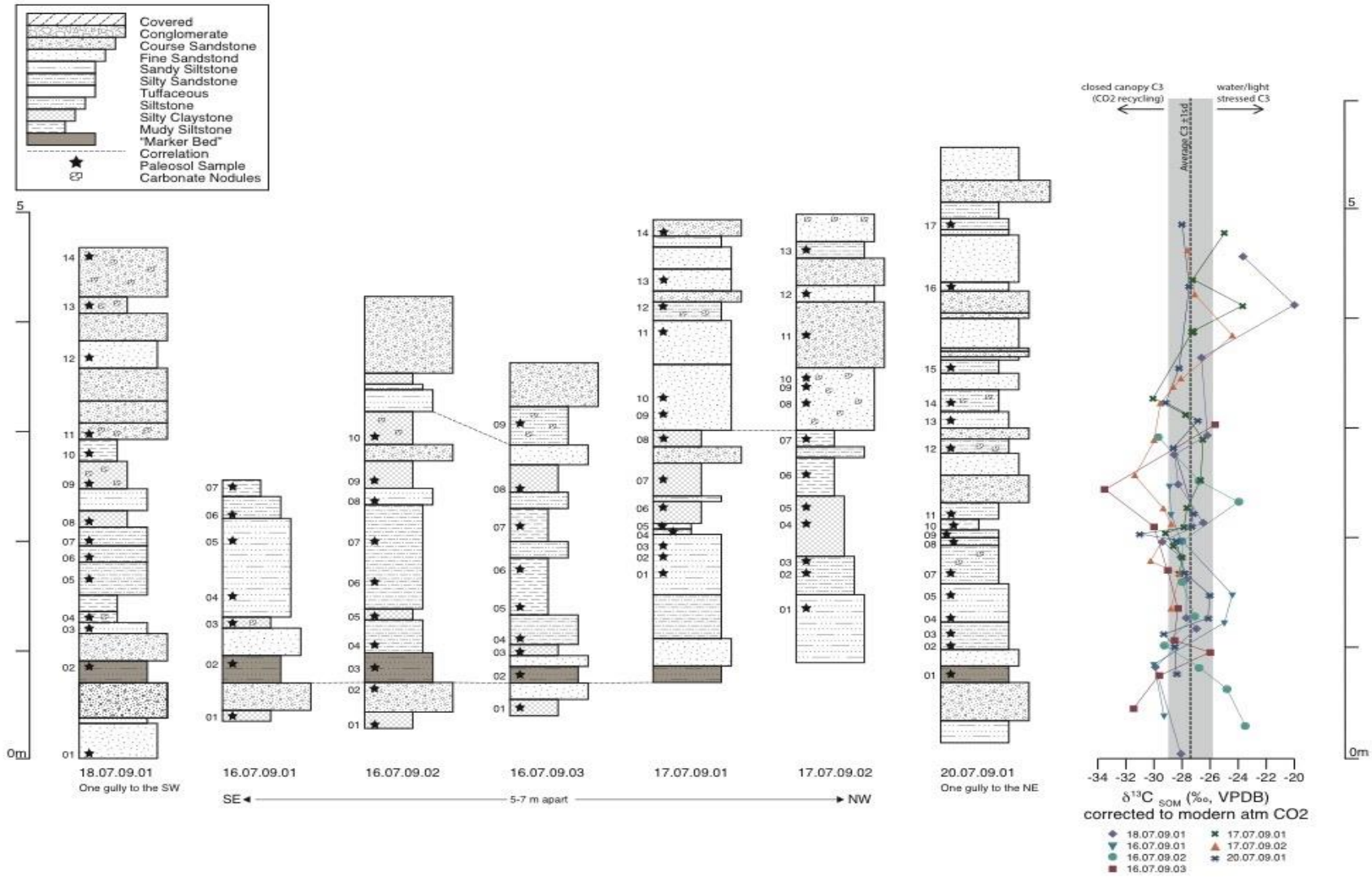

Table 8. Carbon isotope composition of *n*-alkanes and *n*-alkanoic acids, as well as corresponding bulk SOM $\delta^{13}C$ values, of selected paleosol samples. All $\delta^{13}C$ values corrected to modern atmospheric CO_2.

					n-alkanoic acids							*n*-alkanes						SOM
							$\delta^{13}C$ (‰)							$\delta^{13}C$ (‰)					
Sample	**Lab ID**	**Locality[§]**	**Grain Size**	**Possible contaminant**	**ACL**	**CPI**	**C_{26}**	**C_{28}**	**C_{30}**	**C_{32}**	**C_{34}**	**ACL**	**CPI**	**C_{27}**	**C_{29}**	**C_{31}**	**C_{33}**	**C_{35}**	**$\delta^{13}C$ (‰)**
12.07.09.02.04	KU155	W	muddy silt		30.4	1.7	-31.8	-32.1	-32.8	-33.9	-34.6			-30.1	-31.7	-33.3	-34.3	-31.5	-29.6
12.07.09.02.12a	KU157	W	sandy silt		28.4	3.1	-28.7	-30.5	-32.1	-27.1	-29.1								-29.5
12.07.09.02.12b	KU158	W	silty sand		29.3	2.1	-29.3	-30.6	-31.0	-30.6	-31.4								-28.3
12.07.09.02.13	KU145	W	silty sand	modern roots	28.3	2.2	-25.2	-29.2	-29.9	-28.1	-27.6								-26.2
12.07.09.02.15a	KU163	W	silty sand	modern roots	27.9	2.7	-24.2	-25.2	-25.1	-24.1	-22.5								-20.3
12.07.09.02.17	KU152	W	silty sand	modern veg?	27.8	2.8	-26.0	-27.0	-26.9	-25.4	-27.0								-30.2
14.07.09.01.01	KU149	N	silt		27.6	2.5	-25.6	-27.8	-28.8	-30.2	-29.4								-30.6
14.07.09.01.08	KU148	N	sand		28.8	2.2	-29.9	-29.2	-31.5	-32.0	-32.6								-30.0
14.07.09.02.03	KU147	K	silty mud		29.3	1.4	-31.9	-32.7	-33.8	-34.5	-34.8			-31.2	-31.2	-33.2	-34.4	-32.4	-28.7
14.07.09.02.06	KU151	K	silty mud		28.7	2.1	-22.9	-29.0	-30.8	-30.0	-29.3								-27.3
16.07.09.01.01	KU164	W	silty clay		28.1	2.3													-29.3
16.07.09.01.04	KU146	W	sandy silt	modern veg?	30.2	2.0	-27.2	-26.9	-27.9	-26.1	-25.7								-24.4
16.07.09.02.06	KU159	W	sandy silt		29.4	1.5	-31.9	-32.9	-33.2	-33.7	-33.6			-29.9	-31.4	-32.3	-33.1	-29.6	-28.0

Sample	Lab ID	Locality[§]	Grain Size	Possible contaminant	*n*-alkanoic acids							*n*-alkanes							SOM
							$\delta^{13}C$ (‰)							$\delta^{13}C$ (‰)						$\delta^{13}C$ (‰)
					ACL	CPI	C_{26}	C_{28}	C_{30}	C_{32}	C_{34}	ACL	CPI	C_{27}	C_{29}	C_{31}	C_{33}	C_{35}	
17.07.09.01.10	KU160	W	silty clay		28.4	2.0	-27.1	-30.8	-31.7	-32.7	-32.7								-30.0
17.07.09.01.12	KU156	W	silty clay	modern CO_3?	28.5	2.8	-29.2	-31.0	-31.0	-28.9	-28.0								-23.7
17.07.09.02.01	KU161	W	sandy silt		29.6	1.5	-31.9	-33.4	-34.1	-34.3	-34.8			-32.2	-31.4	-32.8	-33.9	-34.5	-28.8
17.07.09.02.10	KU150	W	silty clay		28.8	1.8	-28.5	-29.2	-28.7	-28.9	-28.7								-28.1
17.07.09.02.11	KU154	W	sandy silt		29.3	4.3	-27.3	-27.9	-28.1	-24.8	-26.7								-24.4
18.07.09.01.02	KU162	W	sandy clay		29.0	2.1	-29.1	-29.2	-30.2	-28.6	-28.1								-29.9
18.07.09.01.12	KU153	W	sandy silt		28.8	3.9	-30.2	-30.7	-31.7	-26.5	-26.8								-26.7

[§] "W" indicates Waregi, "N" indicates Nyamsingula, and "K" indicates Kaswanga Point.

CHAPTER 3: STABLE ISOTOPE PALEOECOLOGY OF EARLY MIOCENE RUSINGA ISLAND MAMMALIAN COMMUNITIES FROM THE KULU AND HIWEGI FORMATIONS

Chapter Summary

The fossils from Rusinga Island provide one of the best comparative collections for understanding the evolution and diversification of early Miocene mammals. In addition to more than eighty-five mammalian species, the Rusinga faunal community includes a number of primate species key to understanding the evolution and diversification of catarrhines, such *Dendropithecus*, *Limnopithecus*, and *Nyanzapithecus*, as well as the primitive hominoid *Ekembo*. Placing the mammalian community within a clear ecological context is crucial to our understanding of the evolutionary forces that shaped these species. While there have been numerous past paleoenvironmental reconstructions for these early Miocene deposits, they have resulted in conflicting interpretations, with habitats ranged from closed forests, woodlands and rainforests, to open and semi-arid environments. Here we present the carbon and oxygen isotope composition of mammalian tooth enamel of anthracotheres, suids, sanitherids, tragulids, chalicotheres, titanohyracids, rhinocerotids, gomphotheres, and deinotheres from the early Miocene Hiwegi and Kulu Formations on Rusinga. The results of this analysis indicates a range of C_3 habitats, including those experiencing water and/or light stress were present during these time periods, and were actively exploited by a number of species. Although the presence of a dense close-canopy forest has been recently documented on Rusinga, the evidence from the fauna sampled here exhibits only rare indications of foraging in these habitats, which may be due to sampling bias or demonstrate a marked heterogeneity in

the regional ecosystem. Additionally, this study documents a significant difference in the oxygen isotope composition of meteoric water available to the Hiwegi Formation fauna and the Kulu Formation fauna, indicating either an increase in mean annual temperature, an increase in aridity, a decrease in mean annual precipitation, or some combination of the three climatic factors in the Kulu Formation, and demonstrating marked differences in paleoenvironmental stressors facing this early Miocene mammalian communities.

Introduction

The fossil-bearing early Miocene Rusinga Group on Rusinga Island, Kenya (ca. 15-20.5 Ma; **Fig. 11**) are exceptional in that they contain some of the richest samples of early Miocene East African floral and faunal communities, preserving fossils of more than 100 vertebrate species, including a significant number of holotypes (Pickford, 1986a; Werdelin and Sanders, 2010). During the more than eight decades of field research since its discovery, Rusinga Island has been systematically collected multiple times. The diversity of mammalian orders represented in the collection as well as the overall quantity and quality of preservation makes the Rusinga Island fossil faunas one of the best comparative collections for the paleobiology of early Miocene mammals in East Africa.

Importantly, the fossil deposits on Rusinga Island provide an excellent setting to examine the adaptation and diversification of catarrhines and early hominoids, which is a necessary foundation for our understanding of the evolutionary history of all apes,

including humans. The fossil primate community of Rusinga includes the extensive remains of the primitive hominoid *Ekembo* (traditionally referred to as *Proconsul*; see McNulty et al., 2015), including specimens of every bony element, many partial skeletons, and the type specimens of both *Ekembo nyanzae* and *Ekembo heseloni* (Leakey, 1943; MacInnes, 1943; Napier and Davis, 1959; Walker and Teaford, 1988; Walker, 2007). Additionally, the primates recovered from Rusinga include multiple partial skeletons of *Dendropithecus macinnesi* (Andrews and Simons, 1977), and specimens from the less well-known catarrhines *Limnopithecus legetet* and *Nyanzapithecus vancouveringorum* (Harrison, 2002). As these primate assemblages are key references for understanding the evolution and diversification of crown catarrhines, placing the primate community within a clear ecological context is crucial to our understanding of the evolutionary forces that shaped early ape evolution. This paleoenvironmental framework will allow for future morphological analyses to better address questions regarding habitat preferences, feeding ecologies, and spatial/temporal ranges of the early Miocene primate community.

The many previous paleoenvironmental reconstructions for Rusinga have yielded a wide range of often conflicting results and interpretations, ranging from closed forests, woodland, or rainforest, mosaic habitats of both open and closed habitats, and even semi-arid environments (e.g., Chesters, 1957; Andrews and Van Couvering, 1975; Andrews et al., 1979; Pickford, 1983; Collinson, 1985; Pickford, 1985; Bestland, 1990; Bestland and Retallack, 1993; Thackray, 1994; Bestland and Krull, 1999; Retallack, 2002; Forbes et al., 2004; Andrews and Kelley, 2007; Collinson et al., 2009). The

majority of these reconstructions have focused on the Hiwegi Formation –from which most of the fossils derive – and none has addressed the potential for environmental change during the ca. 5 Myr of deposition of the Rusinga Group. The assumption that the entire Rusinga Group represents a stable paleoenvironment that is relatively unchanged through time, which we test in this study, has been justified by the seeming taxonomic composition stability of faunal assemblages, collected from various fossil localities throughout the sequence (Pickford, 1981; Pickford, 1984; Andrews et al., 1997; Peppe et al., 2009). However, three factors call this assumption into question. First, similar faunal lists throughout the Rusinga Group may not equate with unchanging habitats; stratigraphic resolution for formally testing for faunal turnover is not available for most of the fossil assemblages. Second, the latest magnetostratigraphic results indicate that even Rusinga's "Fossil Bed Member," from the Hiwegi Formation (see **Figs. 11-12**), the source of most fossil specimens, does not represent a single short interval across its outcrop area as has been previously assumed (Van Couvering, 1972; Bestland et al., 1995), but instead consists of different time slices at different localities (McCollum et al., 2013). Finally, our recent work at multiple localities in the Hiwegi Formation suggests more open, drier woodland habitats low in the Hiwegi Formation that transition to a dense, closed canopy forest up section. Notably, the same species of catarrhines are found in both intervals, which may imply these species are flexible in habitat preferences or that our paleoenvironmental reconstructions are not identifying the full range of habitats in the region.

Here we present carbon and oxygen isotope compositions[11] of tooth enamel of anthracotheres, suids, sanitherids, tragulids, chalicotheres, titanohyracids, rhinocerotids, gomphotheres, and deinotheres from the Hiwegi and Kulu Formations of the Rusinga Group on Rusinga (**Fig. 11**). The isotope composition of mammalian enamel provides direct evidence for the diet of these species, reflecting the resources exploited by an animal and therefore readily available in its habitat. These types of analyses require neither modern analogs for an extinct species, nor assumptions based on taxonomic uniformitarianism (see Sponheimer et al., 1999). If the Rusinga Group fauna is inhabiting a stable habitat unchanging through time, the $\delta^{13}C$ and $\delta^{18}O$ enamel values would also be relatively stable and unchanging across both time and space with a relatively small amount of variability, as all of the fauna would be consuming vegetation and obtaining their water from one widespread stable ecosystem. Our results however, are broadly consistent with recent reconstructions based on paleosols for the Hiwegi Formation (**Chapter 2**), and suggest a high degree of spatial variability in both the Kulu and Hiwegi Formation habitats throughout the early Miocene succession on Rusinga. The $\delta^{13}C$ values of the Kulu and Hiwegi Formation fauna span the full range of extant C_3 vegetation, with strong evidence for animals consuming vegetation from both average C_3 habitats (i.e., neither closed-canopy forests nor drought stressed) as well as water/light stressed C_3 habitats. The $\delta^{18}O$ values indicate a significant difference between the local climate experience by proboscideans and rhinocerotids from the Kulu and Hiwegi Formations. Taken together, these results indicate that the Rusinga Group habitats, and

[11] $\delta^{13}C$ and $\delta^{18}O$ values are presented in parts per thousand (permil, ‰), where $\delta X=(R_{sample}/R_{standard}-1) *1000$, X is ^{13}C or ^{18}O, R is $^{13}C/^{12}C$ and $^{18}O/^{16}O$ respectively, and the standard for carbon is Vienna Pee Dee Belemnite (V-PDB) and for oxygen is Vienna Standard Mean Ocean Water (V-SMOW).

therefore the key environments for early crown catarrhine evolution, were not unchanged through time but rather dynamic on both spatial and temporal scales incorporating open and closed ecosystems.

Geological Background of Rusinga Island

Rusinga Island (0°24'S, 34°0'E; **Figs. 11A-B**) is a near-shore island on the eastern edge of Lake Victoria in present-day Kenya. The early Miocene Rusinga Group strata contain ~300m of sediment that records a history of the eruption and erosion of the Kisingiri volcano, active during the early Miocene (Shackleton, 1951; McCall, 1958; Van Couvering, 1972; LeBas, 1977; Pickford, 1986b; Bestland et al., 1995). The hyper-alkaline, volatile rich debris from this volcano facilitated exceptional preservation throughout the Rusinga Group.

The Rusinga Group (**Fig. 11C**), which comprises in stratigraphic order, the Wayando Formation, Kiahera Formation, Rusinga Agglomerate, Hiwegi Formation, and Kulu Formation, includes highly fossiliferous volcaniclastic strata with weakly-developed paleosols and lacustrine and fluvial deposits (Peppe et al., 2009; Peppe et al., 2011a; Peppe et al., 2011b). Although there are mammals located throughout the Rusinga Group strata, the majority of fossils are found within the Hiwegi Formation (see **Table 9** for a list of mammalian fauna). The majority of mammals sampled from this study can be reliably placed within either the Hiwegi or Kulu Formation.

Hiwegi Formation

The Hiwegi Formation, which is the most fossiliferous of the Rusinga Group strata, contains intercalcated sheet-flood (or stream) and paleosol deposits (Van Couvering, 1972; Retallack et al., 1995; Michel et al., 2014). Weakly developed paleosols, which are generally brittle red-weathering grey-green clayey silts (Drake et al., 1988), found within the Hiwegi Formation include pedogenic features such as slickensides, carbonate nodules, mm-cm scale mica fragments, pressure faces, and calcified root and *in situ* tree stump casts. The Hiwegi Formation comprises four volcaniclastic-tuffaceous units, in stratigraphic order the Kaswanga Point Member, Grit Member, Fossil Bed Member and Kibanga Member (**Fig. 12**; Van Couvering, 1972; Drake et al., 1988). Historically, all of the paleontological and paleoenvironmental studies of the Hiwegi Formation have considered all of the fossil sites from the various members to be contemporaneous and treated the deposits as synchronous (e.g., Van Couvering, 1972; Bestland et al., 1995). The latest magnetostratigraphic analyses documented normal and reversed polarity throughout the formation indicating the fossil localities do not represent a single, short synchronous interval as previously thought (McCollum et al., 2013). As such, these fossil collections and subsequent paleoenvironmental reconstructions, which were provenienced by locality, are now understood to be time-averages of multiple separate fossil-bearing units and levels. Recent work in the Hiwegi Formation has provided new stratigraphic information allowing for reconsideration of the temporal and geological context for the faunal communities and has identified multiple different paleoenvironments within this formation. The majority of the fossil mammals from this

study were sampled from the Grit/Fossil Bed Members sampled from the R1, R5, and R106 localities and from the Kibanga Member (R3 locality). The Grit and Fossil Bed Members of the Hiwegi Formation are combined here due to lack of fossil provenience in the historical collections and because they are thought to be roughly contemporaneous (McCollum et al., 2013), however based on field observations, the fossils likely all come from the Fossil Bed Member.

The Grit and Fossil Bed Members exhibit sedimentary features indicative of fluvial processes, including cut and fill architecture, trough cross-bedding, and fining upward succession. Salt hoppers, satin-spar calcite after gypsum, and teepee structures provide significant evidence for high-levels of evaporation at the Grit Member-Fossil Bed Member contact. The paleosols found within the Grit Member have very little clay and stage II soft powdery calcite indicative of semi-arid to arid conditions and evaporations rates in excess of precipitation rates.

The Kibanga Member at R3 preserves, within a single paleosol, a number of closely spaced, large-diameter (18-160 cm) tree-stump casts as well as many calcite-cemented casts of root networks. Found within this paleosol is strong evidence for biogenic activity, as shown by bee brood casts, termite termitaria, oribatid mite fecal pellets and roots, in addition to evidence for strong seasonality with marked wet and dry periods, as indicated by incipient pressure facies (Michel et al., 2014). This forest paleosol layer at the R3 locality documents a widespread, close-canopied (dense and multi-storied) tropical seasonal forest.

Kulu Formation

The Kulu Formation, which is the youngest of the Rusinga Group strata, is distinct from the rest of the Rusinga Group in that it is primarily a non-volcanic lacustrine unit of fine-grained shale, siltstones, and sandstones that was occasionally incised by high-energy currents that deposited conglomerate lenses (Bestland and Krull, 1999; Peppe et al., 2009). The Kulu Formation includes partial skeletons of medium and large-sized mammals, but small-bodied mammals are rarely preserved; most fossils included here were found at the Nyamsingula site (R4 locality; Peppe et al., 2009). While debate has surrounded the stratigraphic placement and age of the Kulu Formation within the Rusinga Group strata (see Shackleton, 1951; Van Couvering and Miller, 1961; Van Couvering, 1972; Drake et al., 1988; Bestland, 1991), recent stratigraphic work has resolved this, identifying the Kulu Formation as the youngest of the Rusinga Group strata with an age between 15-17 Ma (Peppe et al., 2009).

Stable Isotope Composition of Mammalian Tooth Enamel

The carbon isotope composition of mammalian tooth enamel varies based on the $\delta^{13}C$ values of atmospheric CO_2, the photosynthetic pathway of the source vegetation (the Calvin-Benson or C_3 pathway and the Hatch-Slack or C_4 pathway), and environmental factors such as light intensity, aridity, and water stress. C_3 and C_4 plants fractionate carbon isotopes to different degrees during photosynthesis due to anatomical and

biochemical differences associated with each pathway, resulting in distinct and non-overlapping distributions of $\delta^{13}C$ values for large samples of modern plants (mean modern C_3 mean: -27.4 ± 1.6‰; mean modern C_4: -12.7 ± 1.1‰; O'Leary, 1981, Passey et al., 2002; Cerling et al., 2003; Kohn, 2010; Diefendorf et al., 2010). However, prior to the global expansion of C_4 grasslands during the Late Miocene to Pleistocene (Edwards et al., 2010), equatorial African habitats would have been composed of exclusively C_3 vegetation (Cerling, 1997). Pure C_3 ecosystems are commonly assumed to be closed habitats consisting of woody vegetation, yet 97% of extant terrestrial plant species utilize the C_3 photosynthetic pathway including shrubs, temperate grass species, and a number of other open-habitat species (Jacobs et al., 1999). Importantly, extant examples of pure C_3 ecosystems are extremely rare as even high latitude grasslands dominated by C_3 species still include some C_4 grasses (Teeri and Stowe, 1976; Stowe and Teeri, 1978; Ehleringer et al., 1991; Tieszen et al., 1997; Sage et al., 1999).

Of particular importance for paleoenvironmental reconstructions of fossil localities that pre-date the expansion of C_4 plants (i.e., for C_3-only ecosystems), are the environmental factors that drive variation in the carbon isotope composition of C_3 plants. Under light and water stress in open habitats, the physiological and biochemical response by plants, which works to prevent excess water loss, decreases fractionation during carbon fixation, resulting in ^{13}C enriched tissues and higher than average $\delta^{13}C$ values (mean: -24.6 ± 1.1‰; Ehlringer and Cooper, 1988; Cerling and Harris, 1999; Passey et al., 2002). Conversely, in closed forests, photosynthetic recycling of plant respired CO_2 results in ^{13}C depleted plant tissues with lower than average $\delta^{13}C$ values and a vertical gradient of

$\delta^{13}C$ with the most negative values near the ground and the highest values at the top of the canopy (the canopy effect; van der Merwe and Medina, 1991).

The carbon isotope composition of hydroxyapatite in tooth enamel reflects the $\delta^{13}C$ values of the plants consumed during enamel mineralization, with tissue-specific enrichments relative to diet, and persists without remodeling (as seen in bone) throughout the lifetime of the animal. Enamel can therefore be used as a proxy for diet during the time over which tooth enamel was mineralizing, which occurs early in an animal's life. The generally accepted enrichment factor for tooth enamel relative to diet for large-bodied ungulates is +14.1±0.5‰, which is the mean value for numerous large-bodied ungulates (ruminant and non-ruminant species of artiodactyls and perissodactyls; Cerling and Harris, 1999; Passey et al., 2002).

Notably, the isotope composition of enamel apatite from large-bodied animals is understood to be generally resistant to diagenesis during the fossilization process due to its highly crystalline state and extremely low organic content (DeNiro and Epstein, 1978; Sullivan and Krueger, 1981; Tieszen et al., 1983; Ambrose and DeNiro, 1986; Lee-Thorp et al., 1989; LeGeros, 1991; Wang and Cerling, 1994; Cerling and Harris, 1999; Kohn et al., 1999; Lee-Thorp, 2000; Lee-Thorp and Sponheimer, 2013). The total time of enamel mineralization in a single tooth is finite and relatively short (months to a few years) compared to bone, which, due to the process of remodeling, is dynamic and will represent an average of an animal's diet over the many years before death (~10 years in humans for example). As mammals typically move around the landscape, the spatial scale integrated

in an enamel isotopic signal can be quite large for species with large home ranges (Kingston, 2007), providing a short temporal and large spatial snapshot of the animal's habitat.

The oxygen isotope composition of tooth enamel reflects the $\delta^{18}O$ value of body water/fluids and body temperature, and climate, diet, and physiology all play a role in the oxygen isotope composition of mammalian body water (Longinelli, 1984; Luz et al., 1984; Luz and Kolodny, 1985; Koch et al., 1989; Kohn, 1996; Kohn et al., 1996; Sponheimer and Lee-Thorp, 1999). The oxygen isotope composition of mammalian tooth enamel primarily reflects the $\delta^{18}O$ value of ingested water because mammals with a body mass >1kg have a body temperature near 37°C, and enamel precipitation occurs in equilibrium with body water, which is almost entirely ingested water (Longinelli, 1984; Luz et al., 1984). For species that are not obligate drinkers (i.e., obtain their water from food sources such as leaves), the $\delta^{18}O$ value of enamel will reflect the amount of aridity and evaporation, as leaf water will be ^{18}O enriched relative to meteoric water due to preferential evapotranspiration of the lighter $H_2{}^{16}O$ molecules (Sternberg et al., 1989; Levin et al., 2006).

Reconstructing the average $\delta^{18}O$ value of surface and plant water available for at a site or in a region based on estimates of the $\delta^{18}O$ of local meteoric water is often a key component of paleoclimatic reconstructions. Using oxygen mass balance models, Bryant and Froelich (1995) and Kohn (1996) found that large carnivores and obligate-drinking herbivores reliably track changes in meteoric water $\delta^{18}O$ values. Extant proboscideans

are obligate water drinkers that consume large volumes of surface water daily, and studies of fossil proboscidean enamel suggest that proboscideans faithfully records of meteoric water $\delta^{18}O$ values for potentially the entire Cenozoic (Ayliffe et al., 1992; Guilderson et al., 1994; Sánchez Chillón et al., 1994; Bryant et al., 1996; Reinhard et al., 1996; Koch et al., 1998; Fox and Fisher, 2001; Fox et al., 2007).

Materials and Methods

Eighty-nine teeth were sampled from early Miocene Rusinga faunas chosen to document a wide range of taxa from as many localities as possible. Seventy-one of these included accurate and reliable provenience information from seven Rusinga localities in the Hiwegi and Kulu Formations; the majority of these were identifiable to genus and species. A small number of specimens from the historical collections do not have reliable locality information and therefore cannot be placed into one of the Rusinga Group formations, but were included to accurately assess variability within species. Five additional samples were taken from mammals collected from the R74 locality, which has been considered to be either the Kulu or Wayando Formation, but as this locality is bounded by faults and surrounded by discontinuous exposures of the Kiahera formation (see Geraads et al., 2016), these specimens cannot be reliably placed into any formation and are included to show the full range of within taxa variation. Two additional specimens each were sampled from Mfangano Island and the nearby contemporaneous mainland site of Karungu (also Kisingiri volcano sites) and were chosen to allow

comparison to these nearby, and roughly contemporaneous, localities. Below is a detailed discussion of the taxon sampled by clade.

Anthracotheriidae

The extinct clade Anthracotheriidae is represented on Rusinga by four species, *Brachyodus aequatorialis*, *Kulutherium kenyensis*, *Sivameryx africanus* and *Sivameryx moneyi*. *B. aequatorialis*, *Sivameryx africanus* and *Sivameryx moneyi* have been recovered from both the Hiwegi and Kulu Formations whereas *K. kenyensis* is restricted to the Kulu Formation (Peppe et al., 2009). Notably, anthracotheres have been described as hydrophilic based on taphonomic evidence (Pickford, 1983), and are likely therefore to be water-dependent similar to modern hippopotamids. The three anthracothere specimens sampled here were taken from molar fragments and were not identifiable to genus and species. Given the scarcity of *Kulutherium* and *Sivameryx*, however, they most likely represent *Brachyodus*.

Suidae

The fossil Suidae from Rusinga are represented by four species, *Kenyasus rusingensis*, *Kubanocheorus anchidens*, *Bunolistriodon jeanelli*, and *Nguruwe kijivium*. All four species have been recovered from the Hiwegi Formation, and only *Kubanochoerus anchidens* is absent from the Kulu Formation. The fifteen suids sampled were identifed to both genus and species and all three of the four species found in both Hiwegi and Kulu

Formations were included (*Kubanochoerus anchidens* was not sampled); note, six of the specimens were from the historical collections and lack locality data.

Sanitheridae

There is one fossil Sanitheridae from Rusinga, *Diamantohyus africanus* (formally in Suidae), which has been recovered from both the Kulu and Hiwegi Formations. The specimen of *Diamantohyus africanus* sampled here is from the contemporaneous mainland site of Karungu (also a Kisingiri volcano fossil site).

Tragulidae

The fossil Tragulidae from Rusinga are represented by three species within the genus *Dorcatherium*. *D. chappuisi*, *D. parvum*, and *D. pigotti* are found in both the Kulu and Hiwegi Formations. Four tragulids were sampled here: three *D. pigotti* from the Grit/Fossil Bed Members of the Hiwegi Formation, and one *Dorcatherium sp.* from neighboring Mfangano Island.

Chalicotheriidae

There is one species of fossil chalicothere found on Rusinga, *Butleria rusingense*, which has been recovered from both the Kulu and Hiwegi Formations. Of the seven chalicotheres sampled, three were from the Fossil/Grit Members of the Hiwegi

Formation, two were from the Kibanga Member of the Hiwegi Formation, and two were recovered from the Kulu Formation.

The extinct fossil chalicotheres are an unusual group of perissodactyls having both dentition apparently adapted for herbivory (specifically browsing) and claws on their digits rather than the more typical hooves. Microwear analyses of a variety of chalicothere species from Asia, Europe, and North America indicate that all of these taxa were browsers with no significant grass in their diets, although many species potentially included hard food objects such as fibrous fruits, seeds, pits, and nuts (Schulz et al., 2007; Semprebon et al., 2011). Chalicotheres have been used as an indicator taxon, suggesting the presence of at least some trees and shrubs in the nearby habitat (Coombs and Cote, 2010).

Rhinocerotidae

The fossil Rhinocerotidae from Rusinga are represented by four species, *Aceratherium acutirostratum*, *Brachypotherium heinzelini*, *Chilotheridium pattersoni*, and *Dicerorhinus leakeyi*. *Aceratherium acutirostratum* and *Dicerorhinus leakeyi* are found in both the Hiwegi and Kulu Formations, whereas *Brachypotherium heinzelini* is limited to the Hiwegi Formation and *Chilotheridium pattersoni* is found only in the Kulu Formation. Of the 29 rhinocerotids sampled, nine were identifiable to genus and species (*Brachypotherium heinzelini*, *Chilotheridium pattersoni*, and *Dicerorhinus leakeyi*), and the remainder were only identifiable to Rhinocerotidae; 21 Rusinga Rhinocerotidae were

from the Fossil/Grit Member of the Hiwegi Formation, two from the Kibanga Member of the Hiwegi Formation, four were from the Kulu Formation, and two from the R74 locality.

Proboscidea

The fossil Proboscidea from Rusinga are represented by three species from three families, *Prodeinotherium hobleyi* (Deinotheriidae), cf. *Archaeobelodon sp.* (Gomphotheriidae), and *Eozygodon morotoensis* (Mammutidae). Both deinotheres and gomphotheres are found in the Hiwegi and Kulu Formations, and the mammutid is found only in the Hiwegi Formation. Of the 23 proboscideans included in this study, fourteen could be identified to the family level: five deinotheres (three from the Kulu Formation and one from R74) and nine gomphotheres (three from the Grit/Fossil Bed Member of the Hiwegi Formation, four from unspecified localities within the Hiwegi Formation, and two from the Kulu Formation). The remaining nine proboscideans included two from the Kibanga Member of the Hiwegi Formation, three from the Kulu Formation, and one from R74.

Hyracoidea

The fossil Hyracoidea on Rusinga are represented by two species, *Afrohyrax championi* and *Meroehyrax bateae*. Whereas *Afrohyrax championi* has been recovered from both the Hiwegi and Kulu Formations, *Meroehyrax bateae* appears to be absent from the Kulu Formation. Of the six sampled hyracoids, four were identifiable to genus and species,

Afrohyrax championi, and two were indeterminate Hyracoidea; five are from the Hiwegi Formation, and one is from R74.

Carnivora and Creodonta

As with the primary consumers discussed above, the enamel $\delta^{13}C$ values of higher level consumers (such as carnivores and creodonts) will reflect the carbon isotope composition of their diet, in this case, that of the ingested prey (Koch, 2007). The fossil Carnivora from Rusinga are represented by four species, *Cynelos euroyodon* and *Cynelos macrodon* (Amphicyonidae), *Afrosmilus africanus* (Barbourofelidae), and *Kichechia zamanae* (Herpesidae). While all four carnivore species are found in the Hiwegi Formation, only *Cynelos euryodon* and *Kichechia zamanae* are found in the Kulu Formation. Two fossil Carnivora were sampled: an *Afrosmilus sp.* from the Kibanga Member of the Hiwegi Formation and a *Cynelos euroyodon* from the Kulu Formation.

The fossil Creodonta (Hyaenodontidae) from Rusinga are represented by ten species, *Anasinopa leakeyi*, *Isohyaenodon andrewsi*, *Isohyaenodon pilgrim*, *Hyainailourus nyanzae*, *Leakeytherium hiwegi*, *Megistotherium sp.*, *Metapterodon kaiseri*, *Teratodon enigma*, *Pterodon nyanzae*, and *Pterodon africanus*, all of which have been recovered from the Hiwegi Formation; *Hyainailourus nyanzae* and *Leakeytherium hiwegi* have also been found in the Kulu Formation. A single indeterminate Hyaenodonitidae specimen was sampled from the Grit/Fossil Bed Member (R5) of the Hiwegi Formation.

Laboratory Analytical Techniques

Approximately 7 mg of tooth enamel were drilled from each specimen using a diamond bur. Care was taken to avoid diagnostic morphology while drilling; slow drill speeds were used to minimize heating and any resulting isotopic fractionation. Sample powders were reacted with 1 M acetic acid with a 1 M calcium acetate buffer (pH: 5) for 24 hours to remove any exogenous carbonate. Samples were rinsed three times with distilled, deionized water and then dried in a 60°C oven for 48+ hours to remove any remaining water.

The cleaned enamel samples and approximately 2 cm of silver thread (to react with any SO_2 generated during acidification) were reacted with 100% phosphoric acid in a Kiel automatic carbonate extraction device. A Finnigan MAT 252 Isotope Ratio Mass Spectrometer in the Stable Isotope Laboratory in the Department of Earth Sciences, University of Minnesota was used to measure the carbon and oxygen isotope composition of the resulting CO_2 gas. Results are reported as conventional $\delta^{13}C$ and $\delta^{18}O$ values in parts per thousand (permil, ‰), where $\delta X=(R_{sample}/R_{standard}-1) *1000$, X is ^{13}C or ^{18}O, R is $^{13}C/^{12}C$ and $^{18}O/^{16}O$ respectively, and the standard for carbon is Vienna Pee Dee Belemnite (V-PDB) and for oxygen is Vienna Standard Mean Ocean Water (V-SMOW).

Using methods described in detail by Garrett et al. (2015), the $\delta^{13}C$ value of early Miocene atmospheric CO_2 was estimated (mean: -6.0±0.2‰; Zachos et al., 2001; Zachos et al., 2008; Tipple et al., 2010), and fossil $\delta^{13}C$ values are expressed throughout as

modern equivalents (shifted by +2‰) based on a modern atmospheric CO_2 $\delta^{13}C$ value of -8.0‰.

Carbon Isotope Results

The carbon isotope composition of the Rusinga mammalian enamel spans the entire range of modern C_3 biomes (-30.9‰ to -23.5‰), and no individuals sampled have $\delta^{13}C$ values that require consumption of C_4 vegetation (**Table 10, Figs. 17-19**). The majority of specimens (71%) fall within one standard deviation of modern mean C_3 vegetation, indicating most sampled animals foraged in environments with neither light/water stressed vegetation nor closed canopies.

Numerous specimens sampled from the Hiwegi and Kulu Formations (*n*=23) have $\delta^{13}C$ values consistent with foraging in more open habitats in which plants experienced light/water stress, but only three specimens – two specimens of the tragulid *Dorcatherium pigotti* from the Hiwegi Formation and one of the rhinocerotid *Chilotherium ringstron* from the Kulu Formation) – have $\delta^{13}C$ values low enough to indicate foraging in a closed-canopy forest. None of the Hiwegi Formation specimens sampled from the R3 locality have $\delta^{13}C$ values that indicate the animals foraged in closed-canopy forests; this is particularly interesting in light of the fossilized forest with tree stump densities indicating an interlocking and therefore closed canopy recently recovered at this locality (see Michel et al., 2014). This may be an artifact of species sampling (i.e., individuals foraging within the close canopy habitats were inadvertently

not included in this study and the individuals sampled foraged elsewhere early in life and were buried in the paleosol layer at R3); however, the fossilized forest remnants indicate a widespread close-canopied forest and this study demonstrates the presence of both average C_3 habitat (such as open-canopy woodlands) as well as water and/or light stressed habitats in the same stratigraphic layers as the fossilized tree stumps and roots at the R3 locality. In addition to the possibility of multiple habitats within an individual's lifetime foraging range, the ^{13}C enrichment in the R3 fauna may be due to the strong seasonality indicated in the paleosol macromorphology and represent water-stressed C_3 vegetation within the close-canopy forest. Below we discuss the results by higher taxon.

Anthracotheriidae

The $\delta^{13}C$ values for the two anthracotheres from the Kulu Formation are -14.2‰ and -11.5‰ (midpoint = -12.9‰), and the $\delta^{13}C$ value from the Grit/Fossil Bed Member Hiwegi Formation (R1) anthracothere is -11.4‰. While one of the Kulu Formation anthracothere specimens was consuming average C_3 vegetation, the $\delta^{13}C$ values from the other Kulu Formation anthracothere as well as from the Grit/Fossil Bed Member of the Hiwegi Formation suggests these two specimens were consuming C_3 vegetation from more open water and/or light stressed habitats such as woodlands or wooded C_3 grasslands. An alternative explanation for the more enriched ^{13}C enamel values for these individuals is the consumption of aquatic plants. Most aquatic plants utilize the C_3 photosynthetic pathway; however, rather than atmospheric CO_2, these plants receive their carbon from dissolved bicarbonate, which is generally ^{13}C enriched relative to

atmospheric CO_2 (Keeley and Sandquist, 1992; Hayes, 1993; Chikaraishi and Naraoka, 2003). Animals consuming marine vegetation would consequently also have more enriched $\delta^{13}C$ enamel values.

Suidae

Three of the four suids sampled from the Grit/Fossil Bed Members indicate they were foraging in more open habitats with C_3 vegetation experiencing light and/or water stress (mean $\delta^{13}C$ = -11.8 ± 1.9‰). Similarly, the one suid (*N. kijinium*) from the Kibanga Member of the Hiwegi Formation also has a ^{13}C-enriched $\delta^{13}C$ value suggesting light and/or water stressed habitats ($\delta^{13}C$ = -10.9‰). The $\delta^{13}C$ values from three suids (two *B. jeanelli* and one *N. kijivium*) from the Kulu Formation indicate these individuals were consuming average C_3 vegetation (mean = -13.1 ± 0.7‰). The six specimens from the Rusinga collections that lack locality data show a similar pattern, with four consuming average C_3 vegetation, and two foraging in more open habitats ($\delta^{13}C$ enamel range: -13.1 to -10.7‰). One additional suid, (*N. kijivium*) from Mfangano Island was included in the dataset and also has a $\delta^{13}C$ value that indicates a diet of water and/or light stressed C_3 vegetation (-11.2‰). Notably, evidence for foraging in more open habitats is exhibited by members of all three suid species.

Extant East African suids exhibit the full range of enamel $\delta^{13}C$ values, from C_3 hyper-browsers (e.g., *Hylochoerus meinertzhageni*), with diets consistent to closed-canopy forest floor vegetation, to C_4 hyper-grazers (e.g., *Phacochoerus africanus*). None of the

Rusinga suids exhibit ^{13}C-depleted $\delta^{13}C$ values indicating closed-canopy browsing, but rather typical C_3 browsing in mixed habitats (including water/light stressed C_3 habitats), most similar to extant *Potamochoerus larvatus*.

Sanitheridae

The $\delta^{13}C$ value for the *Diamantohyus africanus* specimen from Karungu is -9.8‰, which indicates this sanitherid was consuming vegetation that was experiencing light and/or water stress. Interestingly, there is only one Rusinga specimen that had a more positive $\delta^{13}C$ value, a chalicothere from the Kulu Formation, potentially indicating that nearby Karungu included even more water/light stressed habitats than Rusinga and suggests further sampling of the Karungu fauna is warranted to obtain a complete picture of the Kisingiri volcano fossil site paleoenvironmental variation.

Tragulidae

The $\delta^{13}C$ values from the three *D. pigotti* from the Grit/Fossil Bed Members of the Hiwegi Formation (mean $\delta^{13}C = -13.9 \pm 3.5$‰), and one *Dorcatherium sp.* from neighboring Mfangano Island ($\delta^{13}C = -12.6$‰), indicate a wide range of foraging habitats. Interestingly, two tragulids from the Grit/Fossil Bed Members are the only two specimens of any taxa from the Hiwegi Formation with $\delta^{13}C$ values that indicate foraging in a closed-canopy habitat; conversely, the remaining Grit/Fossil Bed Member tragulid has a $\delta^{13}C$ value ^{13}C-enriched enough to indicate foraging in water and/or light stressed

habitats. Microwear analysis on the Rusinga tragulids indicated *Dorcatherium pigotti* was a mixed feeder with microwear textures close to modern grazers/generalists (Ungar et al., 2012). The $\delta^{13}C$ values from four *D. pigotti* specimens span the entire range of extant C_3 plants (-24.0 to -30.9‰) and corroborate their reconstruction of a forested/woodland habitat with the possibility of some grass included in the diet

Chalicotheriidae

The mean $\delta^{13}C$ value for the three chalicotheres from the Fossil/Grit Members of the Hiwegi Formation is -12.2 ± 1.6 ‰, the two chalicotheres from the Kibanga Member of the Hiwegi Formation had $\delta^{13}C$ values of -10.9‰ and -11.9‰ (midpoint $\delta^{13}C$ value = -11.4%), the two chalicotheres from the Kulu Formation had $\delta^{13}C$ values of -9.4‰ and -12.3‰ (mean $\delta^{13}C$ = -10.8%). The $\delta^{13}C$ enamel values from four *B. rusingense* fossils indicate herbivorous diets from habitats that include light/water stressed areas; this includes two from the Fossil/Grit Member of the Hiwegi Formation, one from the Kibanga Member of the Hiwegi Formation, and one from the Kulu Formation. The Rusinga chalicotheres corroborate the microwear studies discussed above indicating a browsing diet (Schulz et al., 2007; Semprebon et al., 2011), and indicate *Butleria rusingense* was in fact a C_3 browser that appears to prefer the more open habitats.

Rhinocerotidae

The carbon isotope composition from the sampled Rusinga rhinocerotids span the entire range of C_3 vegetation types: mean $\delta^{13}C$ for the 21 from the Fossil/Grit Member of the Hiwegi Formation is -12.7 ± 1.0‰, for the two from the Kibanga Member of the Hiwegi Formation is -14.3 ± 0.6‰, for the four from the Kulu Formation is -13.3 ± 1.8‰, and for the two from R74 is -13.5 ± 1.1‰. Four rhinocerotids, which are not identifiable to genus and species, exhibit $\delta^{13}C$ values ^{13}C-enriched enough to indicate foraging in more open habitats where the C_3 vegetation was under water and/or light stress: one from the Kulu Formation (R4 locality; $\delta^{13}C$ = -11.2‰), and three from the Grit/Fossil Bed Member of the Hiwegi Formation (R1 and R106 localities; $\delta^{13}C$ values = -10.4‰, -10.5‰, and -11.2‰).

A single *Chilotheridium pattersoni* from the Kulu Formation (Wakondo locality) is the only Rhinocerotidae sampled that exhibits a $\delta^{13}C$ value ^{13}C-depleted enough to indicate foraging in closed-canopy habitats (-15.4‰). This specimen is the only individual from the Wakondo locality of the Kulu Formation, which, based on this noticeably lighter $\delta^{13}C$ value from the other Kulu Formation specimens, indicates spatial or temporal heterogeneity in habitats in the upland catchment of the lake represented by the Kulu Formation. However, as this is the only specimen sampled from Wakondo, additional specimens would be required to evaluate the total variation in habitats captured by the Kulu Formation lacustrine deposits.

Modern rhinoceratids exhibit both C_3-grazing and C_4-browsing suggesting dietary niche partitioning between the two African species, with *Diceros bicornis* consuming a C_3 dominated diet with a mean $\delta^{13}C$ value of ~-10.5‰ and *Ceratotherium simum* consuming a C_4 dominated diet with a mean $\delta^{13}C$ value of ~0.0‰ (Kingston and Harrison, 2007). Although all of the Rusinga rhinoceratids were consuming pure C_3 diets, a small number of them (~14%) appear to be thriving in more open habitats.

Proboscidea

Five deinotheres were included in this analysis: three from the Kulu Formation (mean $\delta^{13}C$ = -13.4 ± 0.3‰), one from R74 ($\delta^{13}C$=-13.4‰), and one from the mainland locality Karungu ($\delta^{13}C$ = -13.1‰). Nine gomphotheres were sampled: three from the Grit/Fossil Bed Member of the Hiwegi Formation (mean $\delta^{13}C$ = -12.7 ± 0.7‰), four from the Hiwegi Formation (without specific member information; mean $\delta^{13}C$ = -11.3 ± 0.8‰), and two from the Kulu Formation (mean $\delta^{13}C$ = -13.2 ± 0.5‰). Nine proboscideans, without identification to the familial level were also sampled: two from the Grit/Fossil Bed Member of the Hiwegi Formation (mean $\delta^{13}C$ = -12.9 ± 0.8‰), two from the Kibanga Member of the Hiwegi Formation (mean $\delta^{13}C$ = -13.2 ± 1.7‰), three from the Kulu Formation (mean $\delta^{13}C$ = -13.3 ± 0.8‰), one from the R74 locality ($\delta^{13}C$=-13.8‰), and one from an unknown Rusinga locality ($\delta^{13}C$ = -13.6‰). Nearly all of the fossil Proboscidea sampled were consuming average C_3 vegetation, the only exceptions being three Hiwegi Formation gomphotheres, which exhibit evidence for more open habitat preference with a diet including water and/or light stressed C_3 vegetation.

Modern African elephants have a predominantly C_3 diet with only those from the Amboseli and Tsavo regions of Kenya consuming a significant amount (> 20%) of C_4 vegetation. Although modern African elephants are predominantly browsers, the fossil proboscideans show a greater range of dietary variation; while deinotheres consistently consume C_3 vegetation from the early Miocene through the early Pleistocene, starting in the Late Miocene many other proboscideans including gomphotheres consume considerable amounts of C_4 vegetation (Cerling et al., 1999). While the early Miocene Rusinga *Prodeinotherium hobleyi* are consuming an average C_3 diet consistent with other deinotheres studied, the gomphtheres from Rusinga do not show evidence for any C_4 consumption. That being said, of the two types of fossil Proboscideans, it is only the gomphotheres that show any expansion into the water/light stressed open habitats, which may be an early indication of dietary and habitat niche separation between these two families of proboscidean.

Hyracoidea

Both the Grit/Fossil Bed Member hyracoids ($\delta^{13}C$ mean: -13.2 ± 1.6‰; *n*=3) and the Kibanga Member hyracoids ($\delta^{13}C$ mean: -12.6 ± 1.4‰; *n*=2) including specimens that indicate more open habitats with C_3 vegetation experiencing light and/or water stress. The *Afrohyrax championi* specimen from R74 has the most negative $\delta^{13}C$ value for the hyracoids sampled (-14.5‰) although it still falls within one standard deviation of mean modern C_3 plants and does not indicate foraging in a closed-canopy habitat.

Carnivora and Creodonta

The $\delta^{13}C$ value for the single *Afrosmilus sp.* from the Kibanga Member of the Hiwegi Formation sampled is -11.1‰ and for the single *Cynelos euroyodon* from the Kulu Formation sampled is -12.0‰. The ^{13}C-enriched $\delta^{13}C$ value for the *Afrosmilus sp.* indicates its prey was consuming C_3 vegetation from more open C_3 habitats. The single indeterminate Hyaenodonitidae specimen sampled from the Grit/Fossil Bed Member (R5) of the Hiwegi Formation had a $\delta^{13}C$ value of -12.3‰. Although only one specimen from each of the three Carnivora/Creodonta taxa was sampled, there is not a large amount of variation in the $\delta^{13}C$ values of the tooth enamel for these taxa, suggesting limited dietary niche separation among prey items between these three species; however, since this is a small dataset, further analysis would be required to fully understanding prey choice and any competitive exclusion among prey items amongst the early Miocene predators.

Oxygen Isotope Results

The Rusinga fauna exhibits a wide range of variation in enamel $\delta^{18}O$ values (22.4 to 34.0‰; **Table 10, Figs. 18-20**), documenting considerable variation in the oxygen isotope compositions of the animal water sources, evaporative effects on drinking or plant water, and species thermophysiological adaptations. Most of the taxa have a noticeable correlation between their enamel $\delta^{13}C$ and $\delta^{18}O$ values (**Fig. 18**). For example, specimens that have relatively high $\delta^{13}C$ values also have relatively high $\delta^{18}O$

values, indicating they are feeding and obtaining their water, either by obligate drinking or via their food, in the same open (water/light stressed) habitat. This trend is seen in all of the taxa with an adequately large sample size, the proboscideans, rhinocerotids, and suids. The tragulids and chalicotheres do not show this correlative trend between their enamel $\delta^{13}C$ and $\delta^{18}O$ values. This may indicate these two taxa are feeding in a different type of habitat than where they are obtaining water, or this lack of trend may simply be an artifact of their small sample sizes; additional samples are required to make any definitive statements about feeding/drinking preferences for these taxa. Finally, for the proboscideans, rhinocerotids, and suids that do show a correlation between enamel $\delta^{13}C$ and $\delta^{18}O$ values, the specimens from the Kulu Formation have relatively higher $\delta^{18}O$ values than the specimens of the same taxa from the Hiwegi Formation (**Fig. 18**). This trend is apparent even though the $\delta^{13}C$ values do not show any ^{13}C depletion or enrichment relationship to formation for these three taxa suggesting there is a difference in meteoric water $\delta^{18}O$ values between the Kulu and Hiwegi Formations (**Figs. 18-20**).

While there are a number of taxa sampled that will have $\delta^{18}O$ values that record meteoric water $\delta^{18}O$ values (evaporation insensitive obligate drinkers such as proboscideans and rhinoceratids), there is no way to be truly certain if any of the remaining taxa are evaporation sensitive without making assumptions about drinking habits based on taxonomic uniformitarianism. As such, applying an aridity index, such as that defined by Levin et al. (2006) would be speculative. However, it is possible to determine if there were any noticeable trends or changes in meteoric water in the various levels of the Rusinga Groups strata using Student's *t*-tests to compare the $\delta^{18}O$ values of the Rusinga

proboscideans and rhinoceratids that can be reliably placed into the Grit/Fossil Bed Member and Kibanga Member of the Hiwegi Formation, or the Kulu Formation. These statistical tests are used to determine if the oxygen isotope composition from two of the localities are significantly different from each other (see **Table 11**).

The Grit/Fossil Bed Member proboscideans and rhinoceratids (*n*=26) have $\delta^{18}O$ values that range from 24.4-30.6‰, the Kibanga Member proboscideans and rhinoceratids (*n*=4) have $\delta^{18}O$ values that range from 23.7-28.5‰, and the Kulu Formation proboscideans and rhinoceratids (*n*=12) have $\delta^{18}O$ values that range from 27.4-31.3‰. The $\delta^{18}O$ values of proboscideans and rhinoceratids from the Grit/Fossil Bed Member and the Kibanga Member of the Hiwegi Formation are statistically indistinguishable. The Kulu Formation proboscideans and rhinoceratids however, are statistically significantly more ^{18}O-enriched than those from both the Grit/Fossil Bed Member and Kibanga Member of the Hiwegi Formation (**Table 11**). This increase in $\delta^{18}O$ enamel values represents either an increase in mean annual temperature, an increase in aridity (evaporation), a decrease in mean annual precipitation or some combination of the three climatic factors experienced by the Kulu Formation fauna. There are a number of taxa found in the Hiwegi Formation deposits that are missing from the Kulu Formation (**Table 9**), and these changes in faunal composition may be directly related to this climatic difference rather than an issue of sampling or preservation. Future paleosol geochemistry or macrobotanical remains (e.g., percent whole margin or leaf area analyses) may help to establish the climatic basis of the change in the $\delta^{18}O$ value of meteoric water inferred from the tooth enamel data.

Discussion

It is clear from the Rusinga Island mammalian tooth enamel carbon and oxygen isotope compositions that these early Miocene faunal communities did not inhabit a spatially homogeneous habitat that did not change through time as concluded in previous paleoenvironmental analyses. Additionally, the Rusinga habitats were not the wet, tropical, closed-canopy forests often associated with the early Miocene and generally presented as typical hominoid habitats (see Andrews, 1992). Analyzing the carbon isotope composition of the primates themselves, work that is presently underway, will provide information on the diet and habitat for these species. If any of the primate specimens have enriched $\delta^{13}C$ enamel values similar to the rest of the Rusinga fauna, it will confirm that the early members of Hominoidea did not exclusively inhabit close-canopy forests and exhibited adaptations to more open habitats. However, if the primates have depleted $\delta^{13}C$ enamel values similar to the three faunal specimens indicating close-canopy forest foraging, these results will directly tie these primates to dense forest habitats and further verify the conclusion here of high levels of spatial and temporal habitat variability. These analyses will also address questions of habitat or dietary niche separation among the primate community and interestingly, between the two *Ekembo* species.

The range of enamel $\delta^{13}C$ values from the Rusinga fauna presented here suggests a modest degree of habitat variability, which would have included a temporally and/or

spatially dynamic mixture of open-canopy forests/woodlands and more open habitats (such as shrublands, bushlands, or woody grasslands — i.e., habitats with less than 80% woody cover; White, 1983; Cerling et al., 2011). Unfortunately, without high levels of temporal resolution, it is not possible to tell the difference between temporal and spatial variability as the paleosols and lacustrine sediments and the fossils contained therein represent a temporal average of hundreds to thousands of years and the animals can travel large spatial distances during their lifetimes. Some of the ^{13}C enriched enamel values, specifically those from the semi-aquatic anthracotheres, may indicate the consumption of aquatic C_3 flora, rather than water and/or light stressed vegetation. That being said, the consumption of aquatic plants is not indicated for the other fauna that exhibits ^{13}C-enriched enamel values.

Although some lineages of C_4 grasses evolved during the Oligocene (Sage, 2004; Christin et al., 2008; Vicentini et al., 2008; Edwards et al., 2010; Sage et al., 2011; Christin and Osborne, 2014), and therefore could be present in East Africa during the early Miocene, the mammalian carbon isotope compositions analyzed from Rusinga indicate C_4 plants, if present, were not consumed in enough abundance to leave an isotopic signal in the tooth enamel. Although C_4 plants may have still been present in some small quantity in the ecosystem, $\delta^{13}C$ values from paleosol organic matter also indicates an overall lack of C_4 vegetation (see **Chapter 2**) and corroborates the conclusion that the early Miocene Rusinga habitats were composed of pure C_3 vegetation. Notably, $\delta^{13}C$ values of fossil rhinocerotid and proboscidean tooth enamel from the early Middle Miocene site at Tugen Hills (Member 1, Kipsaramon site; 15.8-15.6 Ma) indicate

the inclusion of small amount of C_4 plants in the diet of these animals. The presence of C_4 grasses in the Tugen Hills during the Middle Miocene is also supported by pedogenic carbonate analyses (Kingston, 1992; Kingston et al., 1994; Morgan et al., 1994; Behrensmeyer et al., 2002). The Tugen Hills Member 1 deposit is slightly younger than the youngest of the Rusinga Group strata (i.e., the Kulu Formation) and suggests there is heterogeneity in onset timing and location of C_4 biomass in East Africa, with the Rusinga deposits maintaining a pure C_3 ecosystem, while C_4 grasses had already increased to abundances recognizable in the $\delta^{13}C$ values of mammalian tooth enamel and paleosols in the Tugen Hills.

There does not appear to be any overall trend within the Hiwegi Formation or between the Hiwegi and Kulu Formations carbon isotope composition, but rather the entire dataset suggests predominately average C_3 habitats during deposition of the Hiwegi Formation with some more open water/light stressed habitats. Evidence for closed-canopy habitats is rare – only three specimens sampled indicate foraging in a closed-canopy forest – which is of particular interest in light of the fossil forest found within the Kibanga Member paleosol (Michel et al., 2014). Although it is possible the dense forest habitats present during this time were small and localized, and therefore not large enough for the canopy effect to occur, based on the scale, density, and distribution of tree stump casts over ca. 4.5 kilometers of outcrops of the tree stump casts at multiple localities (R1, R2, and R3; Michel et al., 2014), this seems unlikely. However, paleosol carbon isotope compositions from the R3 paleosol also do not exhibit evidence for CO_2 recycling in a closed canopy forest (see **Chapter 2**). As such, a further analysis of a larger sample of

mammalian enamel, including primates and other fauna likely to be inhabiting and foraging within the dense forest habitats is required to resolve these two disparate pieces of information.

There is a measured difference in the oxygen isotope composition of the meteoric water between the Hiwegi and Kulu Formations, as determined by the enamel $\delta^{18}O$ values of rhinocerotids and proboscideans. The significant ^{18}O enrichment in the Kulu Formation indicates either an increase in mean annual temperature, and increase in aridity (evaporation), a decrease in mean annual precipitation or some combination of the three climatic factors; regardless of which climatic factor, this was a noticeable shift that may have impacted the Kulu Formation fauna and explain differences in faunal community composition. These climatic changes may be directly related to the increasing global temperatures that occurred in the millennia prior to the Mid-Miocene Climatic Optimum (Flower and Kennett, 1994; Zachos et al., 2001).

Many of the previous paleoenvironmental reconstructions for Rusinga have yielded a wide range of often conflicting results and interpretations, indicating habitats ranging from closed forests, woodland, or rainforest, mosaic habitats of both open and closed habitats, and even semi-arid environments. In light of the dataset presented here, the seemingly disparate paleoenvironmental reconstruction may be, in part, a reflection of the spatial and temporal heterogeneity in the early Miocene Rusinga ecosystem rather than the product of conflicting results from different proxies.

The placement of the Rusinga primate community within these spatially and temporally varied habitats indicates they were able to cope and even thrive within this dynamic landscape by inhabiting both closed and more open habitats (see **Chapter 2**). Importantly, the placement of an early member of Hominoidea, *Ekembo*, in habitats that are not dense closed- and interlocking-canopy forests has a direct impact on its locomotor reconstructions. The adaptations for extensive climbing and clambering capabilities seen in *Ekembo*, including the ability for a high degree of hallux flexion and powerful forelimb and hindlimb grasping (Sarmiento, 1983; Langdon, 1986; Rose, 1992; Rose, 1993; Walker et al., 1993; Begun et al., 1994; Rose, 1994; Dunsworth, 2006) and enhanced joint mobility throughout the forelimb (Jenkins, 1973; Rose, 1998) and hindlimb (Rose, 1993; Ward, 1993; Rose, 1994; Ward et al., 1995; Ward, 1997; Bacon, 2001). This suite of adaptations may have been a biological adaptation to environmental and ecosystem fluctuations, suggesting habitat flexibility may be a primitive characteristic for all hominoids. A direct evaluation of the Rusinga primate dietary isotope ecology will allow for an assessment of the diet, and by extension the possibility of niche separation, of the two species of *Ekembo* and the other catarrhines present on Rusinga.

Conclusions

The aim of this study was to test the assumption that the entire Rusinga Group represents a relatively stable (i.e., unchanged through time) paleoenvironment. Although this assumption has been justified by the seeming taxonomic composition stability of faunal

assemblages, collected from various fossil localities throughout the sequence (e.g., Pickford, 1981; Pickford, 1984; Andrews et al., 1997; Peppe et al., 2009), recent studies have indicated more geological complexity is present than previously believed and shown evidence for paleoenvironmental variability including both open, drier woodland habitats and a dense close-canopy forest (for example, McCollum et al., 2013).

The carbon isotope composition of the Rusinga Group mammalian fauna suggest a high degree of spatial variability in both the Kulu and Hiwegi Formation habitats throughout the early Miocene succession on Rusinga. The range of C_3 foods actively exploited by the mammals in this study included a significant number of plants experiencing water and/or light stress. Evidence for exploitation of plant resources from close-canopy forests experiencing CO_2 recycling was rare however. Finally, the oxygen isotope composition of the Rusinga Group mammals documents either an increase in mean annual temperature, an increase in aridity, a decrease in mean annual precipitation, or some combination of the three climatic factors in the Kulu Formation relative to the Hiwegi Formation.

Figures and Tables

Table 9. Early Miocene fossil mammals from Rusinga and Mfangano Islands.

Order	Family	Species	Kulu	Hiwegi
Artiodactyla	Anthracotheriidae	*Brachyodus aequatorialis*	x	x
		Kulutherium kenyensis	x	
		Sivameryx africanus	x	x
		Sivameryx moneyi	x	x
	Giraffidae	*Canthumeryx sirtensis*		x
	Sanitheridae	*Diamantohyus africanus*	x	x
	Suidae	*Kenyasus rusingensis*	x	x
		Kubanochoerus anchidens		x
		Libycochoerus jeanelli	x	x
		Nguruwe kijivium	x	x
	Tragulidae	*Dorcatherium chappuisi*	x	x
		Dorcatherium parvum	x	x
		Dorcatherium pigotti	x	x
	incertae sedis	*Propalaeoryx nyanzae*		x
		Walangania africanus	x	x
Carnivora	Amphicyonidae	*Cynelos euryodon*	x	x
		Cynelos macrodon		x
	Barbourofelidae	*Afrosmilus africanus*		x
	Herpestidae	*Kichechia zamanae*	x	x
Chiroptera	Emballonuridae	indet		x
	Pteropodidae	*Propotto leakeyi*		x
	Megadermatidae	indet		x
	Molossidae	*Tararida rusingae*		x
Creodonta	Hyaenodontidae	*Anasinopa leakeyi*		x
		Isohyaenodon andrewsi		x
		Isohyaenodon pilgrimi		x
		Hyainailourus nyanzae	x	x
		Leakeytherium hiwegi	x	x
		Megistotherium sp.		x
		Metapterodon kaiseri		x
		Teratodon enigma		x
		Pterodon nyanzae		x
		Pterodon africanus		x

Order	Family	Species	Kulu	Hiwegi
Hyracoidea	Titanohyracidae	*Afrohyrax championi*	x	x
	Pliohyracidae	*Mereohyrax (Prohyrax) bateae*		x
Insectivora	Erinaceidae	*Amphechinus rusingensis*	x	x
		Galerix africanus		x
		Gymnurechinus leakeyi	x	x
		Gymnurechinus camptolophus		x
Lagomorpha	Ochotonidae	*Kenyalagomys minor*		x
		Kenyalagomys rusingae	x	x
Macroscelidea	Macroscelididae	*Hiwegicyon juvenalis*		x
		Miorhynchocyon clarki	x	x
		Miorhynchocyon rusingae		x
		Myohyrax oswaldi	x	x
Perissodactyla	Chalicotheriidae	*Butleria rusingense*	x	x
	Rhinocerotidae	*Aceratherium acutirostratum*	x	x
		Brachypotherium heinzelini		x
		Chilotheridium pattersoni	x	
		Dicerorhinus leakeyi	x	x
Primates	Dendropithecidae	*Dendropithecus macinnesi*	x	x
	Galagidae	*Komba minor*		x
		Komba robustus		x
		Komba walker		x
		Progalago songhorensis		x
	Lorisidae	*Mioeuoticus bishopi*		x
		Mioeuoticus shimpani		x
	incertae sedis	*Ekembo heseloni*	x	x
		Ekembo nyanzae	x	x
		Limnopithecus legetet		x
		Nyanzapithecus vancouveringorum		x
Proboscidea	Deinotheriidae	*Prodeinotherium hobleyi*	x	x
	Gomphotheriidae	cf. *Archaeobelodon sp.*	x	x
	Mammutidae	*Zygolophodon morotoensis*		x
Rodentia	Anomaluridae	*Paranomaluris soniae*		x
		Paranomaluris walkeri		x
	Bathyergidae	*Proheliophobius leakeyi*		x
	Kenyamyidae	*Kenyamys mariae*		x
		Simonimys genovefae		x

Order	Family	Species	Kulu	Hiwegi
	Muridae	*Protarsomys macinnesi*		x
	Myophiomyidae	*Elmerimys woodi*		x
		Myophiomys arambourgi		x
	Nesomyidae	*Notocricetodon petteri*		x
	Pedetidae	*Megapedetes pentadactylus*		x
		indet		x
	Phiomyidae	*Diamantomys luederitzi*		x
	Sciuridae	*Vulcanisciurus africanus*		x
	Thryonomyidae	*Epiphiomys coryndoni*		x
		Paraphiomys pigotti	x	x
		Paraphiomys stromeri	x	x
	incertae sedis	*Lavocatomys aequatorialis*		x
Tenrecoidea	Tenrecidae	*Parageogale aletris*		x
		Protenrec tricuspis		x
Tubulidentata	Orycteropodidae	*Myorycteropus africanus*	x	x

Table 10. Carbon and oxygen isotope composition of mammalian enamel samples from Rusinga and Mfangano Islands analyzed at the University of Minnesota Stable Isotope Lab. Formation and locality information provided for Rusinga Island specimens when known. All $\delta^{13}C$ values corrected to modern atmospheric CO_2.

Taxon	Field No.	Sample No.	Formation	Locality	$\delta^{13}C$ value (‰; VPDB)	$\delta^{18}O$ value (‰; VSMOW)
Artiodactyla						
Anthracotheriidae						
Anthracothere	RU2008-176	07.07.11.01	Hiwegi	R1	-11.37	27.21
Anthracothere	RU2009-963	07.07.11.11	Kulu	R4	-14.19	27.01
Anthracothere	RU2009-1016	07.07.11.12	Kulu	R4	-11.54	28.06
Suidae						
Kenyasus rusingensis	RU 2007-890	26.02.15.47	Hiwegi	R1	-11.27	25.12
Kenyasus rusingensis	RU-2006-487	26.02.15.33	Hiwegi	R5	-14.51	25.92
Kenyasus rusingensis	RU 2007-1104	26.02.15.41	Kulu	R4	-13.52	24.18
Kenyasus rusingensis	RU 2008-280	26.02.15.61	Kulu	R4	-12.31	25.69
Libycochoerus jeanneli	none	26.02.15.42	Hiwegi	R1	-10.34	28.02
Libycochoerus jeanneli	none	26.02.15.43			-10.76	27.18
Libycochoerus jeanneli	R 113 '47	26.02.15.28	Kulu	R4	-13.50	27.38
Libycochoerus jeanneli	none	26.02.15.29			-12.40	27.24
Libycochoerus jeanneli	830'56	26.02.15.51			-12.14	24.52
Nguruwe kijivium	R1A (RS 1A)	26.02.15.60	Hiwegi	R1	-10.96	25.02
Nguruwe kijivium	R 590:50	26.02.15.45	Hiwegi	R3	-10.92	28.28
Nguruwe kijivium	R 759:50	26.02.15.55			-13.08	24.10
Nguruwe kijivium	R58:51	26.02.15.56			-12.85	22.37
Nguruwe kijivium	R576:48	26.02.15.49			-11.22	25.89

Taxon	Field No.	Sample No.	Formation	Locality	$\delta^{13}C$ value (‰; VPDB)	$\delta^{18}O$ value (‰; VSMOW)
Nguruwe kijivum	RU2010-1131	06.07.11.04		Mfangano	-11.24	28.79
Artiodactyla Cont.						
Sanitheridae						
Diamanfohyus africanus	RU2010-1030	06.07.11.05		Karungu†	-9.75	28.15
Tragulidae						
Dorcatherium sp.	RU2010-952	08.07.11.01	Wayando	Mfangano	-12.59	29.15
Dorcatherium pigotti	RU2009-1399	06.07.11.08	Hiwegi	R106	-16.77	31.24
Dorcatherium pigotti	RU2010-065	06.07.11.06	Hiwegi	R106	-14.94	31.22
Dorcatherium pigotti	RU2009-1290	06.07.11.07	Hiwegi	R106	-9.92	29.83
Perissodactyla						
Chalicotheriidae						
Butleria rusingense	RU2010-448	06.07.11.02	Hiwegi	R1	-13.99	29.11
Butleria rusingense	RU2010-119	06.07.11.03	Hiwegi	R106	-10.88	30.39
Butleria rusingense	RU2006-427	06.07.11.01	Kulu	R4	-9.37	34.02
Butleria rusingense	RU2009-1231	07.07.11.19	Hiwegi	R106	-11.58	28.37
Chalicothere	RU2009-1499	07.07.11.21	Hiwegi	R3	-10.94	30.53
Chalicothere	RU2009-1496	07.07.11.18	Hiwegi	R3	-11.91	28.37
Chalicothere	RU2009-1121	07.07.11.20	Kulu	R4	-12.30	29.57
Rhinocerotidae						
Brachypotherium heinzelini	RU2010-002	05.07.11.07	Hiwegi	R5	-12.10	26.66
Chilotheridium pattersoni	R506:1950	26.02.15.53	Kulu	Wakondo	-15.44	27.44

Taxon	Field No.	Sample No.	Formation	Locality	$\delta^{13}C$ value (‰; VPDB)	$\delta^{18}O$ value (‰; VSMOW)
Perissodactyla Cont.						
Rhinocerotidae Cont.						
Chilotheridium pattersoni	R 695: 1949	26.02.15.50		R74	-13.28	26.97
Dicerorhinus leakeyi	R 596:1947	26.02.15.24	Hiwegi	R1	-13.77	27.13
Dicerorhinus leakeyi	R 84:1950	26.02.15.26	Hiwegi	R1-1a	-13.02	28.11
Dicerorhinus leakeyi	R 85:1950	26.02.15.25	Hiwegi	R1-1a	-12.65	28.72
Dicerorhinus leakeyi	R 80:1950	26.02.15.38	Hiwegi	R1-1a	-12.43	28.37
Dicerorhinus leakeyi	RU-2006-308	26.02.15.18	Hiwegi	R106	-13.72	26.26
Dicerorhinus leakeyi	R 1385:1951	26.02.15.23	Hiwegi	R5	-13.22	26.30
Rhinocerotidae	RU2009-773	07.07.11.15	Hiwegi	R1	-10.38	30.57
Rhinocerotidae	F 3091	26.02.15.35	Hiwegi	R1	-13.13	27.25
Rhinocerotidae	R547:49	26.02.15.36	Hiwegi	R1	-12.58	28.50
Rhinocerotidae	RU2009-1353	07.07.11.14	Hiwegi	R106	-13.06	29.92
Rhinocerotidae	RU2009-1309	07.07.11.13	Hiwegi	R106	-12.99	29.25
Rhinocerotidae	RU2010-216	05.07.11.10	Hiwegi	R106	-12.14	29.92
Rhinocerotidae	RU2009-1359	07.07.11.17	Hiwegi	R106	-11.19	30.14
Rhinocerotidae	RU2009-1349	07.07.11.16	Hiwegi	R106	-10.49	30.33
Rhinocerotidae	R 30 '48	26.02.15.20	Hiwegi	R106	-13.99	24.53
Rhinocerotidae	R807:47	26.02.15.32	Hiwegi	R3	-14.75	23.67
Rhinocerotidae	83 '56	26.02.15.34	Hiwegi	R3	-13.94	28.25
Rhinocerotidae	RU2010-018	05.07.11.09	Hiwegi	R5	-12.60	28.76
Rhinocerotidae	R 924-71	26.02.15.12	Hiwegi	R5	-14.26	25.71
Rhinocerotidae	R 107 '71	26.02.15.17	Hiwegi	R5	-13.40	27.00

Taxon	Field No.	Sample No.	Formation	Locality	$\delta^{13}C$ value (‰; VPDB)	$\delta^{18}O$ value (‰; VSMOW)
Perissodactyla Cont.						
Rhinocerotidae Cont.						
Rhinocerotidae	R 30 '71	26.02.15.16	Hiwegi	R5	-13.22	24.39
Rhinocerotidae	R8'73	26.02.15.22	Hiwegi	R5	-13.15	25.25
Rhinocerotidae	none	12.07.11.09	Kulu	R4	-13.72	30.10
Rhinocerotidae	RU2010-688	05.07.11.08	Kulu	R4	-11.20	30.02
Rhinocerotidae	RU-2007-327	26.02.15.52	Kulu	R4	-12.84	30.58
Rhinocerotidae	RU-2007-733	26.02.15.62		R74	-13.70	28.13
Proboscidea						
Deinotheriidae						
Deinotherium	RU2007-461	07.07.11.03/04	Kulu	R4	-13.11	28.88
Deinotherium	RU2009-1070	07.07.11.05	Kulu	R4	-13.31	29.96
Deinotherium	RU2007-726	07.07.11.02		R74	-13.41	29.07
Prodeinotherium hobleyi	RU2010-685	05.07.11.06	Kulu	R4	-13.71	29.68
Prodeinotherium hobleyi	RU2010-1013	05.07.11.05		Karungu†	-13.13	29.76
Gomphotheriidae						
cf. *Archaeobeledon* sp.	RU2007-1066	05.07.11.01/02	Hiwegi	Sienga	-11.74	24.93
cf. *Archaeobeledon* sp.	R 2030:50	26.02.15.63	Hiwegi	Sienga	-10.06	27.25
cf. *Archaeobelodon* sp.	RU 2007-1066	26.02.15.15	Hiwegi	Sienga	-11.77	23.38
Gomphothereiidae	R 235-48	26.02.15.03	Hiwegi	Hiwegi	-11.57	26.83
Gomphothereiidae	R 106	26.02.15.06	Hiwegi	R106	-12.41	25.28
Gomphothereiidae	R 106	26.02.15.07	Hiwegi	R106	-12.26	27.09

Taxon	Field No.	Sample No.	Formation	Locality	$\delta^{13}C$ value (‰; VPDB)	$\delta^{18}O$ value (‰; VSMOW)
Proboscidea Cont.						
Gomphotheriidae Cont.						
Gomphothereiidae	RU 1050 ‘84	26.02.15.09	Hiwegi	R5	-13.46	24.48
Gomphothereiidae	R 1153 50	26.02.15.05	Kulu	R4	-12.87	28.19
Gomphotherium(?)	RU2009-953	07.07.11.07	Kulu	R4	-13.60	31.29
Unknown Family						
Proboscidea	RU2009-564	07.07.11.08	Hiwegi	R1	-13.50	27.67
Proboscidea	RU2009-775	07.07.11.09	Hiwegi	R1	-12.38	29.03
Proboscidea	RU2009-1489	07.07.11.06	Hiwegi	R3	-14.44	27.48
Proboscidea	RU2008-145	05.07.11.03	Hiwegi	R3	-12.04	28.54
Proboscidea	RU2009-925	07.07.11.22	Kulu	R4	-14.74	30.33
Proboscidea	RU2009-1082	07.07.11.10	Kulu	R4	-13.07	30.58
Proboscidea	R 11-73	26.02.15.10	Kulu	R4	-12.22	27.43
Proboscidea	RU 2007-760	26.02.15.14		R74	-13.75	26.49
Proboscidea	F 3085:41	26.02.15.11			-13.58	27.47
Carnivora						
Amphicyonidae						
Cynelos euryodon	RU2010-699	06.07.11.16	Kulu	R4	-12.04	32.34
Barbourofelidae						
Afrosmilus sp.	RU2008-128	06.07.11.13	Hiwegi	R3	-11.14	30.34

Taxon	Field No.	Sample No.	Formation	Locality	$\delta^{13}C$ value (‰; VPDB)	$\delta^{18}O$ value (‰; VSMOW)
Creodonta						
Hyaenodontidae						
Hyaenodontida	RU2007-648	06.07.11.14	Hiwegi	R5	-12.34	27.86
Hyracoidea						
Titanohyracidae						
Afrohyrax championi	RU2010-198	08.07.11.03	Hiwegi	R106	-14.09	29.52
Afrohyrax championi	RU2010-608	06.07.11.11	Hiwegi	R3	-13.56	28.37
Afrohyrax championi	RU2010-583	08.07.11.02	Hiwegi	R3	-11.64	29.44
Afrohyrax championi	RU2010-1058	06.07.11.12		R74	-14.45	29.95
Hyracoidea?	RU2010-201	06.07.11.09	Hiwegi	R106	-11.32	31.24
Hyracoidea?	RU2010-004	06.07.11.10	Hiwegi	R5	-14.20	31.09

[†]Two specimens from Karungu (nearby mainland Kenya), which are roughly contemporaneous, were included in the specimens chosen for sampling.

Figure 17. Enamel carbon isotope composition by taxa. Fossil specimens have been corrected to modern atmospheric CO_2 (see text). The grey dashed line represents the mean of modern C_3 plants and the grey bar throughout represents the mean of modern C_3 plants ± 1 standard deviation. Animals with enamel $\delta^{13}C$ values within this range were eating plants experiencing neither CO_2 recycling nor light/water stress. Animals with enamel $\delta^{13}C$ values more negative than the mean C_3 ± 1 SD range are eating foods experiencing closed canopy CO_2 recycling. Animals with enamel $\delta^{13}C$ values less negative than the mean C_3 ± 1 SD range are eating foods experiencing light and/or water stress.

FIGURE ON NEXT PAGE

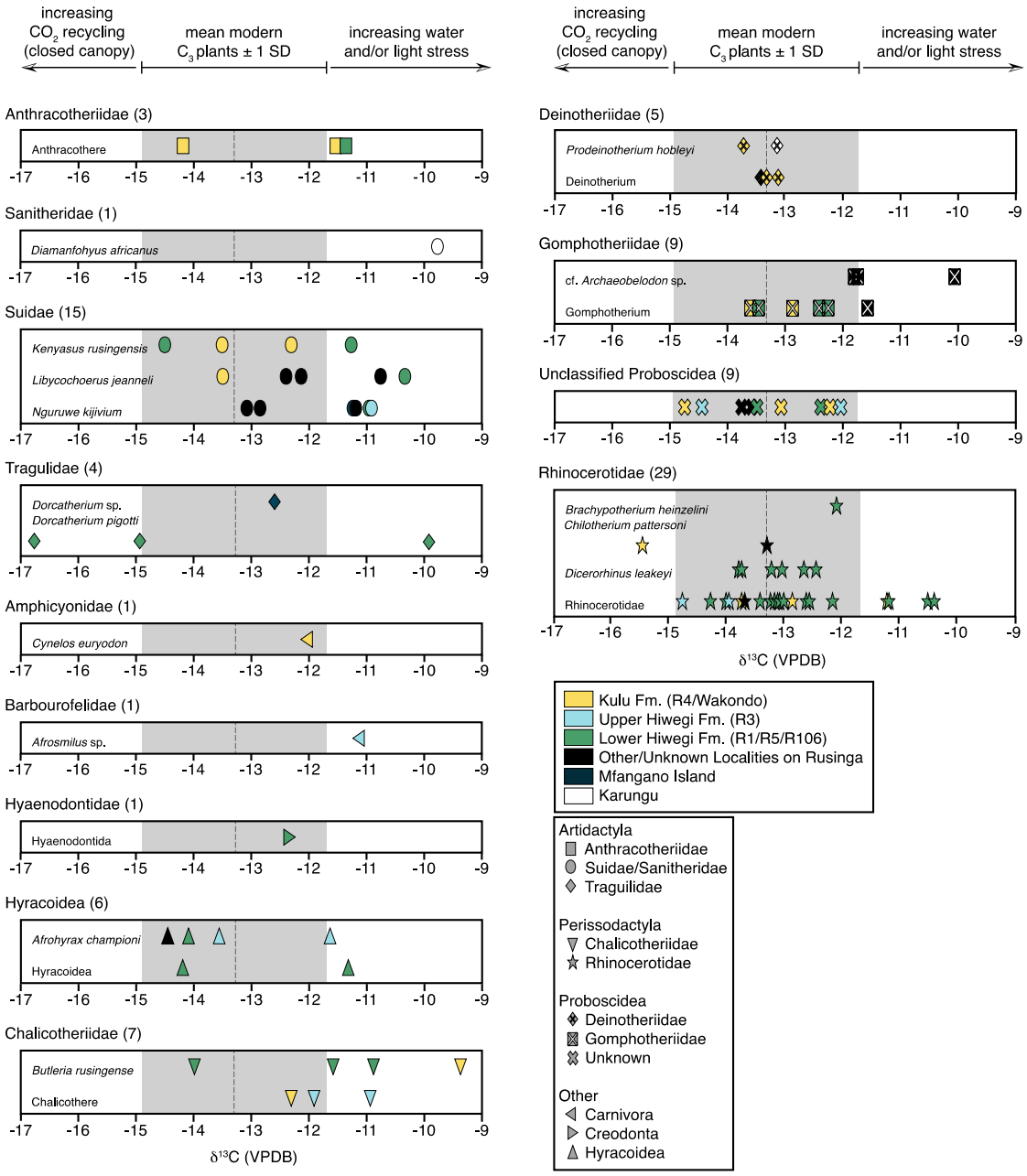
increasing CO2 recycling (closed canopy)
mean modern C3 plants ± 1 SD
increasing water and/or light stress
Anthracotheriidae (3)
Anthracothere
Sanitheridae (1)
Diamanfohyus africanus
Suidae (15)
Kenyasus rusingensis
Libycochoerus jeanneli
Nguruwe kijivium
Tragulidae (4)
Dorcatherium sp.
Dorcatherium pigotti
Amphicyonidae (1)
Cynelos euryodon
Barbourofelidae (1)
Afrosmilus sp.
Hyaenodontidae (1)
Hyaenodontida
Hyracoidea (6)
Afrohyrax championi
Hyracoidea
Chalicotheriidae (7)
Butleria rusingense
Chalicothere
-17 -16 -15 -14 -13 -12 -11 -10 -9
δ13C (VPDB)
Deinotheriidae (5)
Prodeinotherium hobleyi
Deinotherium
Gomphotheriidae (9)
cf. Archaeobelodon sp.
Gomphotherium
Unclassified Proboscidea (9)
Rhinocerotidae (29)
Brachypotherium heinzelini
Chilotherium pattersoni
Dicerorhinus leakeyi
Rhinocerotidae
Kulu Fm. (R4/Wakondo)
Upper Hiwegi Fm. (R3)
Lower Hiwegi Fm. (R1/R5/R106)
Other/Unknown Localities on Rusinga
Mfangano Island
Karungu
Artidactyla
Anthracotheriidae
Suidae/Sanitheridae
Traguilidae
Perissodactyla
Chalicotheriidae
Rhinocerotidae
Proboscidea
Deinotheriidae
Gomphotheriidae
Unknown
Other
Carnivora
Creodonta
Hyracoidea

Figure 18. Mammalian enamel carbon and oxygen isotope composition by taxa. (A) Enamel isotopic composition of all sampled rhinocerotids and proboscideans. (B) Enamel isotopic composition of all remaining fauna sampled.

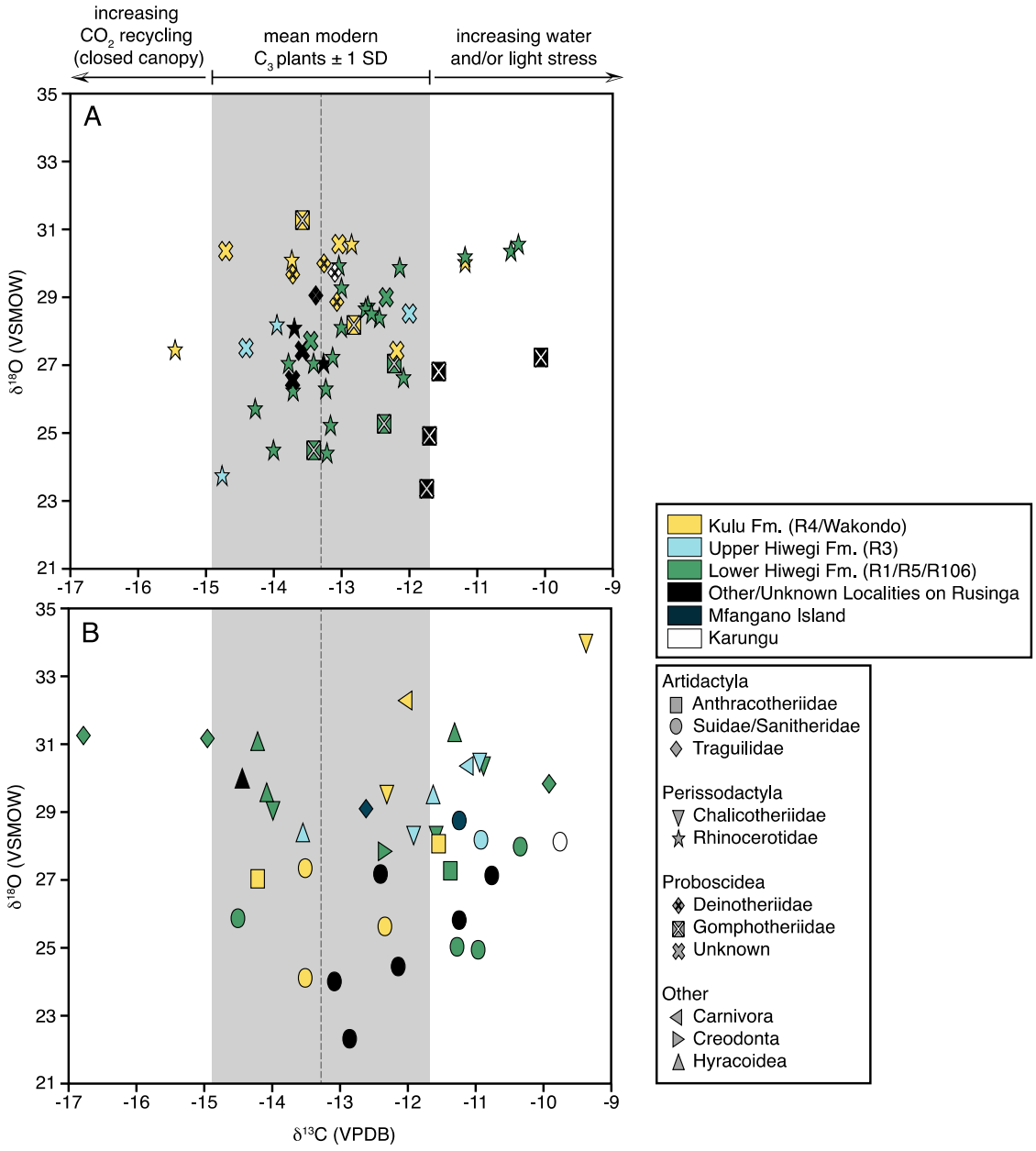

Figure 19. Mammalian enamel carbon and oxygen isotope composition by stratigraphic location. Seventy-one of the 91 total specimens can be accurately placed within the Kulu Formation or Hiwegi Formation, including relevant locality information, and only those specimens are included in this figure. (A) Generalized stratigraphy of early Miocene Rusinga Group strata on Rusinga Island. (B) Enamel isotopic composition of Kulu Formation fauna. Solid/black symbols indicate the Wakondo locality; yellow symbols indicate the R4 localitiy. (C) Enamel isotopic composition of the Upper Hiwegi Formation fauna. Light blue symbols indicate the R3 locality. (D) Enamel isotopic composition of the Lower Hiwegi Formation fauna. Open/white symbols indicate the R106 locality; light green symbols indicate the R1 locality; dark green symbols indicate the R5 locality. All fossil $\delta^{13}C$ values have been corrected to modern atmospheric CO_2 (see text).

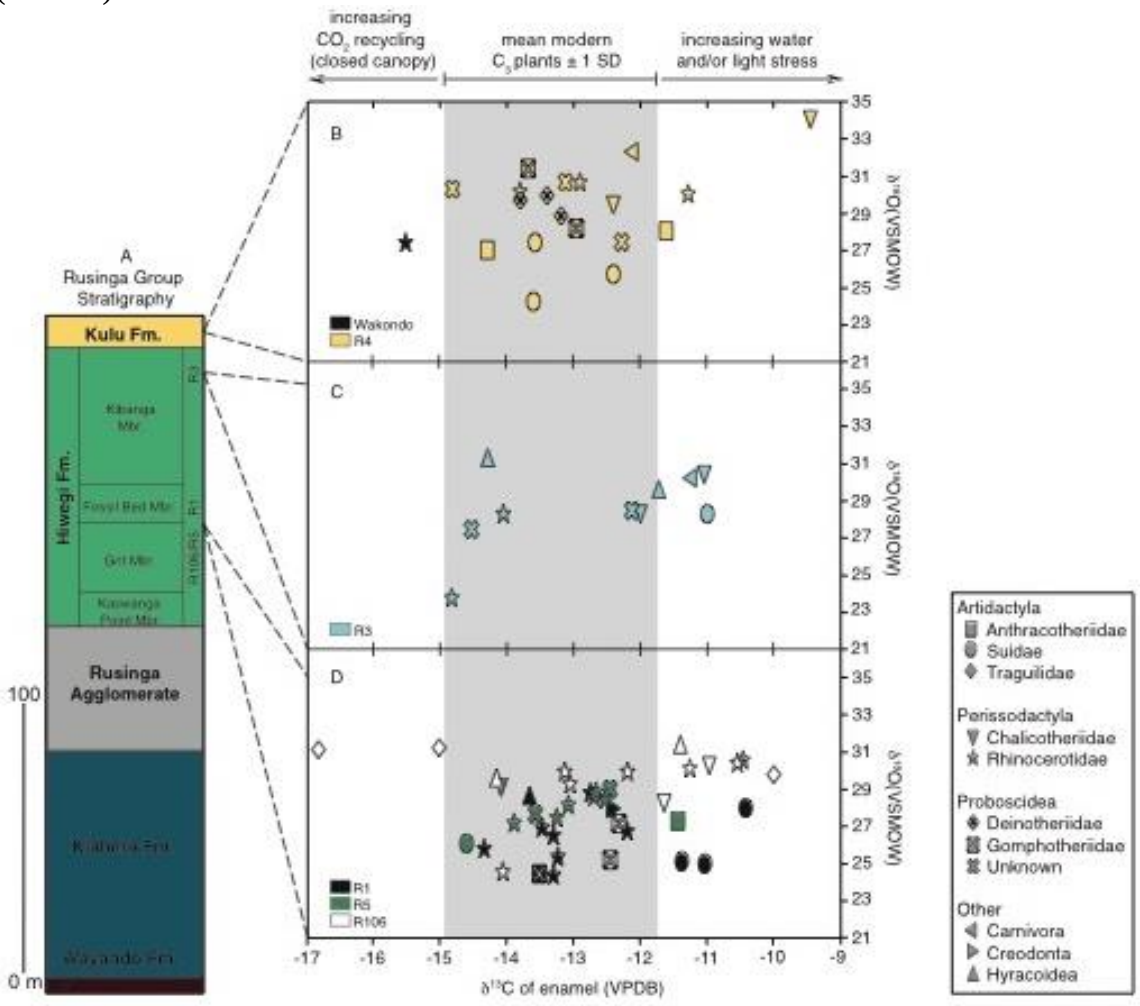

Figure 20. Enamel oxygen isotope composition by taxa.

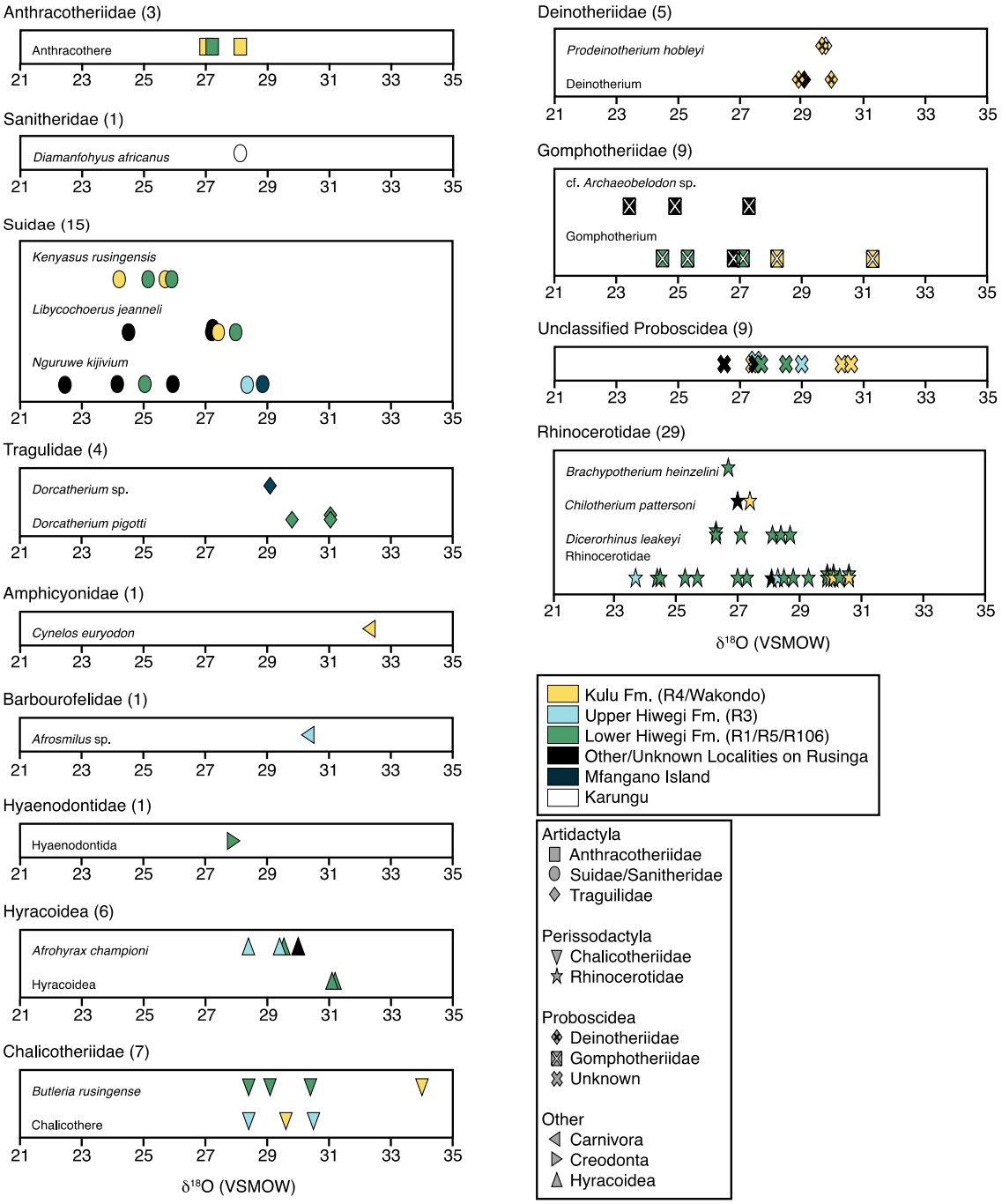

Table 11. Results of Student's t-test used to compare the $\delta^{18}O$ values of the rhinocerotids and proboscideans from the Grit/Fossil Bed Member of the Hiwegi Formation, the Kibanga Member of the Hiwegi Formation, and the Kulu Formation. Bonferroni-adjusted p-values are reported and those that show a significant difference are in boldface.

Member; Formation	**$\delta^{18}O$ mean**	**SD**	***n***	***df***	***t*-value**	***p*-value**
Grit/Fossil Bed; Hiwegi	27.6	1.9	26	28	0.57	0.9999
Kibanga; Hiwegi	27.0	2.3	4			
Kibanga; Hiwegi	**27.0**	**2.3**	**4**	**14**	**2.76**	**0.0459**
Kulu	**29.5**	**1.3**	**12**			
Grit/Fossil Bed/Hiwegi	**27.6**	**1.9**	**26**	**36**	**3.13**	**0.0105**
Kulu	**29.5**	**1.3**	**12**			

CONCLUSION

The fossiliferous sediments on Rusinga and Mfangano Islands provide an ideal location to reconstruct past habitats as a means for documenting the environmental pressures faced by the various primates that have inhabited the area. With deposits from both the Late Pleistocene and early Miocene, this includes both early *Homo sapiens* as well as primitive hominoids.

Chapter 1 of this dissertation is a paleoenvironmental reconstruction of the Late Pleistocene deposits on Rusinga and Mfangano Islands. This chapter analyzes the local habitat where the fauna and Middle Stone Age artifacts accumulated as well as the larger regional ecosystem exploited by the mammalian fauna including the early modern humans. Understanding of the environmental pressures faced by early modern humans and how those pressures mediated the behavioral and biological diversity of early modern humans and their migration patterns provides a rare look into the behaviors and adaptations of modern *Homo sapiens* during this formative time in human biogeography. The data suggest that humans were able to remain in East Africa, even during hyper-arid periods with expanded C_4 grasslands in the greater region, by retreating to locally closed and well-watered riverine woodland habitats, such as those documented on Rusinga and Mfangano. This analysis is also consistent with other studies suggesting a dramatically reduced Lake Victoria during this period of the Late Pleistocene.

Chapters 2-3 of this dissertation are detailed paleoenvironmental reconstructions of the early Miocene deposits on Rusinga Island. The fossil mammalian assemblage at this site provides critical information about the evolutionary pressures that shaped the adaptive morphologies of the early Miocene catarrhine community, which is a necessary foundation for our understanding of the evolutionary history of all later hominoids. Although previous paleoenvironmental reconstructions have attempted to document the early Miocene habitats present on Rusinga, the results have yielded a wide range of conflicting interpretations, which has hindered our ability to fully understand the behavior and ecology of these important early Miocene primates. The results document a spatially and temporally dynamic mixture of C_3 habitats ranging from close-canopy forests undergoing CO_2 recycling to open or unshaded habitats with plants experiencing light and/or water stress. Additionally, this analysis indicates the habitats present and exploited by the faunal community (i.e., in the greater region) were not stable though time, which may explain some differences in faunal community composition. The catarrhine community however, remains consistent throughout the early Miocene deposits, which demonstrates that the early Miocene primates were not living in a single stable habitat, but rather were able to thrive in a range of habitats for an extended period of hominoid evolutionary history. Additionally, this habitat flexibility exhibited by the primitive hominoids present on Rusinga suggests this adaptation may have been an important primitive characteristic for all of Hominoidea.

BIBLIOGRAPHY

Agrawal, S., Galy, V., Sanyal, P., Eglinton, T., 2014. C_4 plant expansion in the Ganga Plain during the last glacial cycle: insights from isotopic composition of vascular plant biomarkers. Org. Geochem. 67, 58-71.

Andrews, P., 1973. Vegetation of Rusinga Island. J. East Afr. Nat. Hist. 142,1-8.

Andrews, P., 1992. Community evolution in forest habitats. J. Hum. Evol. 22, 423-438.

Andrews, P., 2015. An Ape's View of Human Evolution. Cambridge University Press, Cambridge, 397 pp.

Andrews, P., Begun, D., Zylstra, M., 1997. Interrelationships between functional morphology and paleoenvironments in Miocene hominoids. In: Begun, D., Ward, C., Rose, M. (Eds.), Function, Phylogeny, and Fossils: Miocene Hominoid Evolution and Adaptations. Plenum Press, New York, pp. 29-58.

Andrews, P., Kelley, J., 2007. Middle Miocene dispersals of apes. Folia Primatol. 78, 328-343.

Andrews, P., Lord, J., Nesbit Evans, E.M., 1979. Patterns of ecological diversity in fossil and modern mammalian faunas. Biol. J. Linn. Soc. Lon. 11, 177-205.

Andrews, P., Simons, E., 1977. A new African Miocene gibbon-like genus, *Dendropithecus* (Hominoidea, Primates) with distinctive postcranial adaptations: its significance to origin of Hylobatidae. Folia Primatol. 28, 161-170.

Andrews, P., Van Couvering, J.A.H., 1975. Paleoenvironments in the East African Miocene. In: Szalay, F. (ed.) Approaches to Primate Paleobiology. Kargel, Basel, pp. 62-103.

Ambrose, S.H., DeNiro, M.J., 1986. The isotopic ecology of East African mammals. Oecologia. 69, 395-406.

Ambrose, S.H., Norr, L., 1993. Experimental evidence for the relationship of the carbon isotope ratios of while diet and dietary protein to those of bone collagen and carbonate. In: Lambert, J., Grupe, G. (Eds.), Prehistoric Human Bone, Archaeology at the Molecular Level. Springer-Verlag, Berlin, pp. 1-37.

Amundson, R., 1989. The use of stable isotopes in assessing the effect of agriculture on arid and semi-arid soils. In: Rundel, P.W., Ehleringer, J.R., Nagy, K.Y. (Eds.), Stable Isotopes in Ecological Research. Springer-Verlag, New York, pp. 318-341.

Assefa, Z., Lam, Y.M., Mienis, H.K., 2008. Symbolic use of terrestrial gastropod opercula during the Middle Stone Age at Porc-Epic Cave, Ethiopia. Curr. Anthropol. 49, 746-756.

Ayliffe, L.K., Lister, A.M., Chivas, A.R., 1992. The preservation of glacial-interglacial climatic signatures in the oxygen isotopes of elephant skeletal phosphate. Palaeogeogr. Palaeoclim. Palaeoecol. 99, 179-191.

Baas, M., Pancost, R., van Geel, B., Damsté, J.S.S., 2000. A comparative study of lipids in *Sphagnum* species. Org. Geochem. 31, 535-541.

Bacon, A.M., 2001. La locomotion des primates du Miocene d'Afrique et d'Europe. Analyse fonctionnelle des os longs du membre pelvien et systematique. Cahiers de Paleoanthropologie. CNRS, Paris.

Bartholomew, G.A., Bridsell, J.B., 1953. Ecology and the protohominids. Am. Anthropol. 55, 481-498.

Balesdent, J.C., Girardin, C., Mariotti, A., 1993. Site-related $\delta^{13}C$ of tree leaves and soil organic matter in a temperate forest. Ecology. 74, 1713-1721.

Basell, L.S., 2008. Middle Stone Age (MSA) site distributions in eastern Africa and their relationship to Quaternary environmental change, refugia and the evolution of Homo sapiens. Quaternary Sci. Rev. 27, 2484-2498.

Beard, K.C., 2002. Basal anthropoids. In: Hartwig, W.C. (Ed.), The Primate Fossil Record. Cambridge University Press, Cambridge, pp. 133-149.

Beard, K.C., 2005. Mammalian biogeography and anthropoid origins. In: Lehman, S.M., Fleagle, J.G. (Eds.), Primate Biogeography: Progress and Prospects. Springer, New York, pp. 439-467.

Begun, D.R., Teaford, M.F., Walker, A., 1994. Comparative and functional anatomy of *Proconsul* phalanges from the Kaswanga Primate Site, Rusinga Island, Kenya. J. Hum. Evol. 26, 89-165.

Behrensmeyer, A.K., Deino, A.L., Hill, A., Kingston, J.D., Saunders, J.J., 2002. Geology and geochronology of the middle Miocene Kipsaramon site complex, Muruyur Beds, Tugen Hills, Kenya. J. Hum. Evol. 42, 11-38.

Besnard, G., Muasya, A.M., Russier, F., Roalson, E.H., Salamin, N., Cristin, P. -A., 2009. Phylogenomics of C_4 photosynthesis in sedges (Cyperaceae): multiple appearances and genetic convergence. Mol. Bio. Evol. 26, 1909-1919.

Bestland, E.A., 1990. Miocene Volcaniclastic Deposits and Paleosols of Rusinga Island, Kenya. PhD Dissertation, University of Oregon.

Bestland, E.A., 1991. A Miocene Gilbert-type fan-delta from a volcanically influenced lacustrine basin, Rusinga Island, Lake Victoria, Kenya. J. Geol. Soc. London 148, 1067-1078.

Bestland, E.A., Krull, E.S., 1999. Palaeoenvironments of Early Miocene Kisingiri volcano *Proconsul* sites: evidence from carbon isotopes, paleosols, and hydromagmatic deposits. J. Geol. Soc. London 156, 965-976.

Bestland, E.A., Retallack, G.J., 1993. Volcanically influenced calcareous palaeosols from the Miocene Kiahera Formation, Rusinga Island, Kenya. J. Geol. Soc. London 150, 293-310.

Bestland, E.A., Thackray, G.D., Retallack, G.J., 1995. Cycles of Doming and Eruption of the Miocene Kisingiri Volcano, Southwest Kenya. J. Geol. 103, 598-607.

Bibi, 2007. Dietary niche partitioning among fossil bovids in Late Miocene C_3 habitats: Consilience of functional morphology and stable isotope analysis. Palaeogeogr. Palaeoclim. Palaeoecol. 253, 529-538.

Bishop, L.C., 2010. Suoidea. In: Werdelin, L., Sanders, W.J. (Eds.), Cenozoic Mammals of Africa. University of California Press, Berkeley, pp.821-842.

Blegen, N., Tryon, C.A., Faith, J.T., Peppe, D.J., Beverly, E., 2014. Tephrostratigraphy and the archaeology of the Late Pleistocene, eastern Lake Victoria Basin, Kenya: a refined stratigraphic context for Late Pleistocene human evolution in East Africa. PaleoAnthropology Abstracts.

Blome, M.W., Cohen, A.S., Tryon, C.A., Brooks, A.S., Russel, J., 2012. The environmental context for the origins of modern human diversity: a synthesis of regional variability in African climate 150,000-30,000 years ago. J. Hum. Evol. 62, 563-592.

Bocherens, H., Koch, P.L., Mariotti, A., Geraads, D., Jaeger, J., 1996. Isotopic biogeochemistry (^{13}C, ^{18}O) of mammalian enamel from African Pleistocene hominid sites. Palaios. 11, 306-318.

Bonnefille, R., 1995. A reassessment of the Plio-Pleistocene pollen record of East Africa. In: Vrba, E.S., Denton, G.H., Partridge, T.C., and Burckle, L.H. (Eds.) Paleoclimate and Evolution, with Emphasis on Human Origins. Yale University Press, New Haven, pp. 299-310.

Brandt, S.A., Fisher, E.C., Hildebrand, E.A., Vogelsang, R., Ambrose, S.A., Lesur, J., Wang, H., 2012. Early MIS 3 occupation of Mochena Borago Rockshelter, Southwest Ethiopian Highlands: implications for Late Pleistocene archaeology, paleoenvironments, and modern human dispersals. Quaternary Int. 274, 38-54.

Broecker, W.C., Peteet, D., Hajdas, I., Lin, J., 1998. Antiphasing between rainfall in Africa's Rift Valley and North America's Great Basin. Quaternary Res. 50, 12-20.

Bryant, J.D., Froelich, P.N., 1995. A model of oxygen isotope fractionation in body water of large mammals. Geochim. Cosmochim. Acta 59, 4523-4537.

Bryant, J.D., Froelich, P.N., Showers, W.J., Genna, B.J., 1996. Biologic and climatic signals in the oxygen isotopic composition of Eocene-Oligocene equid enamel phosphate. Palaeogeogr. Palaeoclim. Palaeoecol. 126, 75-89.

Buchmann, N., Brooks, J.R., Rapp, K.D., Ehleringer, J.R., 1996. Carbon isotope composition of C_4 grass as influenced by light and water supply. Plant Cell Environ. 19, 392-402.

Campisano, C.J., Feibel, C.S. 2008. Tephrostratigraphy of the Hadar and Busidima Formations at Hadar, Afar Depression, Ethiopia. In: Quade, J., Wynn, J.G. (Eds.), The Geology of Early Humans in the Horn of Africa. Geological Society of America Special Paper 446, Boulder, CO, pp. 135-162.

Carto, S.L., Weaver, A.J., Hetherington, R., Lam, Y., Wiebe, E.C., 2009. Out of Africa and into an ice age: on the role of global climate change in the Late Pleistocene migration of early modern humans out of Africa. J. Hum. Evol. 56, 139-151.

Cerling, T.E., 1991. On the isotopic composition of carbon in soil carbon dioxide. Geochim. Cosmochim. Acta. 55, 3403-3405.

Cerling, T.E., 1992. Development of grasslands and savannas in East Africa during the Neogene. Palaeogeogr. Palaeoclim. Palaeoecol. 97, 241-247.

Cerling, T.E., 1997. Late Cenozoic vegetation change, atmospheric CO_2, and tectonics. In: Ruddiman, W.F. (Ed.), Tectonic Uplift and Climate Change. Plenum Press, New York, pp. 313-327.

Cerling, T.E., Harris, J.M., 1999. Carbon isotope fractionation between diet and bioapatite in ungulate mammals and implications for ecological and paleoecological studies. Oecologia. 120, 347-363.

Cerling, T.E., Harris, J.M., Hart, J.A., Kaleme, P., Klingel, H., Leakey, M.G., Levin, N.E., Lewison, R.L., Passey, B.H., 2008. Stable isotope ecology of the common hippopotamus. J. Zool. 276, 204-212.

Cerling, T.E., Harris, J.M., Leakey, M.G., 1999. Browsing and grazing in elephants: the isotope record of modern and fossil proboscideans. Oecologia. 120, 364-374.

Cerling, T.E., Harris, J.M., Passey, B.H., 2003. Diets of East African Bovidae based on stable isotope analysis. J. Mammal. 82, 456-470.

Cerling, T.E., Levin, N.E., Quade, J., Wynn, J.G., Fox, D.L., Kingston, J.D., Klein, R.G., Brown, F.H., 2010. Comment on paleoenvironment of Ardipithecus ramidus. Science. 328, 1105-d.

Cerling, T.E., Quade, J., 1993. Stable carbon and oxygen isotopes in soil carbonates. In: McKenzie, J.A., Savin, S. (Eds.), Climate Change in Continental Isotopic Records (Geophysical Monograph). American Geophysical Union, Washington, D.C., pp. 217-231.

Cerling, T.E., Wynn, J.G., Andanje, S.A., Bird, M.E., Korir, D.K., Levin, N.E., Mace, W., Macharia, A.N., Quade, J., Remin, C.H., 2011. Woody cover and hominin environments in the past 6 million years. Nature. 476, 51-56.

Chen, Q., Shen, C., Sun, Y., Peng, S., Yi, W., Li, Z., Jiang, M., 2005. Spatial and temporal distribution of carbon isotopes in soil organic matter at the Dinghushan Biosphere Reserve, South China. Plant Soil. 273, 115-128.

Chesters, K.I.M., 1957. The Miocene flora of Rusinga Island, Lake Victoria, Kenya. Palaeontographica 101, 30-67.

Chikaraishi, Y., Naraoka, H., 2001. Organic hydrogen–carbon isotope signatures of terrestrial higher plants during biosynthesis for distinctive photosynthetic pathways. Geochem. J. 35, 451-458.

Chikaraishi, Y., Naraoka, H., 2003. Compound-specific δD and $\delta^{13}C$ analyses of *n*-alkanes extracted from terrestrial and aquatic plants. Phytochemistry. 63, 361-371.

Chikaraishi, Y., Naraoka, H., 2007. $\delta^{13}C$ and δD relationships among three *n*-alkyl compound classes (*n*-alkanoic acid, *n*-alkane, and *n*-alkanol) of terrestrial higher plants. Org. Geochem. 38, 198-215.

Christin, P.-A., Besnard, G., Samaritani, E., Duvall, M.R., Hodkinson, T.R., Savolainen, V., Salamin, N., 2008. Oligocene CO_2 decline promoted C_4 photosynthesis in grasses. Curr. Biol. 18, 37-43.

Christin, P.-A., Osborne, C.P., 2014. The evolutionary ecology of C_4 plants. New Phytologist 204, 765-781.

Christin, P.-A., Osborne, C.P., Chatelet, D.S., Columbus, J.T., Besnard, G., Hodkinson, T.R., Garrison, L.M., Vorontsova, M.S., Edwards, E.J., 2013. Anatomic enablers and the evolution of C_4 photosynthesis in grasses. Proc. Natl. Acad. Sci. USA. 110, 1381-1386.

Clementz, M.T., Fox-Dobbs, K., Wheatley, P.V., Koch, P.L., Doak, D.F., 2009. Revisiting old bones: coupled carbon isotope analysis of bioapatite and collagen as an ecological and palaeoecological tool. Geol. J. 44, 605-620.

Clementz, M.T., Fordycem R.E., Peek, S.L., Fox, D.L., 2014. Ancient marine isoscapes and isotopic evidence of bulk-feeding by Oligocene cetaceans. Palaeogeogr. Palaeoclim. Palaeoecol. 400, 28-40.

Codron, D., Brink, J.S., Rossouw, L., Clasuss, M., 2008. The evolution of ecological specialization in southern African ungulates: competition or physical environmental turnover. Oikos. 117, 334-353.

Codron, D., Codron, J., Lee-Thorp, J.A., Sponheimer, M., De Ruiter, D., Brink, J.S., 2006. Dietary variation in impala *Aepyceros melampus* recorded by carbon isotope composition of feces. Acta Zoological Sinica. 52, 1015-1025.

Collinson, M., 1985. Revision of East African Miocene floras: a preliminary report. International Association of Angiosperm Paleontology Newsletter 8, 4-12.

Collinson, M., Andrews, P., and Bamford, M.K. 2009. Taphonomy of early Miocene flora, Hiwegi Formation, Rusinga Island, Kenya. J. Hum. Evol. 57, 149-162.

Collister, J.W., Rieley, G., Stern, B., Eglinton, G., and Fry, B., 1994. Compound-specific δ13C analyses of leaf lipids from plants with differing carbon dioxide metabolisms. Org. Geochem. 21, 619-627.

Comte, M.H., Weber, J.C., Carlson, P.J., and Flanagan, L.B., 2003. Molecular and carbon isotopic composition of leaf wax in vegetation and aerosols in a northern prairie ecosystem. Oecologia. 135, 67–77.

Conrad, J.L., Jenkins, K., Lehmann, T., Manthi, F.K., Peppe, D.J., Nightingale, S., Cosette, A., Dunsworth, H.M., Harcourt-Smith, W.E.H., and McNulty, K.P.,

2013. New specimens of '*Crocodylus*' *pigotti* (Crocodylidae) from Rusinga Island, Kenya, and generic reallocation of the species. J. Vertebr. Paleontol. 33, 629-646.

Coombs, M.C., Cote, S.M., 2010. Chalicotheriidae. In: Werdelin, L., Sanders, W.J. (Eds.), Cenozoic Mammals of Africa, University of California Press, pp.659-668.

Compton, J.S., 2011. Pleistocene sea-level fluctuations and human evolution on the southern coastal plain of South Africa. Quaternary Sci. Rev. 30, 506-527.

Cote, S.M., 2008. Sampling and ecology in three Early Miocene catarrhine assemblages from East Africa. PhD Dissertation, Harvard University.

Cowling, S.A., Cox, P.M., Jones, C.D., Maslin, M.A., Peros, M., Spall, S.A., 2008. Simulated glacial and interglacial vegetation across Africa: implications for species phylogenies and trans-African migration of plants and animals. Glob. Chang. Bio. 14, 827-840.

Craig, H., 1965. The measurement of oxygen isotope paleotemperature. In: Tongiori, E. (Ed.), Stable Isotopes in Oceanographic Studies and Paleotemperatures. V. Lischi, pp. 161-182.

Crul, R.C.M., 1995. Limnology and hydrology of Lake Victoria. UNESCO, Paris.

Dart, R.A., 1925. *Australopithecus africanus:* the man-ape of South Africa. Nature. 115, 195-199.

Darwin, C., 1871. The Descent of Man, and Selection in Relation to Sex. John Murray, London.

Daver, G., Nakatsukasa, M., 2015. *Proconsul heseloni* distal radial and ulnar epiphyses from the Kaswanga Primate Site, Rusinga Island, Kenya. J. Hum. Evol. 80, 17-33.

DeConto, R.M., Pollard, D., 2003. Rapid Cenozoic glaciation of Antarctica induced by declining atmospheric CO_2. Nature. 421, 245-249.

Deines, P., Langmuir, D., Harmon, R.S., 1974. Stable carbon isotope ratios and existence of a gas phase in the evolution of carbonate ground water. Geochim. Cosmochim. Acta. 38, 1147-1164.

del Moral, R., Wood, D.M., 1993. Early primary succession on the volcano Mount St. Helens. J. Veg. Sci. 4, 223-234.

deMenocal, P.B., 2011. Climate and human evolution. Science. 331, 540-542.

DeNiro, M.J., Epstein, S., 1978. Influence of diet on the distribution of carbon isotopes in animals. Geochim. Cosmochim. Acta. 42, 495-506.

Denslow, J.D., 1980. Patterns of plant species diversity during succession under different disturbance regimes. Oecologia. 46, 18-21.

Dewar, R.E., 1986. Discovering settlement systems of the past in New England site distributions. Man in the Northeast. 31, 77-88.

Diefendorf A.F., Mueller K.E., Wing S.L., Koch P.L., Freeman K.H. 2010. Global patterns in leaf ^{13}C discrimination and implications for studies of past and future climate. Proc. Natl. Acad. Sci. 107, 5738–5743.

Domingo, L., Koch, P.L., Hernandez Fernandez, M., Fox, D.L., Domingo, M.S., Alberdi, M.T., 2013. Late Neogene and Early Quaternary Paleoenvironmental and Paleoclimatic Conditions in Southwestern Europe: Isotopic Analyses on Mammalian Taxa. PLOS One 8, e63739.

Domínguez-Rodrigo, M., Mabulla, A., Luque, L., Thompson, J.W., Rink, J., Bushozi, P., Díez-Martin, F., Alcala, L., 2008. A new archaic *Homo sapiens* fossil from Lake Eyasi, Tanzania. J Hum. Evol. 54, 899-903.

Drake, R.E., Van Couvering, J.A., Pickford, M.H., Curtis, G.H., Harris, J.A., 1988. New chronology for the Early Miocene mammalian faunas of Kisingiri, Western Kenya. J. Geol. Soc. 145, 479-491.

Dunsworth, H.M., 2006. *Proconsul heseloni* feet from Rusinga Island Kenya. PhD Dissertation, Pennsylvania State University.

Edwards, E.J., Osborne, C.P., Stromberg, C.A.E., Smith, S.A., Bond, W.J., Christin, P.-A., Cousins, A.B., Duvall, M.R., Fox, D.L., Freckleton, R.P., Ghannoum, O., Hartwell, J., Huang, Y., Janis, C.M., Keeley, J.E., Kellogg, E.A., Knapp, A.K., Leakey, A.D.B., Nelson, D.M., Saarela, J.M., Sage, R.F., Sala, O.E., Salamin, N., Still, C.J., Tipple. B., 2010. The origins of C_4 grasslands: integrating evolutionary and ecosystem science. Science. 328, 587-591.

Eglinton, G., Hamilton, R.J., 1967. Leaf epicuticular waxes. Science. 156, 1322-1335.

Ehleringer, J.R., Cooper, T.A., 1988. Correlations between carbon isotope ratio and microhabitat in desert plants. Oecologia. 76, 562-566.

Ehleringer, J.R., Sage, R.F., Flanagan, L.B., Pearcy, R.W., 1991. Climate change and the evolution of C_4 photosynthesis. Trends Ecol. Evol. 6, 95-99.

Erez, J., Luz, B., 1983. Experimental paleotemperature equation for planktonic foraminifera. Geochim. Cosmochim. Acta. 47, 1025– 1031.

Faith, J.T., Choiniere, J.N., Tryon, C.A., Peppe, D.J., Fox, D.L., 2011. Taxonomic status and paleoecology of *Rusingoryx atopocranion* (Mammalia, Artiodactyla), an extinct Pleistocene bovid from Rusinga Island, Kenya. Quaternary Res. 75, 697-707.

Faith, J.T., Potts, R., Plummer, T.W., Bishop, L.C., Marean, C.W., Tryon, C.A., 2012. New perspectives on middle Pleistocene change in the large mammal faunas of East Africa, *Damaliscus hypsodon* sp. nov. (Mammalia, Artiodactyla) from Lainyamok, Kenya. Palaeogeogr. Palaeoclim. Palaeoecol. 361-362, 84-93.

Faith, J.T., Tryon, C.A., Peppe, D.J., 2016. Environmental change, ungulate biogeography, and their implications for early human dispersals in equatorial East

Africa. In: Jones, S.C., Stewart, B.A. (Eds.), Africa from MIS 6-2, Population Dynamics and Paleoenvironments. Springer.

Faith, J.T., Tryon, C.A., Peppe, D.J., Fox, D.L., 2013. The fossil history of Grévy's zebra (*Equus grevyi*) in equatorial East Africa. J. Biogeogr. 40, 359-369.

Faith, J.T., Tryon, C.A., Peppe, D.J., Beverly, E.J., Blegen, N., 2014. Biogeographic and evolutionary implications of an extinct Late Pleistocene impala from the Lake Victoria Basin. J. Mamm. Evol. 21, 213-222.

Feakins, S.J., deMenocal, P.B., and Eglinton, T.E., 2005. Biomarker records of late Neogene changes in northeast African vegetation. Geology. 33, 977-980.

Feakins, S.J., Eglinton, T.I., and deMenocal, P.B., 2007. A comparison of biomarker records of northeast African vegetation from lacustrine and marine sediments (ca. 3.40 Ma). Org. Geochem. 38, 1607-1624.

Feranec, R.S., Hadly, E.A., Paytan A., 2009. Stable isotopes reveal seasonal competition for resources between Late Pleistocene bison (*Bison*) and horse (*Equus*) from Rancho La Brea, southern California. Palaeogeogr. Palaeoclim. Palaeoecol. 271, 153-160.

Feranec, R.S., Pagnac, D., 2013. Stable carbon isotope evidence for the abundance of C_4 plants in the middle Miocene of southern California. Palaeogeogr. Palaeoclim. Palaeoecol. 388, 42-47.

Ferring, C.R., 1986. Rates of fluvial sedimentation: implications for archaeological variability. Geoarchaeol. 1, 259-274.

Ficken, K.J., Li, B., Swain, D.L., and Eglinton, G., 2000. An *n*-alkane proxy for the sedimentary input of submerged floating freshwater aquatic macrophytes. Org. Geochem. 31, 745-749.

Fillinger, U., Sonye, G., Killeen, G.F., Knols, B.G.J., Becker, N., 2004. The practical importance of permanent and semipermanent habitats for controlling aquatic stages of *Anopheles gambiae sensu lato* mosquitoes: operational observations from a rural town in western Kenya. Trop. Med. Int. Health 9, 1274-1289.

Flanagan, L.B., Comstock, J.P., Ehleringer, J.R., 1991. Comparison of modeled and observed environmental influences on the stable oxygen and hydrogen isotope composition of leaf water in *Phaseolus vulgaris* L. Plant. Physiol. 96, 588-596.

Flower, B.P., Kennett, J.P., 1994. The middle Miocene climatic transition: East Antarctic ice sheet development, deep ocean circulation and global carbon cycling. Palaeogeogr. Palaeoclim. Palaeoecol. 108, 537-555.

Forbes, M.S., Bestland, E.A., Krull, E.S., and Dicker, D.G., 2004. Palaeoenvironmental mosaic of *Proconsul* habitats: geochemical and sedimentaological interpretation of Kisingiri fossil sites, Western Kenya. J. Afr. Earth Sci. 39, 63-79.

Foster, G.L., Lear, C.H., Rae, J.W.B., 2012. The evolution of pCO_2, ice volume and climate during the middle Miocene. Earth Planet Sci. 341-344, 243-254.

Fox, D.L., Fisher, D.C., 2001. Stable isotope ecology of a late Miocene population of *Gomphotherium* (Mammalia, Proboscidea) from Port of Entry Pit, Oklahoma: diet, climate and diagenesis. Palaios. 16, 279-293.

Fox, D.L., Fisher, D.C., Vartanyan, S., Tikhonov, A.N., Mol, D., Buigues, B., 2007. Paleoclimatic implications of oxygen isotopic variation in late Pleistocene and Holocene tusks of *Mammuthus primigenius* from northern Eurasia. Quaternary Int. 169-170, 154-165.

Fricke, H.C., Clyde, W.C., O'Neil, J.R., 1998. Intra-tooth variations in $\delta^{18}O$ (PO_4) of mammalian tooth enamel as a record of seasonal variations in continental climate variables. Geochim. Cosmochim. Acta. 62, 1839-1850.

Friedli, H., Lötscher, H., Oeschger, H., Siegenthaler, U., Stauffer, B., 1986. Ice core record of the $^{13}C/^{12}C$ ratio of atmospheric CO_2 in the past two centuries. Nature. 324, 237-238.

Garrett, N.D., Fox, D.L., McNulty, K.P., Faith, J.T., Peppe, D.J., Van Plantinga, A., Tryon, C.A., 2015. Stable isotope paleoecology of Late Pleistocene Middle Stone Age humans from the Lake Victoria Basin, Kenya. J. Hum. Evol. 82, 1-14.

Gehler, A., Tütken, T., Pack, A., 2012. Oxygen and Carbon Isotope Variations in a Modern Rodent Community – Implications for Palaeoenvironmental Reconstructions. PLOS One 7, e49531.

Gelpi, E., Schneider, H., Mann, J., and Oró, J., 1970. Hydrocarbons of geochemical significance in microscopic algae. Phytochemistry. 9, 603-612.

Geraads, D., Lehmann, T., Peppe, D.J., McNulty, K.P., 2016. New Rhinoceratidae from the Kisingiri localities (lower Miocene of Western Kenya). J. Vertebr. Paleontol.

Godinot, M., 1994. Early North African primates and their significance for the origin of Simiiformes (=Anthropoidea). In: Fleagle, J.G., Kay, R.F. (Eds.), Anthropoid Origins. Plenum Press, New York, pp. 235-296.

Gonder, M.K., Mortensen, H.M., Reed, F.A., de Sousa, A., Tishkoff, S.A., 2007. Whole mtDNA genome sequence analysis of ancient African lineages. Mol. Biol. Evol. 24, 757-768.

Gröcke, D.R., 2002. The isotopic composition of ancient CO_2 based on higher-plant organic matter. Philos. Transact. A Math Phys. Eng. Sci. 360, 633-658.

Guilderson, T.P., Fairbanks, R.J., Rubenstone, J.L., 1994. Tropical temperature variations since 20,000 years ago: modulating interhemispheric climate change. Science. 263, 663-665.

Han, B.J., McCarthy, E.D., van Hoeven, W., Calvin, M., Bradley, W.H., 1968. Organic geochemical studies, II. A preliminary report on the distribution of aliphatic hydrocarbons in algae, in bacteria, and in a recent lake sediment. Proc. Natl. Acad. Sci. U.S.A. 59, 29-33.

Harris, J.M., Cerling, T.E., 2002. Dietary adaptations of extant and Neogene African suids. J. Zool. 256, 45-54.

Harris, J., Van Couvering, J., 1995. Mock aridity and the paleoecology of volcanically influenced ecosystems. Geology. 23, 593-596.

Harrison, T., 2002. Late Oligocene to middle Miocene catarrhines from Afro-Arabia. In: Kingston, J.D., 1992. Stable isotopic evidence for hominid paleoenvironments in East Africa. Ph.D. dissertation, Harvard University.

Harrison, T., 2010. Later Tertiary Lorisiformes (Strepsirrhini, Primates). In: Werdelin, L., and Sanders, W.J. (eds.) Cenozoic Mammals of Africa. University of California Press, Berkeley, pp. 333-350.

Hartwig, W.C., 2002. (Ed.) The Primate Fossil Record. Cambridge University Press: Cambridge, pp. 311-338.

Hayes, J.M., 1993. Factors controlling ^{13}C contents of sedimentary organic compounds: principles and evidence. Mar. Geol. 113, 111-125.

Hijmans, R.J., Cameron, S.E., Parra, J.L., Jones, P.G., Jarvis, A., 2005. Very high resolution interpolated climate surfaces for global land areas. Int. J. Climatol. 25, 1965-1978.

Heinselman, M.L., 1973. Fire in the virgin forests of the Boundary Waters Canoe Area, Minnesota. *Quaternary Research* 3, 329-382.

Hill, A., Ward, S., 1988. Origin of the Hominidae: the record of African large Hominoid evolution between 14 My and 4 My. Yearb. Phys. Anthropol. 3, 49-83.

Hobbie, E.A., Johnson, M.G., Rygiewicz, P.T., Tingey, D.T., Olszyk, D.M., 2004. Isotopic estimates of new carbon inputs into litter and soils in a four-year climate change experiment with Douglas-fir. Plant Soil. 259, 331-343.

Holbourn, A., Kuhnt, W., Schulz, M., Erlenkeuser, H., 2005. Impacts of orbital forcing and atmospheric carbon dioxide on Miocene ice-sheet expansion. Nature 438, 483-487.

Holdaway, S., Witter, D., Fanning, P., Musgrave, R., Cochrane, G., Doelman, T., Greenwood, S., Pigdon, D., Reeves, J., 1998. New approaches to open site spatial archaeology in Sturt National Park, New South Wales, Australia. Archaeology in Oceania. 33, 1-19.

Holroyd, P.A., Lihoreau, F., Gunnell, G.F., Miller, E.R., 2010. Anthracotheriidae. In: Werdelin, L., and Sanders, W.J. (eds.) Cenozoic Mammals of Africa. University of California Press, Berkeley, pp. 843-851.

Huang, Y., Street-Perrott, F.A., Perrott, R.A., Metzger, P., Eglinton, G., 1999. Glacial-interglacial environmental changes inferred from molecular and compound-specific $\delta^{13}C$ analyses of sediments from Sacred Lake, Mt. Kenya. Geochim. Cosmochim. Acta 63, 1383-1404.

Isaac, G., 1981. Stone Age visiting cards: Approaches to the study of early land-use patterns. In: Hodder, I., Isaac, G., Hammond, N. (Eds.), Patterns of the Past. Cambridge University Press, Cambridge, pp. 131-155.

Jacobs, B.F., Kingston, J.D., Jacobs, J.J., 1999. The origin of grass-dominated ecosystems. Ann. Mo. Bot. Gard. 86, 590-643.

Jacobs, B.F., Pan, A.D., Scotese, C.R., 2010. A review of the Cenozoic vegetation history in Africa. In: Werdelin, L., and Sanders, W.J. (eds.) Cenozoic Mammals of Africa. University of California Press, Berkeley, pp. 45-55.

Jarosewich, E., Nelen, J.A. Norberg, J.A., 1980. Reference samples for electron microprobe analysis. Geostandards Newsletter. 4, 43-47.

Jenkins, F.A., 1973. The functional anatomy and evolution of the mammalian humero-ulnar articulation. Am. J. Anat. 137, 281-297.

Jenkins, K., Faith, J.T., Tryon, C., Peppe, D., Nightingale, S., Ogondo, J., Roure Johnson, C., Driese, S., 2012. New excavations of a Late Pleistocene bonebed and associated MSA artifacts from Rusinga Island, Kenya. Paleoanthropology. 2012, A17.

Jolly, C.J., 1970. The seed eaters: a new model of hominid differentiation based on a baboon analogy. Man 5, 5-26.

Keeley, J.E., Sandquist, D.R., 1992. Carbon: freshwater plants. Plant Cell Environ. 15, 1021-1035.

Keeling, C.D., Piper, S.C., Bacastow, R.B., Wahlen, M., Whorf, T.P., Heimann, M., Meijer, H.A., 2001. Exchanges of atmospheric CO_2 and $^{13}CO_2$ with the terrestrial biosphere and oceans from 1978 to 2000. I. Global aspects, SIO Reference Series, No. 01-06, (Scripps Institution of Oceanography, San Diego), 88 pages.

Kelley, J., 1997. Paleobiological and phylogenetic significance of life history in Miocene hominoids. In: Begun, D.R., Ward, C.V., and Rose, M.D., (eds.) Function, phylogeny, and fossils: Miocene hominoid evolution and adaptation. Plenum Press, New York, pp. 173-208.

Kellogg, E.A., 2001. Evolutionary history of grasses. Plant Physiol. 125, 1198-1205.`

Kendall, R.L., 1969. An ecological history of the Lake Victoria Basin. Ecol. Monogr. 39, 121-176.

Kingdon, J., 1988a. East African Mammals: An Atlas of Evolution in Africa, Volume 3, Part C: Bovids. University of Chicago Press, 404 pages.

Kingdon, J., 1988b. East African Mammals: An Atlas of Evolution in Africa, Volume 3, Part D: Bovids. University of Chicago Press, 358 pages.

Kingston, J.D., 2007. Shifting adaptive landscapes: progress and challenges in reconstructing early hominid environments. Yearb. Phys. Anthropol. 50, 20-58.

Kingston, J.D., Harrison, T., 2007. Isotopic dietary reconstructions of Pliocene herbivores at Laetoli: implications for early hominin paleoecology. Palaeogeogr. Palaeoclim. Palaeoecol. 243, 273-306.

Kingston, J.D., Marino, B.D., Hill, A., 1994. Isotopic evidence for Neogene hominid paleoenvironments in the Kenya Rift Valley. Science. 264, 955-959.

Koch, P.L., 1998. Isotopic reconstruction of past continental environments. Ann. Rev. Earth Planet Sci. 26, 573-613.

Koch, P.L., 2007. Isotopic study of the biology of modern and fossil vertebrates. In: Michener, R., Kajtha, K. (Eds.), Stable Isotopes in Ecology and Environmental Science, 2nd Edition. Blackwell Publishing, Boston, pp. 99-154.

Koch, P.L., Behrensmeyer, A.K., Fogel, M.L., 2001. The isotopic ecology of plants and animals in Amboseli National Park, Kenya. Annual Report of the Director of the Geophysical Laboratory. 163-171.

Koch, P.L., Tuross, N., Fogel, M.L., 1997. The effect of sample treatment and diagenesis on the isotopic integrity of carbonate in biogenic hydroxyapatite. J. Arch. Sci. 24, 417-429.

Kohn, M.J., 1996. Predicting animal $\delta^{18}O$: accounting for diet and physiological adaptation. Geochem. Cosmochem. Acta. 60, 4811-4829.

Kohn, M.J., 2010. Carbon isotope compositions of terrestrial C_3 plants as indicators of (paleo)ecology and (paleo)climate. Proc. Natl. Acad. Sci. U.S.A. 107, 19691-19695.

Kohn, M., Schoeninger, M., Barker, W., 1999. Altered states: effects of diagenesis on fossil tooth chemistry. Geochem. Cosmochem. Acta. 63, 2737-2747.

Kohn, M.J., Schoeninger, M.J., Valley, J.W., 1996. Herbivore tooth oxygen isotope compositions: effects of diet and physiology. Geochem. Cosmochem. Acta. 60, 3889-3896.

Kolattukudy, P., 1969. Plant waxes. *Lipids* 5, 259-275.

Langdon, J., 1986. Functional morphology of the Miocene hominoid foot. Contrib. Primatol. 22, 1-225.

Laporte, L.F., Zhilman, A.L., 1983. Climate and hominoid evolution. S. Afr. J. Sci. 79, 96-110.

Leakey, L.S.B., 1943. A Miocene anthropoid mandible from Rusinga, Kenya. Nature. 152, 319-320

Le Bas, M.J., 1977. Carbonitite-nephelinite volcanism. J. Wiley and Sons, London.

Lee-Thorp, J.A., 2000. Preservation of biogenic carbon isotopic signals in Plio-Pleistocene bone and tooth mineral. In: Ambrose, S.H., Katzenberg, M.A. (Eds.), Biogeochemical Approaches to Paleodietary Analysis. Kluwer Academic/Plenum Publishers, New York, pp. 89-114.

Lee-Thorp, J.A., Beaumont, P.B., 1995. Vegetation and seasonality shifts during the Late Quaternary deduced from $^{13}C/^{12}C$ ratios of grazers at Equus Cave, South Africa. Quaternary Res. 43, 426-432.

Lee-Thorp, J.A., Sealey, J.C., van der Merwe, N.J., 1989. Stable carbon isotope ratio differences between bone collagen and bone apatite, and their relationship to diet. J. Arch. Sci. 16, 585-599.

Lee-Thorp, J.A., Sponheimer, M., 2013. Hominin ecology from hard-tissue biogeochemistry. In: Sponheimer, M., Lee-Thorp, J.A., Reed, K.E., Ungar, P.S. (Eds.), *Early* Hominin Paleoecology. University Press of Colorado, Boulder, Colorado, pp. 281-324.

Lee-Thorp, J.A., van der Merwe, N.J., 1987. Carbon isotope analysis of fossil bone apatite. S. Afr. J. Sci. 83, 71-74.

LeGeros, R.Z., 1991. Calcium Phosphates in Oral Biology and Medicine. Karger Publishers, Paris.

Leuenberger, M., Siegenthaler, U., Langway, C.C., 1992. Carbon isotope composition of atmospheric CO_2 during the last ice age from an Antarctic ice core. Nature. 357, 488-490.

Levin, N.E., Cerling, T.E., Passey, B.H., Harris, J.M., Ehleringer, J.R., 2006. A stable isotope aridity index for terrestrial environments. Proc. Natl. Acad. Sci. U.S.A. 103, 11201-11205.

Longinelli A., 1984. Oxygen isotopes in mammal bone phosphate: A new tool for paleohydrological and paleoclimatological research? Geochim. Cosmochim. Acta 48, 385-390.

Luz, B., Cormie, A.B., Schwarcz, H.P., 1990. Oxygen isotope variations in phosphate of deer bones. Geochim. Cosmochim. Acta. 54, 1723-1728.

Luz, B., Kolodny, Y., 1985. Oxygen isotope variations in phosphate of biogenic apatites. IV. Mammal teeth and bones. Earth and Planetary Sciences Letters 75, 29-36.

Luz B., Kolodny Y., Horowitz M., 1984. Fractionation of oxygen isotopes between mammalian bone-phosphate and environmental drinking water. Geochim. Cosmochim. Acta 48, 1689-1693.

MacInnes, D.G., 1943. Notes on the East African Miocene primates. Journal of East Africa and Uganda Natural History Society 17, 141-181.

MacLatchy, L., 2004. The oldest ape. Evol. Anthropol. 13, 90-103.

Magill, C.R., Ashley, G.M., Freeman, K.H., 2013. Ecosystem variability and early human habitats in Eastern Africa. Proc. Natl. Acad. Sci. U.S.A. 110, 1167-1174.

Marean, C.W., 1992. Implications of late Quaternary mammalian fauna from Lukenya Hill (south-central Kenya) for paleoenvironmental change and faunal extinctions. Quaternary Res. 37, 239-255.

Marean, C.W., 1997. Hunter-gatherer foraging strategies in tropical grasslands: Model-

building and testing in the East African Middle and Later Stone Age. J. Anthropol. Archaeol. 16, 189-225.

Marean, C. W., Gifford-Gonzalez, D., 1991. Late Quaternary extinct ungulates of East Africa and palaeoenvironmental implications. Nature. 350, 418-420.

Marino, B.D., McElroy, M.B., 1991. Isotopic composition of atmospheric CO_2 inferred from carbon in C_4 plant cellulose. Nature. 349, 127-131.

Marivaux, L., Antione, P.-O., Baqri, S.R.H., Benammi, M., Chaimanee, Y., Crochet, J.-Y., de Franceschi, D., Jaeger, I.-J., Métais, G., Roohi, G., Welcomme, J.-L., 2005. Anthropoid primates from the Oligocene of Pakistan (Bugti Hills): data on early anthropoid evolution and biogeography. Proc. Natl. Acad. Sci. USA. 102, 8436-8441.

Marzi, R., Torkelson, B.E., Olson, R.K., 1993. A revised carbon preference index. Org. Geochem. 20, 1303-1306.

Maxbauer, D.P., Peppe, D.J., Bamford, M., McNulty, K.P., Harcourt-Smith, W.E.H., Davis, L.E., 2013. A morphotype catalog and paleoenvironmental interpretations of early Miocene fossil leaves from the Hiwegi Formation, Rusinga Island, Lake Victoria, Kenya. Palaeontol. Electron. 28A, 19p.

McBrearty, S., Brooks, A.S., 2000. The revolution that wasn't: a new interpretation of the origin of human behavior. J. Hum. Evol. 39, 456-563.

McCall, G.J.H., 1958. Geology of the Gwasi Area. Geological Survey of Kenya Report, 45.

McCollum, M.S., Peppe, D.J., McNulty, K.P., Dunsworth, H.M., Harcourt-Smith, W.E.H., Andrews, A.L., 2013. Geo. Sci. Am. Abstracts 45(3), 12.

McDougall, I., Brown, F.H., Fleagle, J.G., 2005. Stratigraphic placement and age of modern humans from Kibish, Ethiopia. Nature. 433, 733-736.

McLean, B.S., Emslie, S.D., 2012. Stable isotopes reflect the ecological stability of two high-elevation mammals from the late Quaternary of Colorado. Quaternary Res. 77, 408-417.

McNulty, K.P., 2010. Apes and tricksters: the evolution and diversification of humans' closest relatives. Evo. Edu. Outreach 3, 322-332.

McNulty, K.P., Begun, D.R., Kelley, J., Manthi, F.K., Mbua, E., 2015. A systematic revision of *Proconsul* with the description of a new genus of early Miocene hominoid. J. Hum. Evol. 84, 42-61.

Michel, L.A., Peppe, D.J., Lutz, J.A., Driese, S.G., Dunsworth, H.M., Harcourt-Smith, W.E.H., Horner, W.H., Lehmann, T., Nightingale, S., McNulty, K.P., 2014. Remnants of an ancient forest provide ecological context for Early Miocene fossil apes. Nature Comm. 5 ,3236. doi: 10.1038/ncomms4236.

Miller, E.R., Gunnell, G.F., Martin, R.D., 2005a. Deep time and the search for anthropod origins. Yearb. Phys. Anthropol. 48, 60-95.

Miller, K.G., Kominz, M.A., Browning, J.G., Wright, J.D., Mountain, G.S., Katz, M.E., Sugarman, P.J., Cramer, B.S., Christie-Blick, N., Pekar, S.F., 2005b. The Phanerozoic record of global sea-level change. Science. 310, 1293-1298.

Miller, C., Urban, D.L., 1999. Forest pattern, fire, and climatic change in the Sierra Nevada. Ecosystems. 2, 76-87.

Milly, P.C.D., 1999. Comment on "Antiphasing between rainfall in Africa's Rift Valley and North America's Great Basin". Quaternary Res. 51, 104-107.

Morgan, M.E., Kingston, J.D., Marino, B.D., 1994. Carbon isotopic evidence for the emergence of C_4 plants in the Neogene from Pakistan and Kenya. Nature. 367, 162-165.

Nagy, K.A., 1989. Doubly-labeled water studies of vertebrate physiological ecology. In: Rundel, P.W., Ehleringer, J.R., Nagy, K.A. (Eds.), Stable Isotopes in Ecological Research. Springer-Verlag, New York, pp. 270-287.

Napier, J.R., Davis, P.R., 1959. The fore-limb skeleton and associated remains of *Proconsul africanus.* In: Fossil Mammals of Africa. London, British Museum of Natural History.

Nesbit Evans, E.M., van Couvering, J.H., Andrews, P., 1981. Palaeoecology of Miocene sites in Western Kenya. J. Hum. Evol. 10, 35-48.

Nordt, L., Von Fischer, J., Tieszen, L., Tubbs, J., 2008. Coherent changes in relative C_4 plant productivity and climate during the late Quaternary in the North American Great Plains. Quaternary Sci. Rev. 27, 1600-1611.

O'Leary, M.H., 1981. Carbon isotope fractionation in plants. Phytochemistry. 20, 553-567.

Pagani, M., Huber, M., Liu, Z., Bohaty, S.M., Henderiks, J., Sijp, W., Krishnan, S., DeConto, R.M., 2011. The role of carbon dioxide during the onset of Antarctic glaciation. Science. 334, 1261-1264.

Pagani, M., Zachos, J.C., Freeman, K.H., Tipple, B., Bohaty, S., 2005. Marked decline in atmospheric carbon dioxide concentrations during the Paleogene. Science. 309, 600-603.

Partridge, T.C., 2010. Tectonics and geomorphology of Africa during the Phanerozoic. In: Werdelin, L., and Sanders, W.J. (eds.) Cenozoic Mammals of Africa. University of California Press, Berkeley, pp. 3-17.

Passey, B.H., Cerling, T.E., Perkins, M.E., Voorhies, M.R., Harris, J.M., Tucker, S.T., 2002. Environmental change in the Great Plains: an isotopic record from fossil horses. J. Geol. 110, 123-140.

Perkins, M.E., Nash, W.P., Brown, F.H., Fleck, R.J., 1995. Fallout tuffs of Trapper Creek, Idaho: a record of Miocene explosive volcanism in the Snake River Plain volcanic province. Geol. Soc. Am. Bull. 107, 1484-1506.

Peppe, D.J., Deino A.L., McNulty, K.P., Lehmann, T., Harcourt-Smith, W.E.H., Dunsworth, H.M., Fox, D.L., 2011b. New age constraints on the early Miocene faunas from Rusinga and Mfangano Islands (Lake Victoria, Kenya). Am. J. Phys. Anthropol. 144, 237.

Peppe, D.J., McNulty, K.P., Cote, S.M., Harcourt-Smith, W.E.H., Dunsworth, H.M., Van Couvering, J.A., 2009. Stratigraphic interpretation of the Kulu Formation (Early Miocene, Rusinga Island, Kenya) and its implications for primate evolution. J. Hum. Evol. 56, 447-461.

Pickford, M., 1981. Preliminary Miocene mammalian biostratigraphy for Western Kenya. J. Hum. Evol. 10, 73–97.

Pickford, M., 1983. On the origins of Hippopotamidae together with descriptions of two new species, a new genus, and a new subfamily from the Miocene of Kenya. Geobios 16, 193-217.

Pickford, M., 1984. Kenya Palaeontology Gazetter. Kenya National Museums Special Publication 1.

Pickford, M., 1985. A new look at *Kenyapithecus* based on recent discoveries in western Kenya. J. Hum. Evol. 14, 113-144.

Pickford, M., 1986a. Cainozoic Palaeontological Sites of Western Kenya. Münchner Geowissenschaftliche Abhandlungen Reihe A: Geologie und Paläontologie 8,1-151.

Pickford, M., 1986b. Sedimentation and fossil preservation in the Nyanza Rift system, Kenya. In: Frostick, L.D., Renaut, R.W., Reid, I., Tiercelin, J.J. (Eds.), Sedimentation in the African Rifts. Geological Society Special Publications, London, pp. 345-362.

Pickford, M., Thomas, H., 1984. An aberrant new bovid (Mammalia) in subrecent deposits from Rusinga island, Kenya. Proc. Koninklijke Akademie des Wetenschappen B. 87, 441-452.

Plummer, T.W., Ditchfield, P.W., Bishop, L.C., Kingston, J.D., Ferraro, J.V., Braun, D.R., Hertel, F., Potts, R., 2009. Oldest evidence of toolmaking hominins in a grassland-dominated ecosystem. PLOS One 4, e7199.

Potts, R., 2012. Evolution and environmental change in early human prehistory. Ann. Rev. Anthropol. 41,151-167

Potts, R., Behrensmeyer, A.K., Ditchfield, P., 1999. Paleolandscape variation and Early Pleistocene hominid activities: Members 1 and 7, Olorgesailie Formation, Kenya. J. Hum. Evol. 37,747-788.

Pouchou, J.L., Pichoir, F., 1985. "PAP", Procedure for Improved Quantitative Microanalysis. In: Armstrong, J.T. (Ed.), Microbeam Analysis Proceedings. San Francisco Press, San Francisco, pp. 104-106.

Pruetz, J.D., and Bertolani, P., 2009. Chimpanzee (*Pan troglodytes*) behavioral responses to stresses associated with living in a savanna-mosaic environment: implications for hominin adaptations to open habitats. PaleoAnthropology 2009, 252-262.

Quade, J., Levin, N.E., 2013. East African hominin paleoecology: isotopic evidence from paleosols. In: Sponheimer, M., Lee-Thorp, J.A., Reed, K.E., Ungar, P.S. (Eds.), Early Hominin Paleoecology. University Press of Colorado, Boulder, Colorado, pp. 59-102.

Reinhard, E., de Torres, T., O'Neil, J., 1996. $^{18}O/^{16}O$ ratios of cave bear tooth enamel: a record of climate variability during the Pleistocene. Palaeogeogr. Palaeoclim. Palaeoecol. 126, 45-59.

Retallack, G.J., 2002. Soils of the Past: an Introduction to Paleopedology, 2nd ed. London, Blackwell Science.

Retallack, G., Bestland, E.A., Dugas, D.P., 1995. Miocene paleosols and habitats of *Proconsul* on Rusinga Island, Kenya. J. Hum. Evol. 29, 53-91.

Robinson, J.T., 1954. Prehominid dentition and hominid evolution. Evolution. 8, 324-334.

Roebroeks, W., De Loecker, D., Hennekens, P., van Ieperen, M., 1995. "A veil of stones": On the interpretation of an early Middle Paleolithic low density scatter at Maastricht-Bélvèdere (The Netherlands). Analecta Praehistorica Leidensia. 25,1-16.

Rogers, M.J., Harris, J.W.K., 1992. Recent investigations in landscape archaeology at East Turkana. Nyame Akuma. 38,41-47.

Romanek, C.S., Grossman, E.L., Morse, J.W., 1992. Carbon isotopic fractionation in synthetic aragonite and calcite: effects of temperature and precipitation rate. Geochim. Cosmochim. Acta. 56, 419-430.

Rommenskirchen, F., Plader, A., Eglinton, G., Chikaraishi, Y., Rullkötter, J., 2006. Chemotaxonomic significance of distribution and stable isotopic composition of long-chain alkanes and alkan-1-ols in C_4 grass waxes. Org. Geochem. 37, 1303-1332.

Rose, M.D., 1988. Another look at the anthropoid elbow. J. Hum. Evol. 17, 193-224.

Rose, M.D., 1992. Kinematics of the trapezium-1st metacarpal joint in extant anthropoids and Miocene hominoids. J. Hum. Evol. 22, 255-266.

Rose, M.D., 1993. Locomotor anatomy of Miocene hominoids. In: Gebo, G.L., (Ed.) Postcranial Adaptation in Nonhuman Primates. Northern Illinois University Press, DeKalb, pp. 252-272.

Rose, M.D., 1994. Quadrupedalism in some Miocene catarrhines. J. Hum. Evol. 26, 387-411.

Rossie, J.B., Seiffert, E.R., 2006. Continental paleobiogeography as phylogenetic evidence. In: Fleagle, J.G., Kay, R.F., (Eds.) Anthropoid Origins. Plenum Press, New York, pp. 469-548.

Ruddiman, W.F., 1997. Tectonic Uplift and Climate Change. Plenum Press, New York, 535pp.

Sage, R.F., 2004. The evolution of C_4 photosynthesis. New Phytol. 161, 341-370.

Sage, R.F., Christin, P.-A., Edwards, E.K., 2011. The C_4 plant lineages of planet Earth. J. Exp. Bot. 62, 3155-3169.

Sage, R.F., Li., M., Monson, R.K., 1999. The taxonomic distribution of C_4 photosynthesis. In: Sage, R.F., Monson, R.K., (Eds.) C_4 Plant Biology. Academic Press, San Diego, pp. 551-584.

Sage, R.F., Wedin, D.A., Li, M., 1999. The biogeography of C_4 photosynthesis: patterns and controlling factors. In: Sage, R.F., and Monson, R.K. (Eds.) C_4 Plant Biology Academic Press, New York, pp. 313–373.

Sánchez Chillón, B., Alberdi, M.T., Leone, G., Bonadonna, F.P., Stenni, B., Longinell, A., 1994. Oxygen isotopic composition of fossil equid tooth and bone phosphate: an archive of difficult interpretation. Palaeogeogr. Palaeoclim. Palaeoecol. 107, 317-328.

Sarmiento, G., 1984. The Ecology of Neotropical Savannas. Cambridge, Harvard University Press.

Schefuss, E., Ratmeyer, V., Stuut, J.B.W., Jansen, J.H.F., Damsté, J.S.S., 2003. Carbon isotope analyses of n-alkanes in dust from the lower atmosphere over the central eastern Atlantic. Geochim. Cosmochim. Acta 67, 1757-1767.

Scholz, C.A., Johnson, T.C., Cohen, A.S., King, J.W., Peck, J.A., Overpeck, J.T., Talbot, M.R., Brown, E.T., Kalindekafe, L., Amoako, P.Y.O., Lyons, R.P., Shanahan, T.M., Castenada, I.S., Heil, C.W., Forman, S.L., McHargue, L.R., Beuning, K.R., Gomex, J., Pierson, J., 2007. East African megadroughts between 135 and 75 thousand years ago and bearing on early-modern human origins. Proc. Natl. Acad. Sci. U.S.A. 104, 16416-16421.

Schulz, E., Fahlke, J.M., Merceron, G., Kaiser, T., 2007. Feeding ecology of the Chalicotheriidae (Mammalia, Perissodactyla, Ancylopoda). Results from dental micro- and mesowear analyses. Verhandlungen des naturwissenschaftlichen Vereins Hamburg 45, 5-31.

Schulze, E.D., Mooney, H.A., Sala, O.E., Jobbagy, E., Buchmann, N., Bauer, G., Canadell, J., Jackson, R.B., Loreti, J., Oesterheld, M., Ehleringer, J.R., 1996. Rooting depth, water availability, and vegetation cover along an aridity gradient in Patagonia. Oecologia. 108, 503-511.

Schoeninger, M.J., Hallin, K., Reeser, H., Valley, J.W., Fournelle, J., 2003. Isotopic alteration of mammalian tooth enamel. Int. J. Osteoarchaeol. 13, 11-19.

Seiffert, E.R., Simons, E.L., Fleagle, J.G., Godinot, M., 2010. Paleogene anthropoids. In: Werdelin, L., and Sanders, W.J. (eds.) Cenozoic Mammals of Africa. University of California Press, Berkeley, pp. 369-391.

Semprebon, G.M., Sise, P.J., Coombs, M.C., 2011. Potential bark and fruit browsing as revealed by stereomicrowear analysis of the peculiar clawed herbivores known as calicotheres (Perissodactyla, Chalicotherioidea). J. Mammal. Evol. 18, 33-55.

Sepulchre, P., Ramstein, G., Fluteau, F., Schuster, M., Tiercelin, J.-J., Brunet, M., 2006. Tectonic uplift and Eastern African aridification. Science. 313, 1419-1423.

Shackleton, R.M., 1951. A contribution to the geology of the Kavirondo Rift Valley. Quarterly J. Geol. Soc. London. 106, 345-392.

Soares, P., Alshamali, F., Pereira, J.B., Fernandes, V., Silva, N.M., Alfonso, C., Costa, M.D., Musilová, E., Macaulay, V., Richards, M.B., Černy, V., Pereira, L., 2012. The expansion of mtDNA haplogroup L3 within and out of Africa. Mol. Biol. Evol. 29, 915-927.

Sponheimer, M., Lee-Thorp, J.A., 1999a. Alteration of enamel carbonate environments during fossilization. J. Arch. Sci. 26, 143-150

Sponheimer, M., Lee-Thorp, J.A., 1999b. Oxygen isotopes in enamel carbonate and their ecological significance. J. Arch. Sci. 26, 723-728.

Sponheimer, M., Lee-Thorp, J.A., 2003. Using carbon isotope data of fossil bovid communities for palaeoenvironmental reconstruction. S. Afr. J. Sci. 99, 273-275.

Sponheimer, M., Grant, C.C., De Ruiter, D., Lee-Thorp, J.A., Codron, D.M., Codron, J., 2003a. Diets of impala from Kruger National Park: evidence from stable carbon isotopes. Koedoe 46, 101-106.

Sponheimer, M., Lee-Thorp, J.A., DeRuiter, D.J., Smith, J.M., van der Merwe, M.J., Reed, K., Grant, C.C., Ayliffe, L.K., Robinson, T.F., Heidelberger, C., Marcus, W., 2003b. Diets of South African Bovidae: stable isotope evidence. J. Mammal. 84, 471-479.

Sponheimer, M., Reed, K.E., Lee-Thorp, J.A., 1999. Combining isotopic and ecomorphological data to refine bovid paleodietary reconstruction: a case study from the Makapansgat Limeworks hominin locality. J. Hum. Evol. 36, 705-718.

Stanhope, M.J., Waddell, V.G., Masden, O., De Jong, W., Hedges, S. B., Cleven, G.C., Kao, D., Springer, M.S., 1998. Molecular evidence for multiple origins of Insectivora and for a new order of endemic insectivore mammals. Proc. Natl. Acad. Sci. U.S.A. 95, 9967-9972.

Stern, N., 1993. The structure of the Lower Pleistocene archaeological record. Cur. Anthropol. 34, 201-225.

Sternberg, L.S.L., 1989. Oxygen and hydrogen isotope ratios in plant cellulose: mechanisms and applications. In: Rundel, P.W., Ehleringer, J.R., Nagy, K.A.

(Eds.) Stable Isotopes in Ecological Research: Ecological Studies: analysis and synthesis. Springer-Verlag, New York, pp. 124-141.

Stevens, N.J., Seiffert, E.R., O'Connor, P.M., Roberts, E.M., Schmitz, M.D., Krause, C., Gorscak, E., Ngasala, S., Hieronymus, T.L., Temu, J., 2013. Palaeontological evidence for an Oligocene divergence between Old World monkeys and apes. Nature. 497, 611-614.

Stowe, L.G., Teeri, J.A., 1978. The geographic distribution of C_4 species of the Dicotyledonae in relation to climate. Am. Nat. 112, 609-623.

Sullivan, C.H., Krueger, H.W., 1981. Carbon isotope analysis of separate chemical phases in modern and fossil bone. Nature. 292, 333-335.

Swap, R.J., Aranibar, J.N., Dowty, P.R., Gilhooly III, W.P., Macko, S.A., 2004. Natural abundance of ^{13}C and ^{15}N in C_3 and C_4 vegetation of southern Africa: patterns and implications. Glob. Change Biol. 10, 350-358.

Talbot, M.R., Jensen, N.B., Laerdal, T., Filippi, M.L., 2006. Geochemical responses to a major transgression in giant African lakes. J. Paleolimnol. 35, 467-489.

Talbot, M.R., Livingstone, D.A., 1989. Hydrogen Index and carbon isotopes of lacustrine organic matter as lake level indicators. Palaeogeogr. Palaeoclim. Palaeoecol. 70, 121-137.

Teeri, J.A., Stowe, L.G., 1976. Climatic patterns and the distribution of C_4 grasses in North America. Oecologia. 23, 1-12.

Thackray, G.D., 1994. Fossil nest of Sweat Bees (Halictinae) from a Miocene Paleosol, Rusinga Island, Kenya. J. Palentol. 68(4), 795-800.

Tieszen, L.L., Boutton, T.W., Tesdahl, K.G., Slade, N.A., 1983. Fractionation and turnover of stable carbon isotopes in animal tissues: implications for the ^{13}C analysis of diet. Oecologia. 57, 32-37.

Tieszen, L.L., Fagre, T., 1993. Effect of diet quality and composition on the isotopic composition of respiratory CO_2, bone collagen, bioapatite, and soft tissue. In: Lambert, J., Grupe, G. (Eds.), Prehistoric Human Bone, Archaeology at the Molecular Level. Springer-Verlag, Berlin, pp. 121-155.

Tieszen, L.L., Reed, B.C., Bliss, N.B., Wylie, B.K., Dejong, D.D., 1997. NDVI, C-3 and C-4 production and distributions in Great Plains grassland land cover classes. Ecol. Appl. 7, 59-78.

Tipple, B.J., Meyers, S.R., Pagani, M., 2010. Carbon isotope ratio of Cenozoic CO_2: a comparative evaluation of available geochemical proxies. Paleoceanography. 25, PA3202.

Tryon, C.A., 2003. The Acheulian to Middle Stone Age Transition: Tephrostratigraphic Context for Archaeological Change in the Kapthurin Formation, Kenya. Ph.D. Dissertation, University of Connecticut, Storrs.

Tryon, C.A., Faith, J.T., 2013. Variability in the Middle Stone Age of Eastern Africa. Curr. Anthropol. 54, S234-S254.

Tryon, C.A., Faith, J.T., Peppe, D.J., Fox, D.L., McNulty, K.P., Jenkins, K., Dunsworth, H.E., Harcourt-Smith, W., 2010. The Pleistocene archaeology and environments of the Wasiriya Beds, Rusinga Island, Kenya. J. Hum. Evol. 59, 657-671.

Tryon, C.A., Faith, J.T., Peppe, D.J., Keegan, W.F., Keegan, K., Nightingale, S., Jenkins, K., Van Plantinga, A., Driese, S., Roure Johnson, C., Beverly, E.J., 2014. Sites on the landscape: Paleoenvironmental reconstruction of Late Pleistocene archaeological sites from the Lake Victoria Basin, Equatorial Africa. Quaternary Int. 331, 20-30.

Tryon, C.A., Peppe, D.J., Faith, J.T., Van Plantinga, A., Nightingale, S., Ogondo, J., Fox, D.L., 2012. Late Pleistocene artefacts and fauna from Rusinga and Mfangano islands, Lake Victoria, Kenya. Azania: Arch. Res. Afr. 47, 14-38.

Tryon, C.A., Faith, J.T., Peppe, D.J., Blegen, N., Beverly, E., Patterson, D., Jacobs, Z., 2013. Pleistocene archaeology and paleoenvironments of the Lake Victoria basin in Kenya. Paleoanthropology Society Meetings Abstracts, Honolulu, HI, 2-3 April 2013. PaleoAnthropology 2013, A37.

Turner, M.G., Bratton, S.P., 1987. Fire, grazing and the landscape heterogeneity of a Georgia barrier island. In: Turner, M.G. (Ed.) Landscape Heterogeneity and Disturbance. Springer-Verlag, New York, pp. 85-101.

Ungar, P.S., Scott, J.R., Curran, S.C., Dunsworth, H.M., Harcourt-Smith, W.E.H., Lehmann, T., Manthi, F.K., McNulty, K.P., 2012. Palaeogeogr. Palaeoclim. Palaeoecol. 342-343, 84-96.

Uno, K.T., Polissar, P.J., Kahle, E., Feibel, C., Harmand, S., Roche, H., deMenocal, P.B., 2016. A Pleistocene palaeovegetation record from plant wax biomarkers from the Nachukui Formation, West Turkana, Kenya. Phil. Trans. R. Soc. B 371: 20150235. http://dx.doi.org/10.1098/rstb.2015.0235.

Van Couvering, J.A., 1972. Geology of Rusinga Island and Correlation of the Kenya Mid-Tertiary Fauna. Ph.D. Dissertation, Cambridge University.

Van Couvering, J.A., Miller, J.A., 1969. Miocene stratigraphy and age determinations, Rusinga Island, Kenya. Nature. 221, 628-632.

van der Merwe, N.J., Medina, E., 1991. The canopy effect, carbon isotope ratios, and foodwebs in Amazonia. J. Archaeol. Sci. 18, 249-259.

Van Plantinga, A., 2011. Geology of the Late Pleistocene artifact-bearing Wasiriya Beds at the Nyamita locality, Rusinga Island, Kenya. M.Sc. thesis, Department of Geology, Baylor University, Waco, TX.

Vicentini A., Barber J.C., Aliscioni S.S., Giussani L.M., Kellogg E.A., 2008. The age of the grasses and clusters of origins of C-4 photosynthesis. Glob. Change Biol. 14, 2963–2977.

von Fischer, J.C., Tieszen, L.L., Schimel, D.S., 2008. Climate controls on C_3 vs. C_4 productivity in North American grasslands from carbon isotope composition of soil organic matter. Glob. Change Biol. 14, 1141-1155.

Walker, A., 1997. *Proconsul*: function and phylogeny. In: Begun, D.R., Ward, C.V., and Rose, M.D., (eds.) Function, phylogeny, and fossils: Miocene hominoid evolution and adaptation. Plenum Press, New York, pp. 209-224.

Walker, A., 2007. Taphonomy and site formation of two early Miocene sites on Rusinga Island, Kenya. In: T. Pickering et al (Eds.) Breathing Life into Fossils. Stone Age Press, Gossport, pp. 107-118.

Walker, A., Teaford, M.F., 1988. The Kaswanga Primate Site: An Early Miocene hominoid site on Rusinga Island, Kenya. J. Hum. Evol. 17, 539-544.

Wang, Y., Cerling, T.E., 1994. A model of fossil tooth and bone diagenesis: implications for paleodiet reconstruction from stable isotopes. Palaeogeogr. Palaeoclim. Palaeoecol. 107, 281-289.

Ward, C.V., 1993. Torso morphology and locomotion in *Proconsul nyanzae*. Am. J. Phys. Anthropol. 92, 291-328.

Ward, C.V., 1997. Functional anatomy and phyletic implications of the hominoid truck and hindlimb. In: Begun, D. (ed.) Miocene Hominoid Fossils: Functional and Phylogenetic Implications. Plenum Press, New York, pp. 101-130.

Ward, C.V., Leakey, M.G., Brown, B., Brown, F., Harris, J., Walker, A., 1999. South Turkwel: A new Pliocene hominid site in Kenya. J. Hum. Evol. 36, 69-95.

Ward, C.V., Ruff, C.B., Walker, A., Teaford, M.F., Rose, M.D., Nengo, I.O., 1995. Functional morphology of *Proconsul* patellas from Rusinga Island, Kenya, with implications for other Miocene-Pliocene catarrhines. J. Hum. Evol. 29, 1-19.

Ward, C.V., Walker, A., Teaford, M.F., 1991. *Proconsul* did not have a tail. J. Hum. Evol. 21, 215-220.

Werdelin, L., Sanders, W.J., 2010. Cenozoic Mammals of Africa. University of California Press, Berkeley, California, 1008 pp.

White, F., 1983. The Vegetation of Africa, Vol. 20. United Nations Scientific and Cultural Organization.

White, T.D., Ambrose, S.H., Suwa, G., Su, D.F., DeGusta, D., Bernor, R.L., Boisserie, J.-R., Brunet, M., Delson, E., Frost, S., Garcia, N., Giaourtsakis, I.X., Haile-Selassie, Y., Howell, F.C., Lehmann, T., Likius, A., Pehlevan, C., Saegusa, H., Semprebon, G., Teaford, M., Vrba, E., 2009. Microvertebrate Paleontology and the Pliocene Habitat of Ardipithecus ramidus. J. Hum. Evol. 326, 87-93.

Winkler, A.J., 2002. Neogene paleobiogeography and East African paleoenvironments: contributions from the Tugen Hills rodents and lagomorphs. J. Hum. Evol. 42, 237-256.

Winkler, A.J., Denys, C., Avery, D.M., 2010. Rodentia. In: Werdelin, L., and Sanders, W.J. (eds.) Cenozoic Mammals of Africa. University of California Press, Berkeley, pp. 263-304.

Wynn, J.G., 2007. Carbon isotope fractionation during decomposition of organic matter in soils and paleosols: implications for paleoecological interpretations of paleosols. Palaeogeogr. Palaeoclim. Palaeoecol. 251, 437-448.

Wynn, J.G., Bird, M.I., Wong, V.N.L., 2005. Rayleigh distillation and the depth profile of $^{13}C/^{12}C$ ratios in soil organic carbon from two soils in Iron Range National Park, Far North Queensland, Australia. Geochim. Cosmochim, Acta. 69, 1961–1973.

Yeakel, J.D., Bennett, N.C., Koch, P.L., Dominy, N.J., 2007. The isotopic ecology of African mole rats inform hypotheses on the evolution of human die. Proc. R. Soc. B. 274, 1723-1730.

Yellen, J., Brooks, A., Helgren, D., Tappen, M., Ambrose, S., Bonnefille, R., Feathers, J., Goodfriend, G., Ludwig, K., Renne, P., Stewart, K., 2005. The archaeology of Aduma Middle Stone Age site in Awash Valley, Ethiopia. PaleoAnthropology. 10, 25-100.

Zachos, J.C., Dickens, G.R., Zeebe, R.E., 2008. An early Cenozoic perspective on greenhouse warming and carbon-cycle dynamics. Nature. 451, 279-283.

Zachos, J., Pagani, M., Sloan, L., Thomas, E., Billups, K., 2001. Trends, rhythms, and aberrations in global climate 65 Ma to present. Science. 292, 686–693.

Zech, M., Rass, S., Buggle, B., Löscher, M., Zöller, L., 2012. Reconstruction of the late Quaternary paleoenvironments of the Nussloch loess paleosol sequence, Germany, using *n*-alkane biomarkers. Quaternary Res. 78, 226-235.

Zhang, R., Jiang, D., Zhang, Z., Yu, E., 2015. The impact of regional uplift of the Tibetan Plateau on the Asian monsoon climate. Palaeogeogr. Palaeoclim. Palaeoecol. 417, 137-150.

Zhang, Y.G., Pagani, M., Liu, A., Bohaty, S.M., DeConto, R., 2013. A 40-million-year history of atmospheric CO_2. Phil. Trans. R. Soc. A. 371, 2130096.

Zhisheng, A., Kutzbach, J.E., Prell, W.L., Porter, S.C., 2001. Evolution of Asian monsoons and phased uplift of the Himalaya–Tibetan plateau since Late Miocene times. Nature. 411, 62-66.

Zomer, R.J., Trabucco, A., Bossio, D.A., van Straaten, O., Verchot, L.V., 2007. A spatial analysis of global land suitability for clean development mechanism afforestation and reforestation. Agric. Ecosys. Environ. 126, 67-80.